Bone: structure and properties… and how to mimic it

Fernando J. Monteiro
fjmont@ineb.up.pt

INSTITUTO DE INVESTIGAÇÃO E INOVAÇÃO EM SAÚDE
UNIVERSIDADE DO PORTO

INEB - Instituto de Engenharia Biomédica
Universidade do Porto, Porto, Portugal

SUMMER SCHOOL Ceramic and Glass Science & Technology
Application to Bioceramics and Bioglasses

MADRID, 17, 18, 19 June 2015

Structure of bone

- **Internal support system in all higher vertebrates**
- **Flat bones**
  - Skull bones, Mandible, Ileum
- **Long bones**
  - Tibiae, Femur, Humerus
- **Mineralized living tissue of marked rigidity and strength while still maintaining some degree of elasticity**

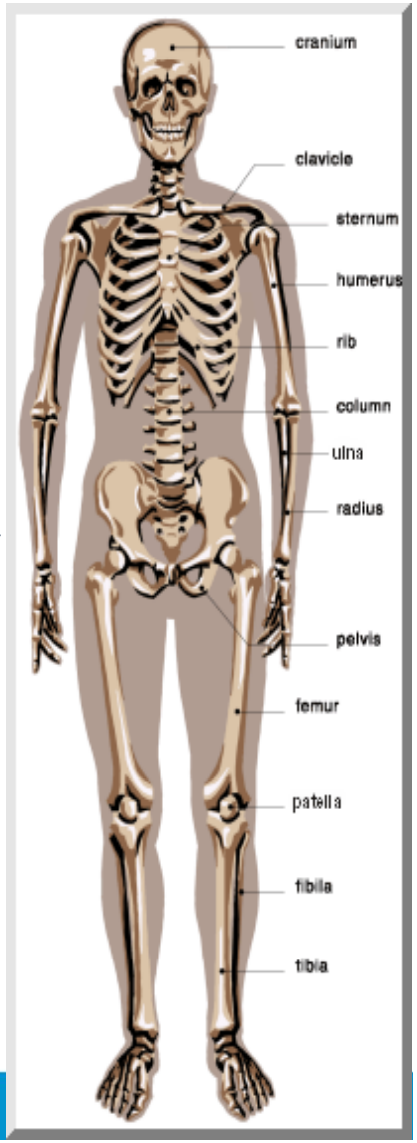

Structure of bone

- **Functions of bone**
  - Mechanical
    - Support and site of muscle attachment for locomotion
  - Protective
    - For vital organs and bone marrow
  - Metabolic
    - Reserve of ions for the entire organism (especially Ca and P)
    - Hematopoiesis

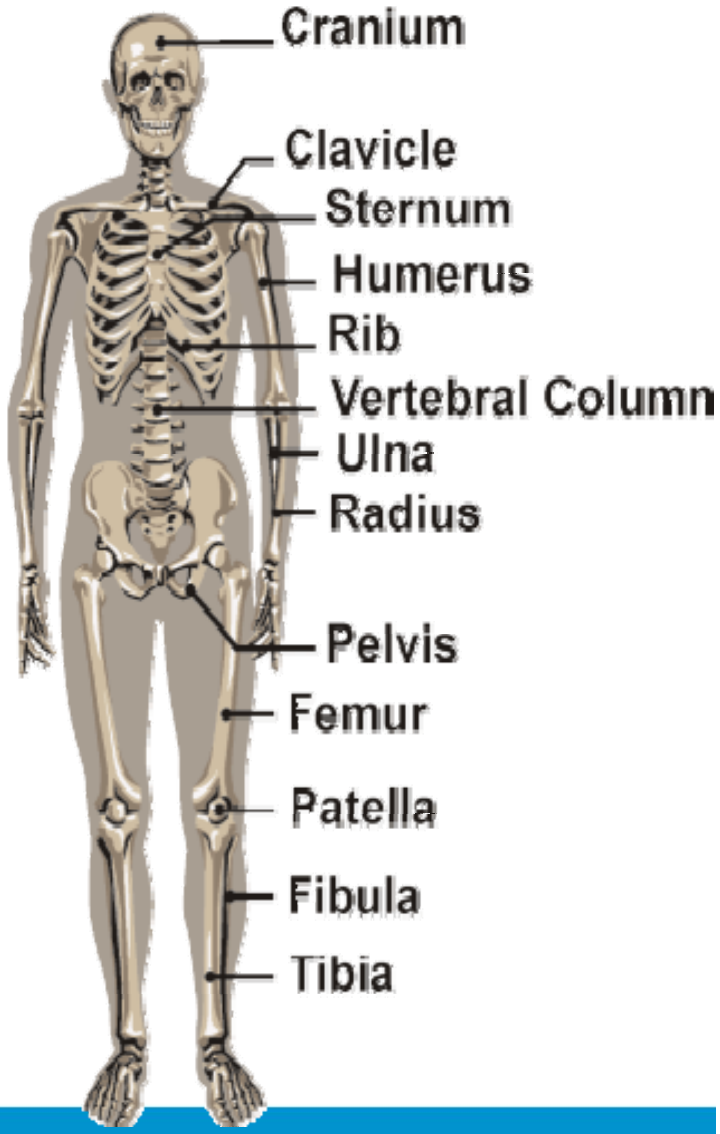

Structure of bone

- **Constituents of bone**
  - Cells
    - Osteoblasts
      - Osteocytes*
    - Osteoclasts
    - Bone lining cells
  - Mineralised extracellular matrix
    - Highly substituted hydroxyapatite
    - Organic compounds
      - Type I collagen (90%)
      - Glicoproteins
      - Proteoglicans

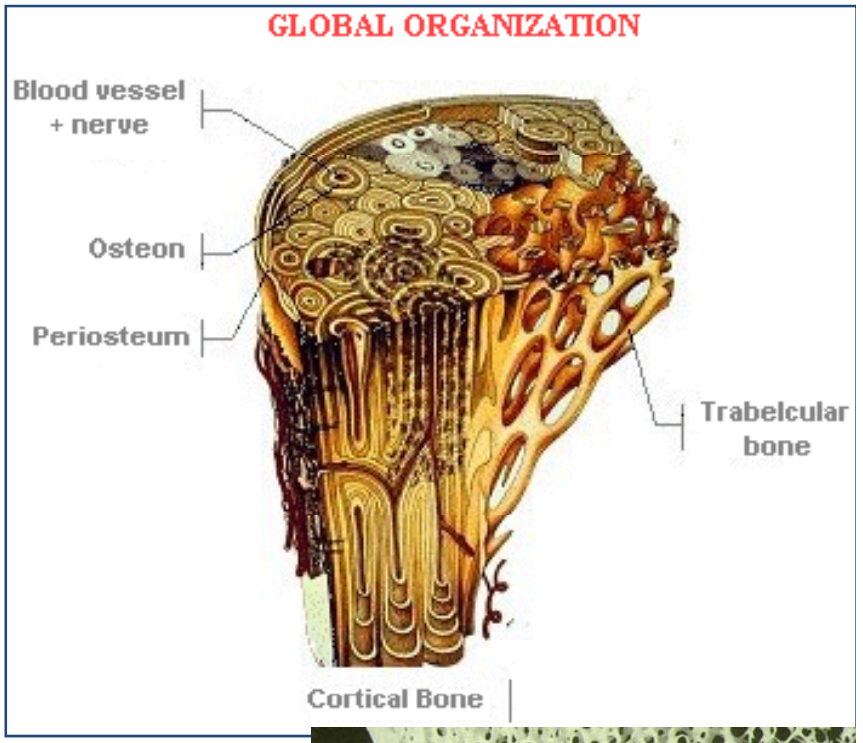

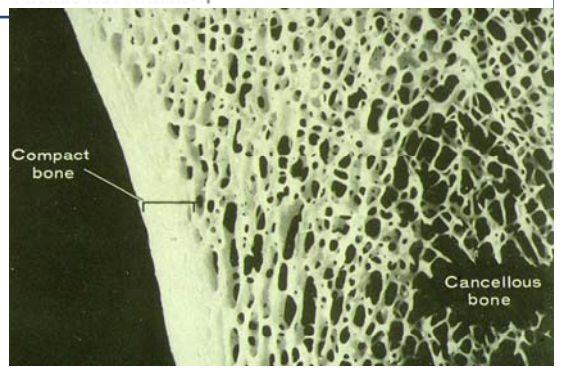

* Osteocytes are osteoblasts that have been entraped into the extracellular matrix

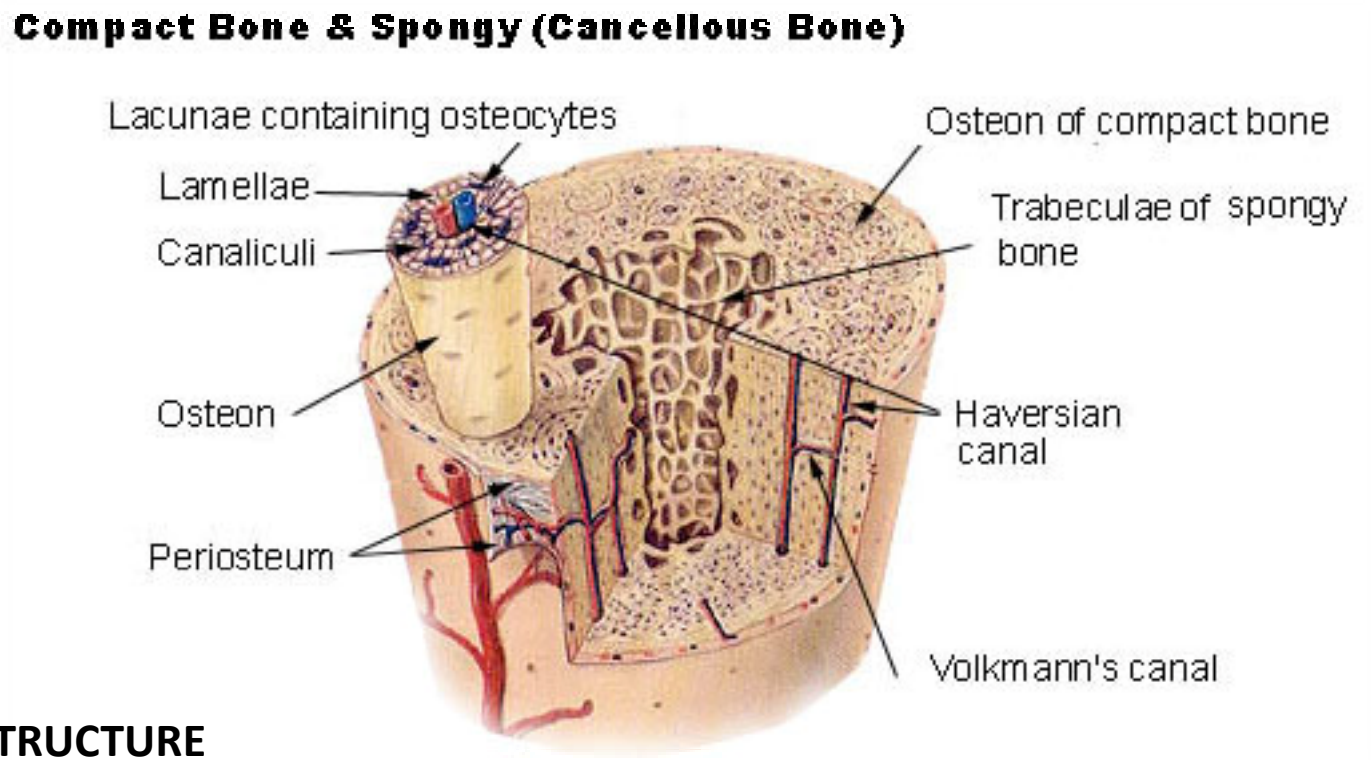

BONE STRUCTURE

Compact bone (dense or cortical)

Trabecular bone (cancellous or spongy bone)

Periosteum

Endosteum

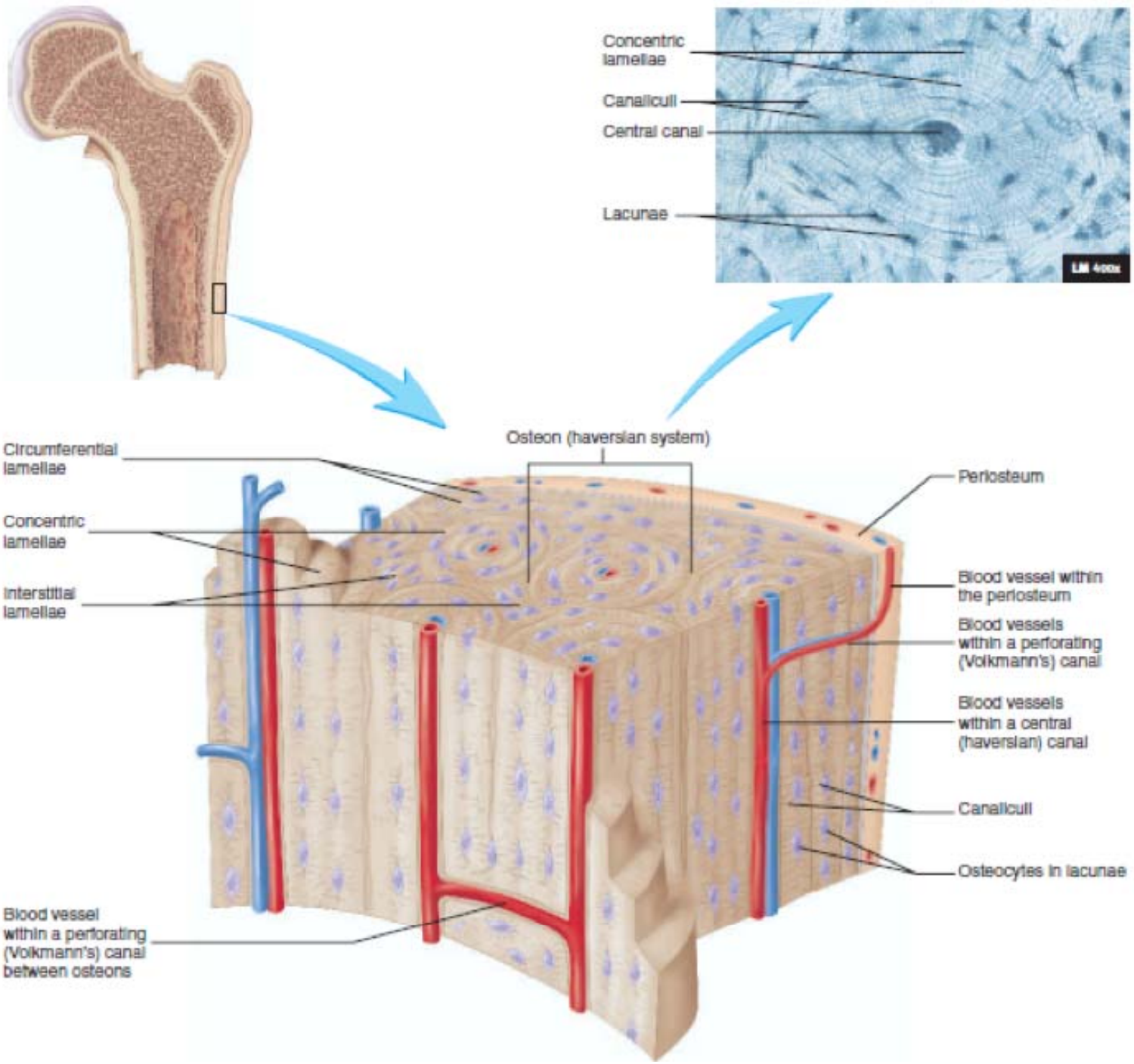
Concentric lamellae
Canaliculi
Central canal
Lacunae
LM 400x
Osteon (haversian system)
Circumferential lamellae
Concentric lamellae
Interstitial lamellae
Periosteum
Blood vessel within the periosteum
Blood vessels within a perforating (Volkmann's) canal
Blood vessels within a central (haversian) canal
Canaliculi
Osteocytes in lacunae
Blood vessel within a perforating (Volkmann's) canal between osteons

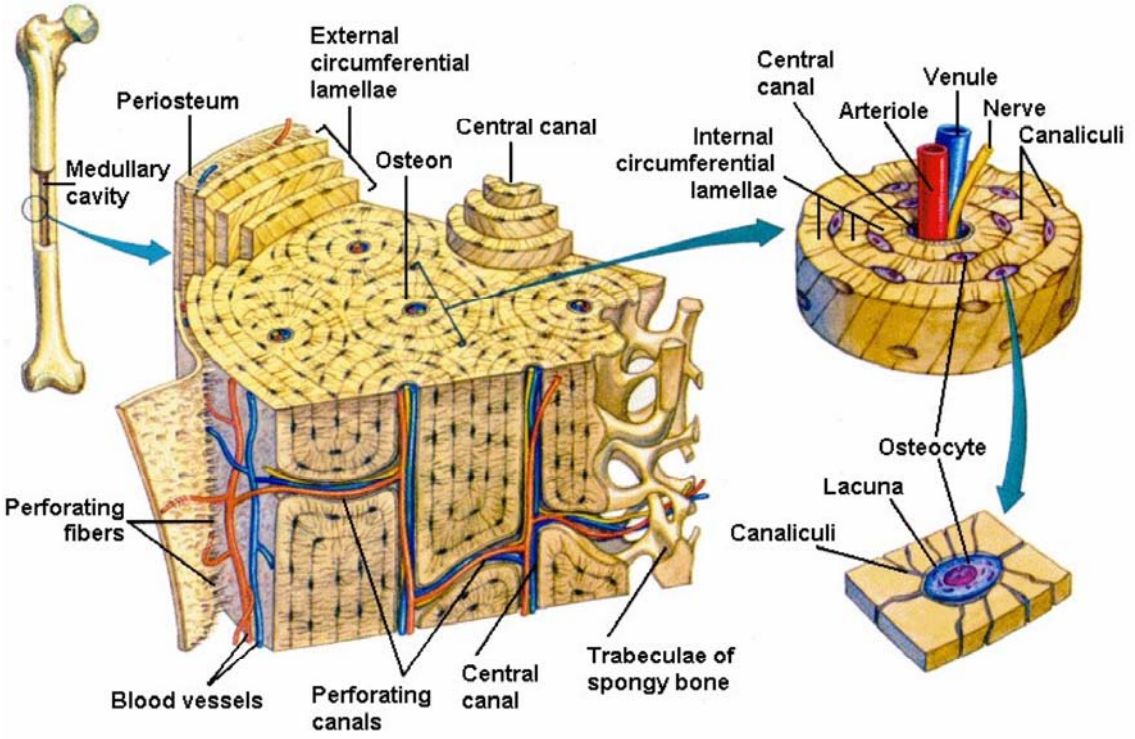

Schematic drawing of the bone architecture. Both cortical and spongy bone can be distinguished. The osteons of cortical bone are displayed including the haversian channels that contain blood vessels and nerves. The periosteum (highly vascularised membrane that covers the bone surface) can also be seen.

Adapted from a figure by the Department of Kinesiology & Physical Education, Lethbridge University.

Table 1. Comparison between structures that compose skeleton [9]

Structure	Water Composition	Proteoglycans Composition	Collagen Composition	Mineral Composition
Tendon/Ligament	Moderate	Low	High	Low
Cartilage	High	High	Low - Moderate	Low
Bone	Low	Low	Moderate	High

Distribution of calcium, magnesium, and phosphate in the body of a 70-kg adult* [2]

Compartment	Calcium (g)	Magnesium (g)	Phosphate (g)
Bones and teeth	1300 (99)	14.0 (54)	600.0 (86)
Extracellular fluid	1 (0.1)	0.3 (1)	0.2 (0.03)
Cells	7 (1.0)	12.0 (46)	100.0 (14)

Note: *Most of calcium is in bone and almost half of magnesium is in cells. Phosphate, as the principal counter ion to calcium and magnesium, has an intermediate proportional distribution. Number in parentheses is the percentage of total content for that mineral.

Mechanical properties of cortical and trabecular (cancellous) bone

Property	Cortical bone	Cancellous bone
Compressive strength (MPa)	100–230	2–12
Flexural, tensile strength (MPa)	50–150	10–20
Strain to failure (%)	1–3	5–7
Fracture toughness ($MPam^{1/2}$)	2–12	–
Young's modulus (GPa)	7–30	0.5–0.05

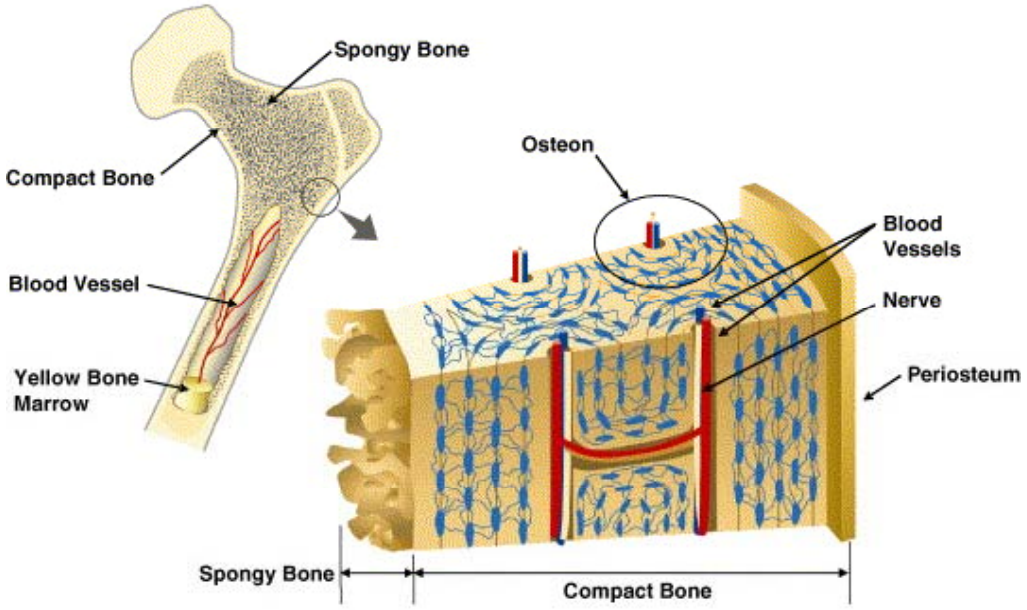
Spongy Bone
Compact Bone
Blood Vessel
Yellow Bone Marrow
Osteon
Blood Vessels
Nerve
Periosteum
Spongy Bone
Compact Bone

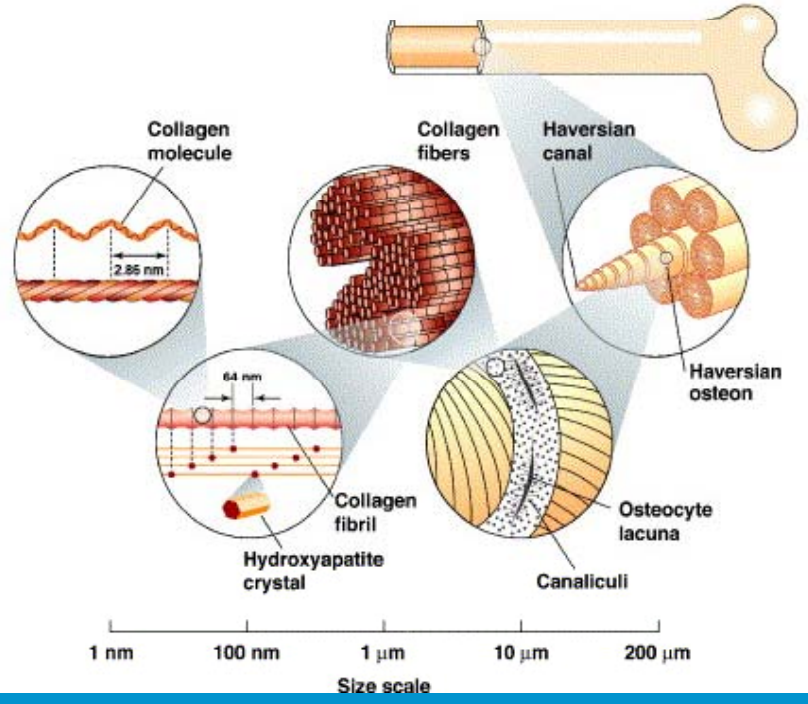
Collagen molecule
2.86 nm
Collagen fibers
Haversian canal
Haversian osteon
64 nm
Collagen fibril
Hydroxyapatite crystal
Osteocyte lacuna
Canaliculi
1 nm
100 nm
1 μm
10 μm
200 μm
Size scale

Osteoblast and bone formation

- **Production of matrix**
  - Recruitment of osteoprogenitor cells
  - Proliferation
  - Differentiation into osteoblasts
  - Osteoblasts
    - Secrete ECM into which mineral is selectively deposited
    - Control the composition of the matrix

Osteoblast and bone formation

Composition of the organic extracellular matrix

- ✓Type I collagen (90%) → ✓Scaffolding; ✓Binds and orients other proteins that play a role on HA deposition
- ✓Proteoglycans
- ✓Glycoproteins
  - ✓ Osteonectin, Bone sialoprotein, Osteopontine, Fibronectine
- ✓G-carboxy glutamin acid containing proteins → ✓Provides appropriate concentrations of phosphate ions to initiate mineralisation
  - ✓ Osteocalcin, Matrix gla-proteins
- ✓Enzymes
  - ✓ Alkaline phosphatase, Collagenase, Proteinases
- ✓Growth factores
  - ✓ FGFs, IGFs, TGFβs, BMPs
- ✓Proteolipids

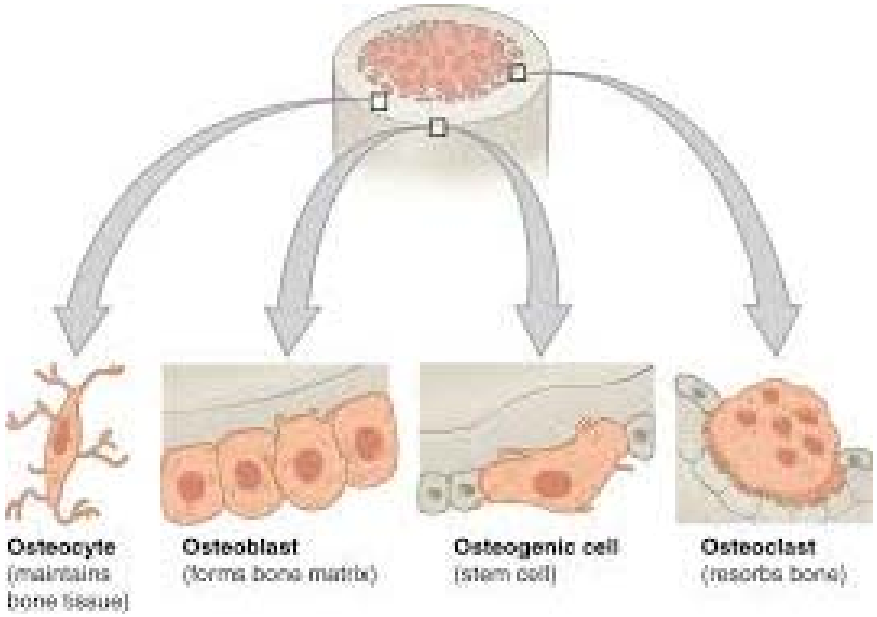
Osteocyte
(maintains
bone tissue)
Osteoblast
(forms bone matrix)
Osteogenic cell
(stem cell)
Osteoclast
(resorbs bone)

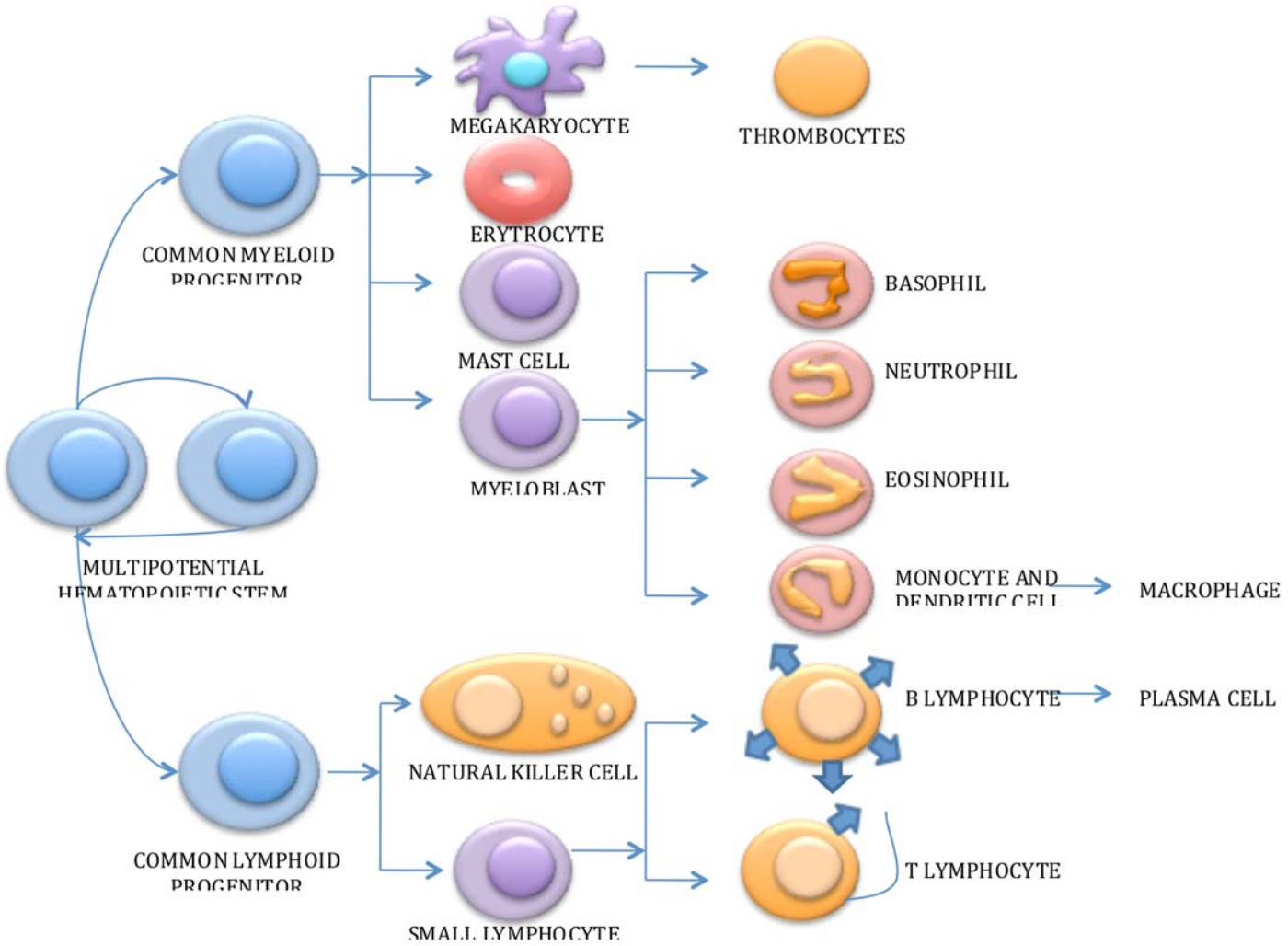

Figure 2. Hematopoiesis pathway

Structure of bone

- **Bone remodelling**
  - Throughout life, bone mass is continuously in a remodelling process

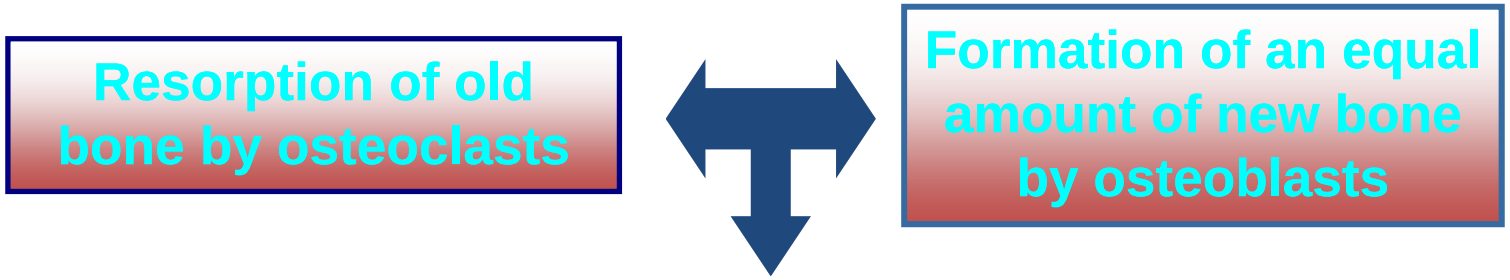

- ✓ Renewal of the skeleton
- ✓ Maintenance of bone tissue integrety
- ✓ Maintenance of mineral homeostasis

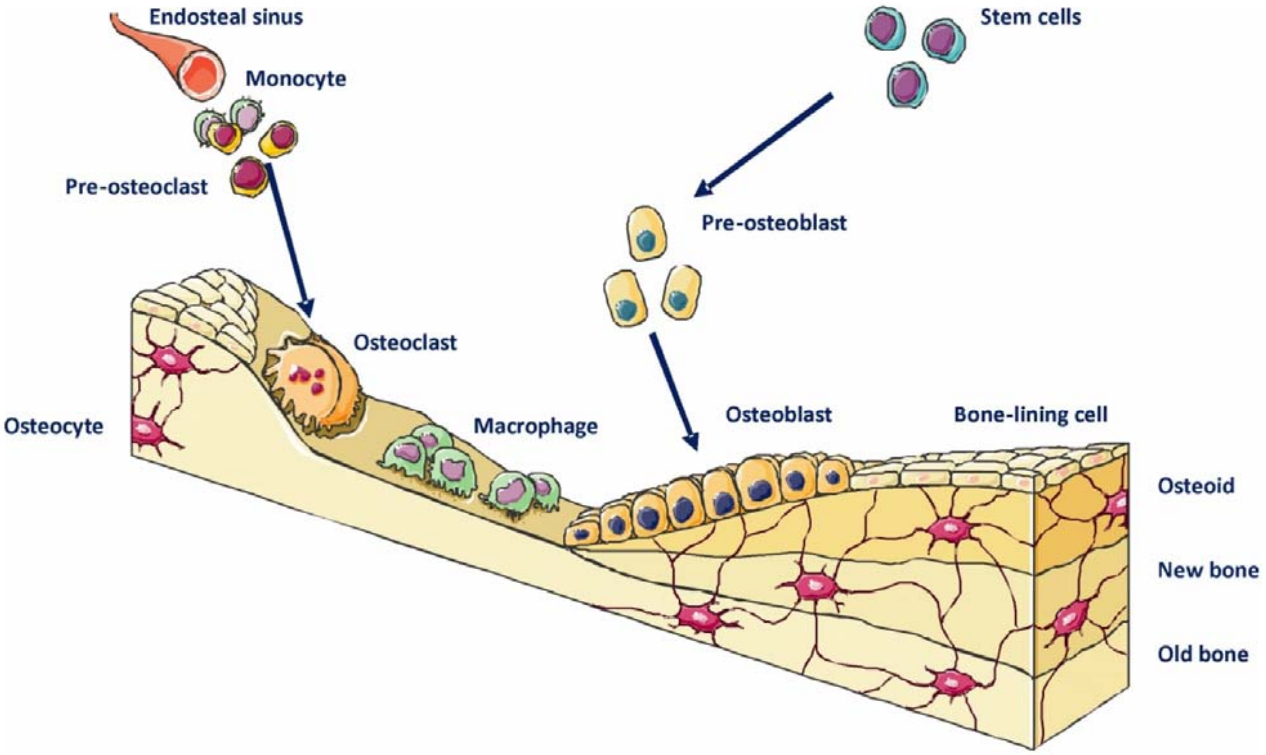

Bone remodeling osteoblasts and osteoclasts differentiation

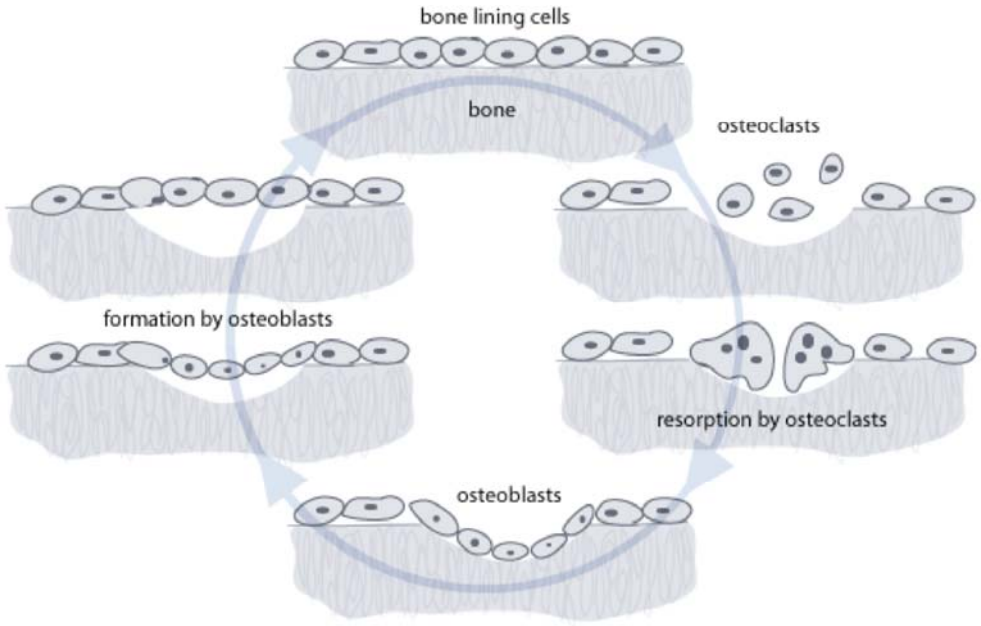

Bone remodelling process. Osteoblasts depend on the osteoclasts to resorb older bone ahead of them. As the bone is resorbed by the osteoclasts, there is the release of cytokines (signalling molecules) that attract osteoblasts and induce them to start laying down new bone tissue. The osteoblasts then incorporate proteins into the bone structure. Once that bone is resorbed by osteoclasts again the proteins are released and act as signals to the osteoblast to return and lay down more bone. This tight coupling of formation and resorption is necessary to prevent a disorganized bone structure from being established. Adapted from *The Science Creative Quarterly*, by Jen Philpot.

Bone matrix composition

Inorganic portion

Hydroxyapatite (HA) crystals
($Ca_{10}(PO_4)_6(OH)_2$)

Organic portion

Collagen type I fibrils

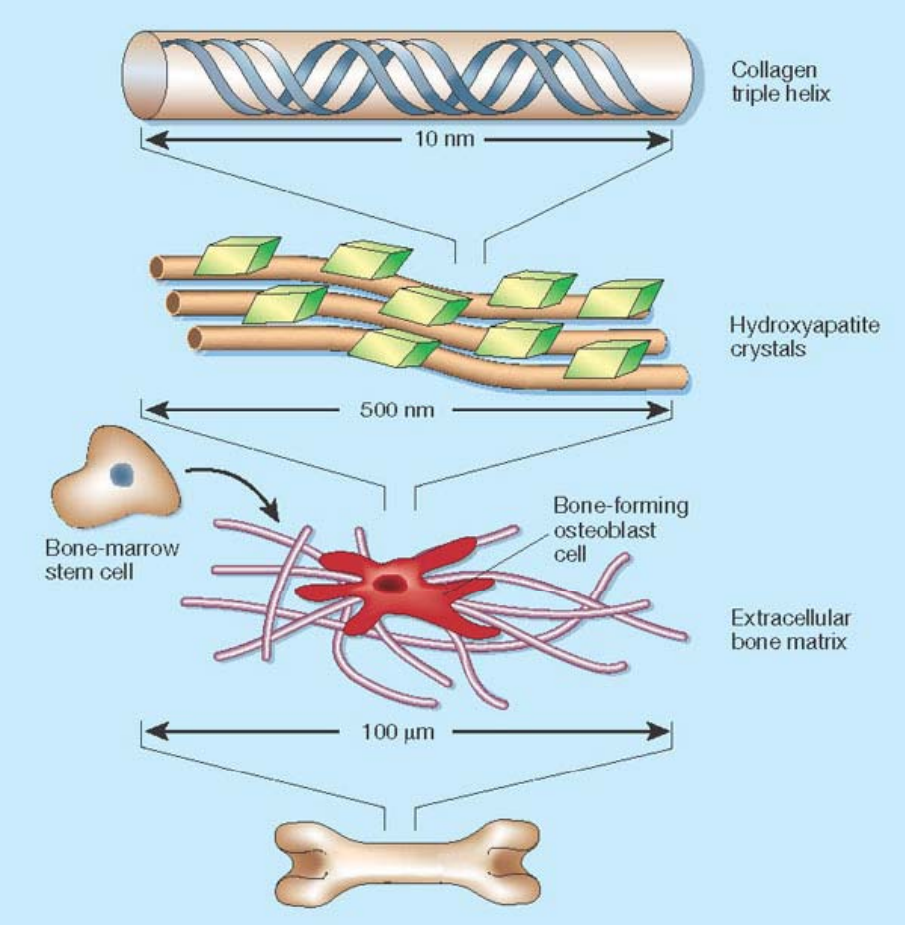

The many scales of organization in natural bone (Taton, 2001).

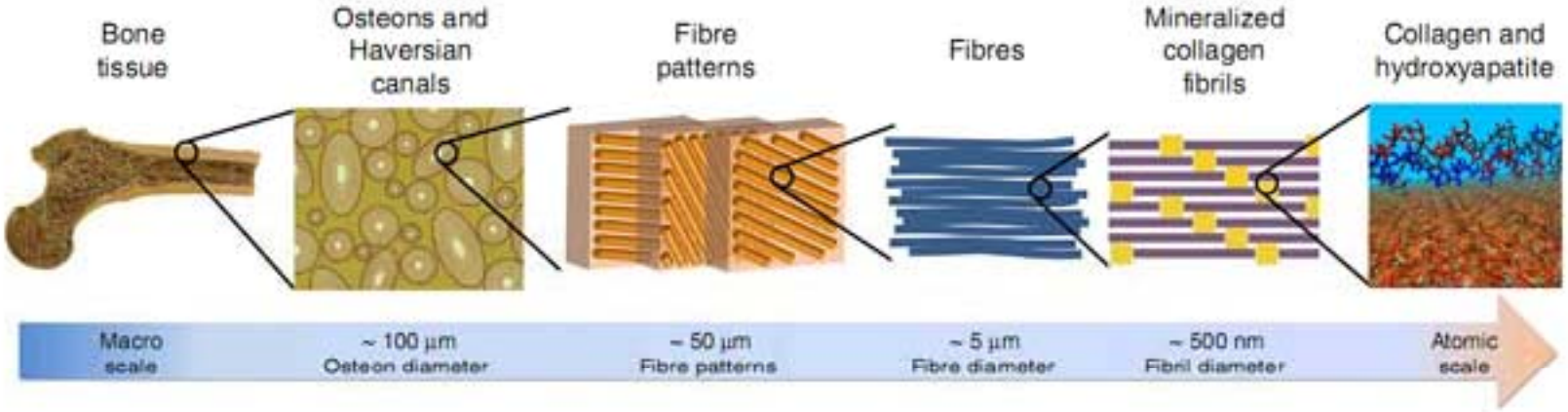
Bone tissue
Osteons and Haversian canals
Fibre patterns
Fibres
Mineralized collagen fibrils
Collagen and hydroxyapatite
Macro scale
~ 100 µm
Osteon diameter
~ 50 µm
Fibre patterns
~ 5 µm
Fibre diameter
~ 500 nm
Fibril diameter
Atomic scale

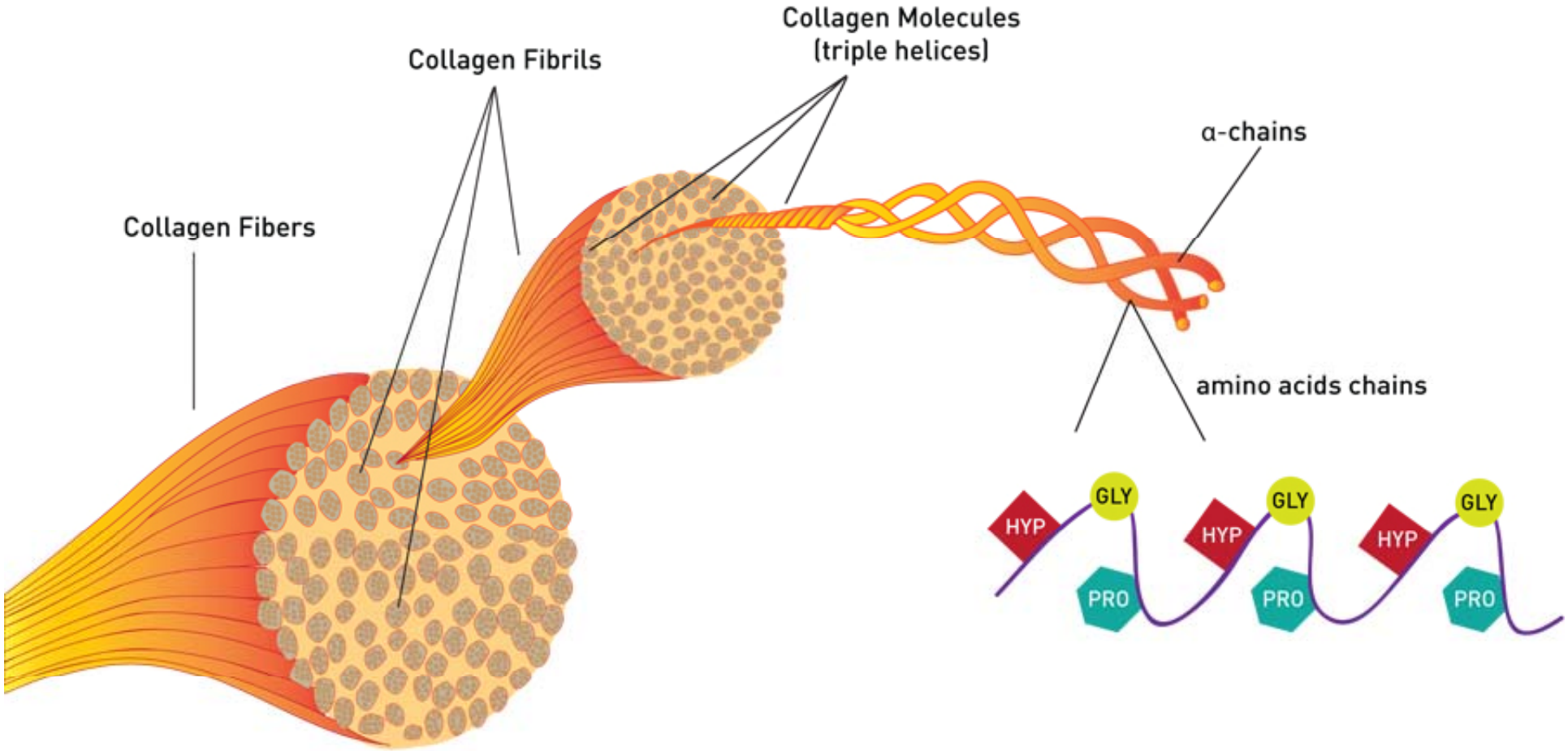
Collagen Molecules
(triple helices)
Collagen Fibrils
α-chains
Collagen Fibers
amino acids chains
HYP
GLY
PRO
HYP
GLY
PRO
HYP
GLY
PRO

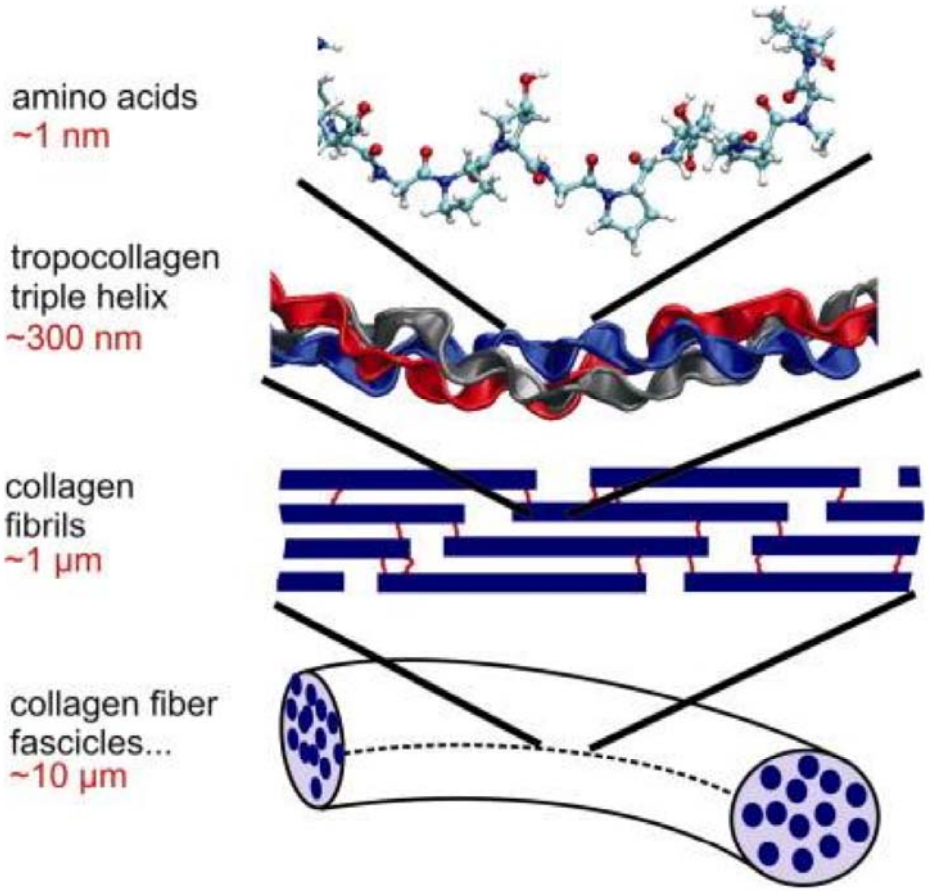

Figure 1. Collagen organization (30).

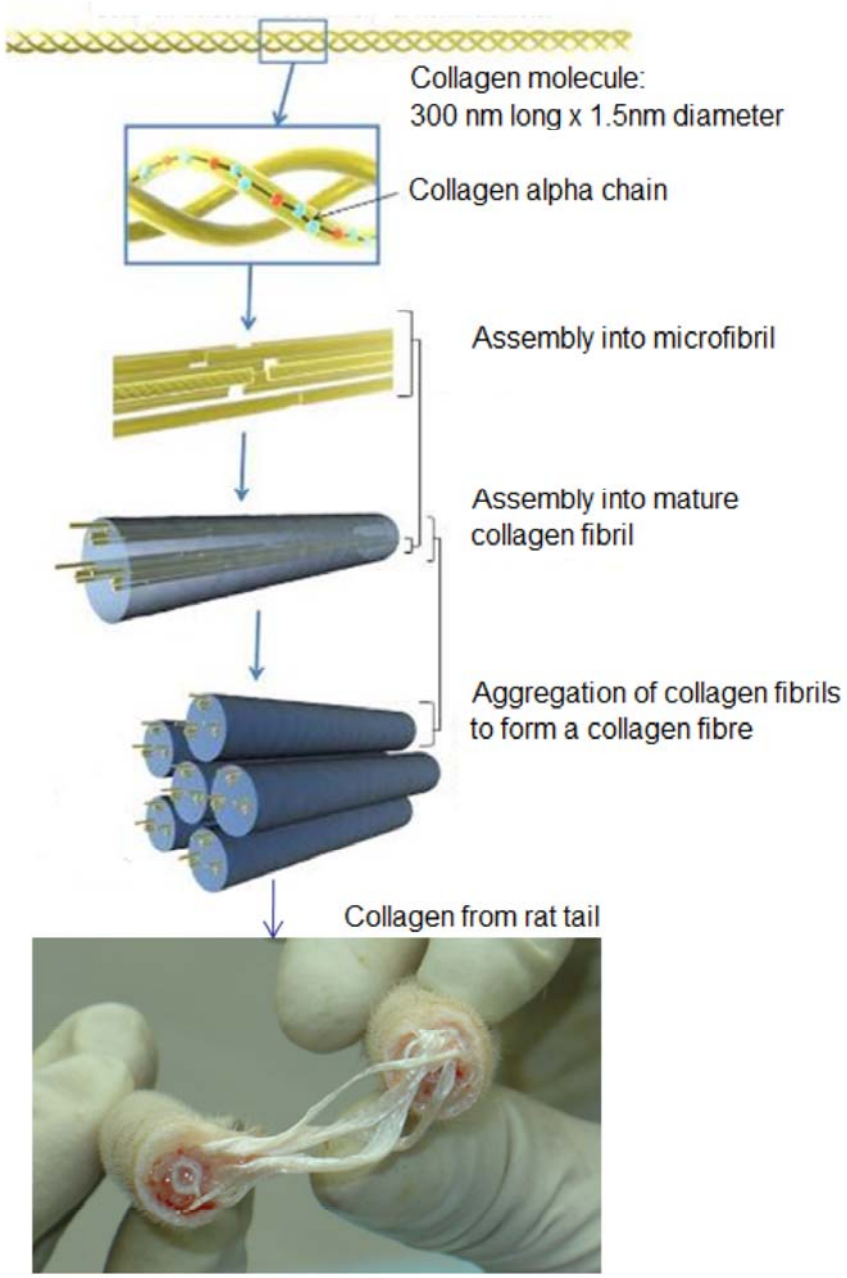

Figure 4. Collagen structure.

Adapted from the source. Source: www.orthoteers.com

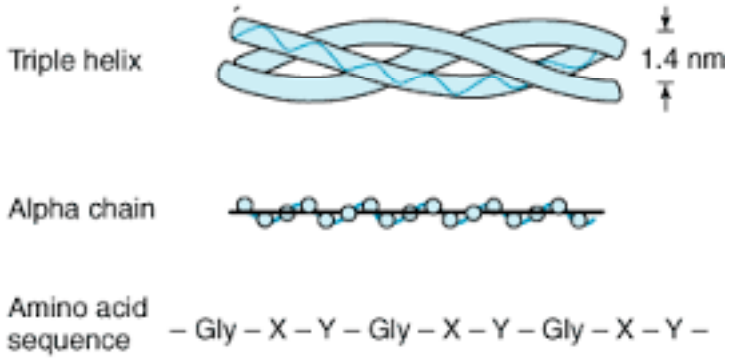

Energy minimized structure of 24-mer collagen triple helix

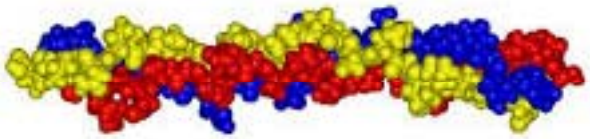

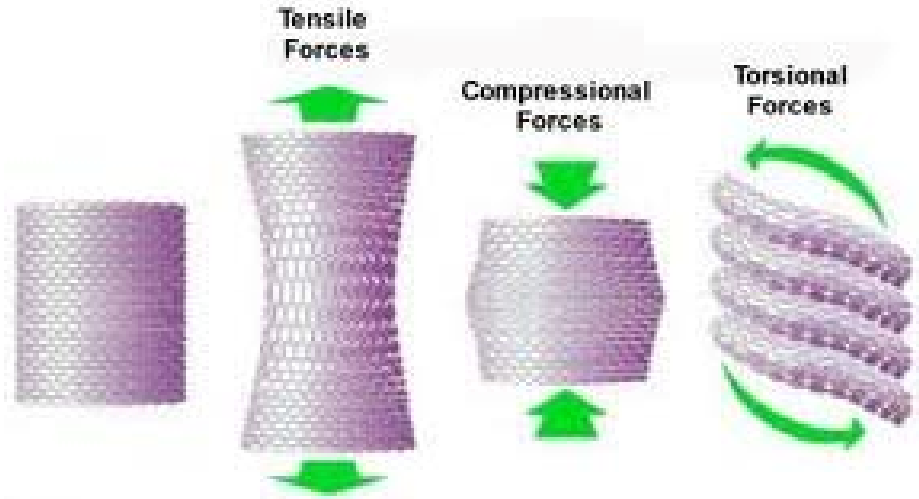
Tensile
Forces
Compressional
Forces
Torsional
Forces

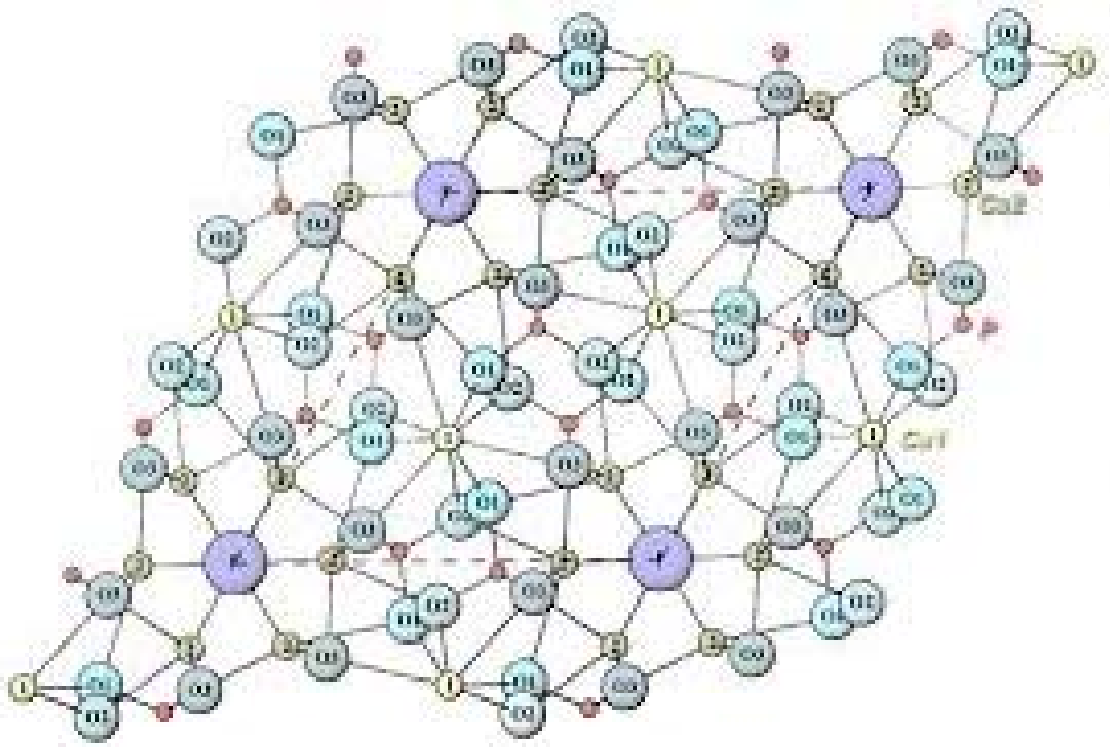

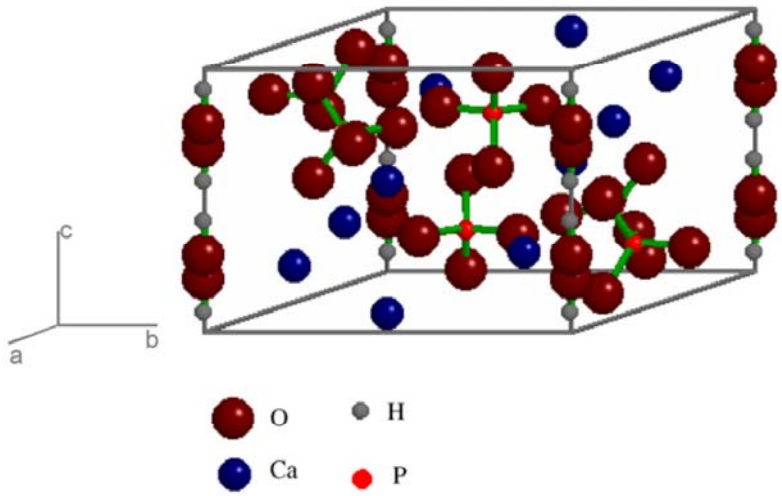

Figure 1: The unit cell of hydroxyapatite (45).

Dentin and Bone

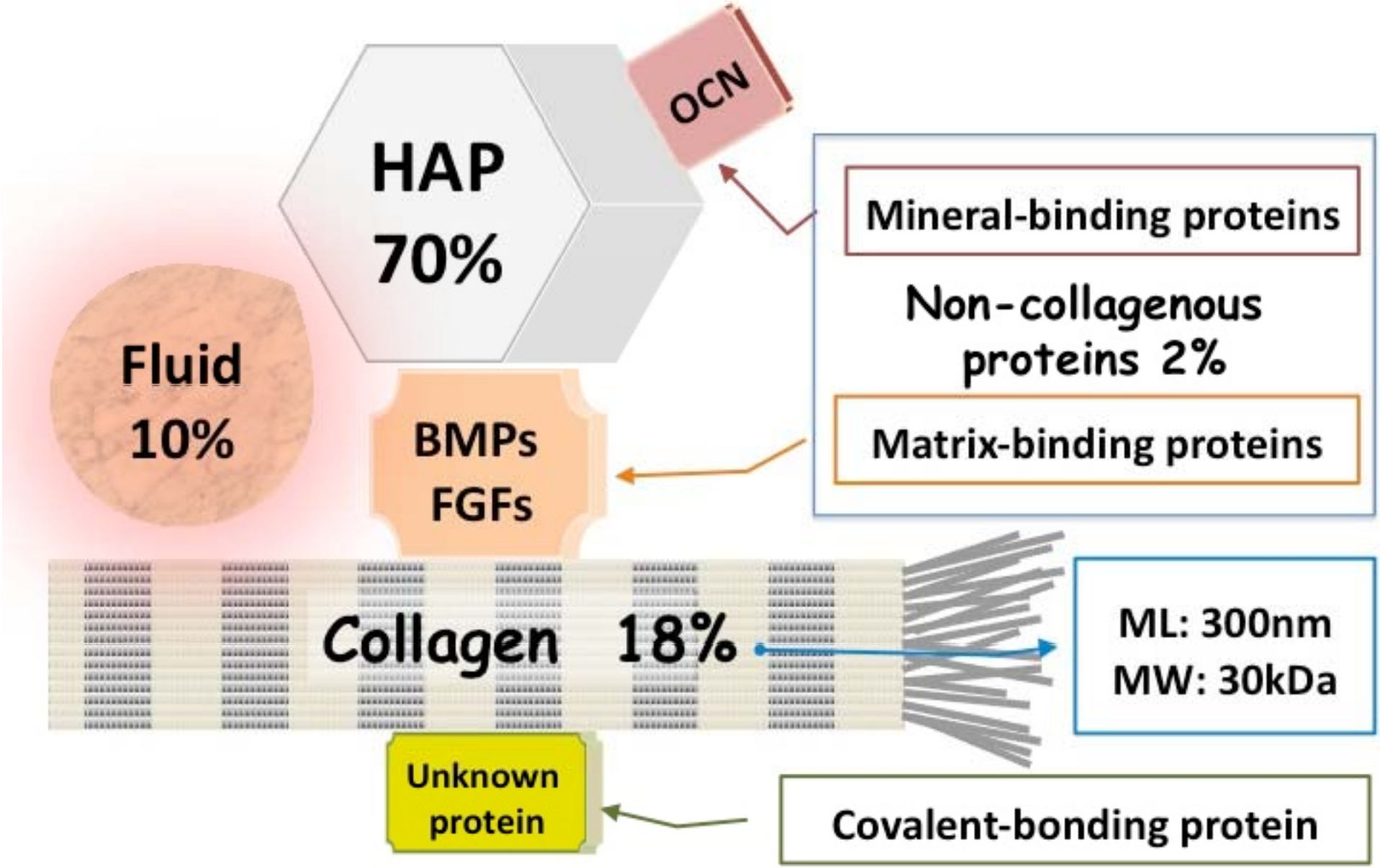

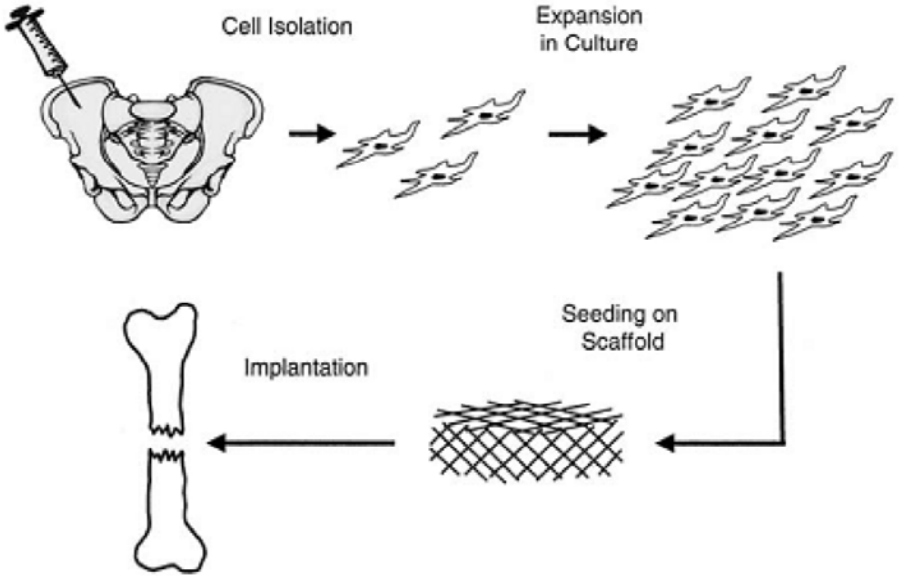

Figure 1. The Tissue Engineering Paradigm (19).

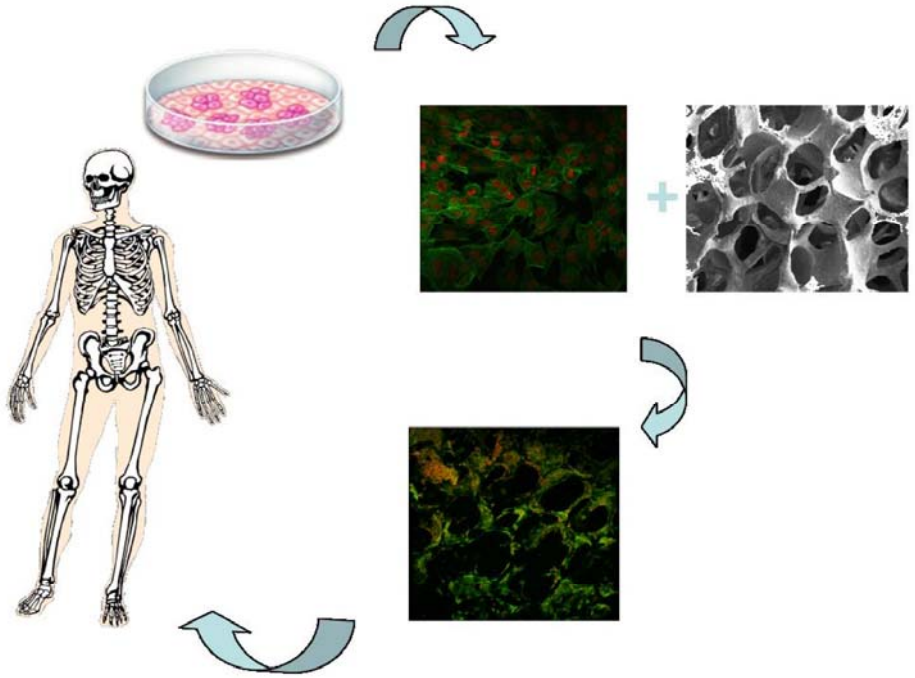

Schematic representation of cell based bone tissue engineering. A fraction of bone marrow obtained by biopsy from the patient will be harvested, and cells will be expanded in vitro. The cells will then be seeded on adequate scaffolds and further cultured, eventually being led to express adequate phenotypic character. The tissue engineering construct will then be implanted back to the patient to heal the bone defect.

Case Study 1

Ceramic based granular structures for bone tissue engineering and drug delivery

T.E.M. Images of HA nanocrystals

INEB

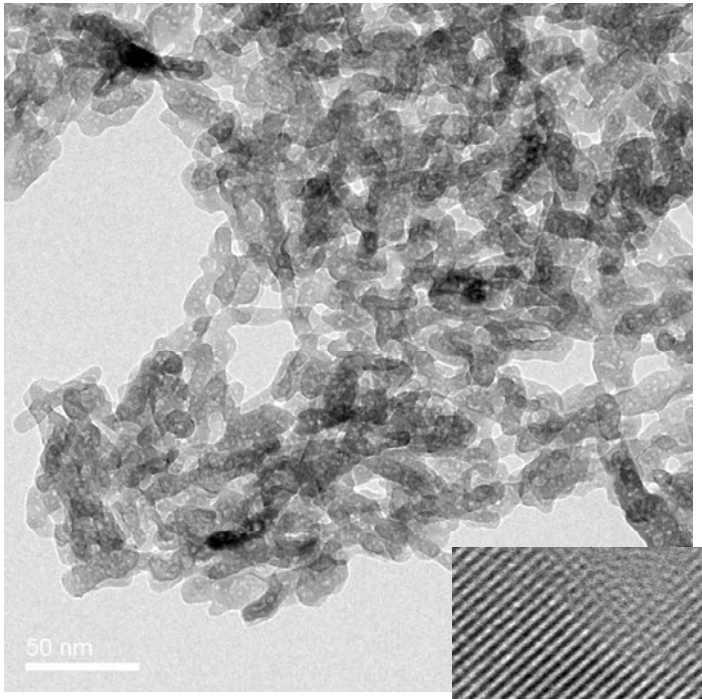

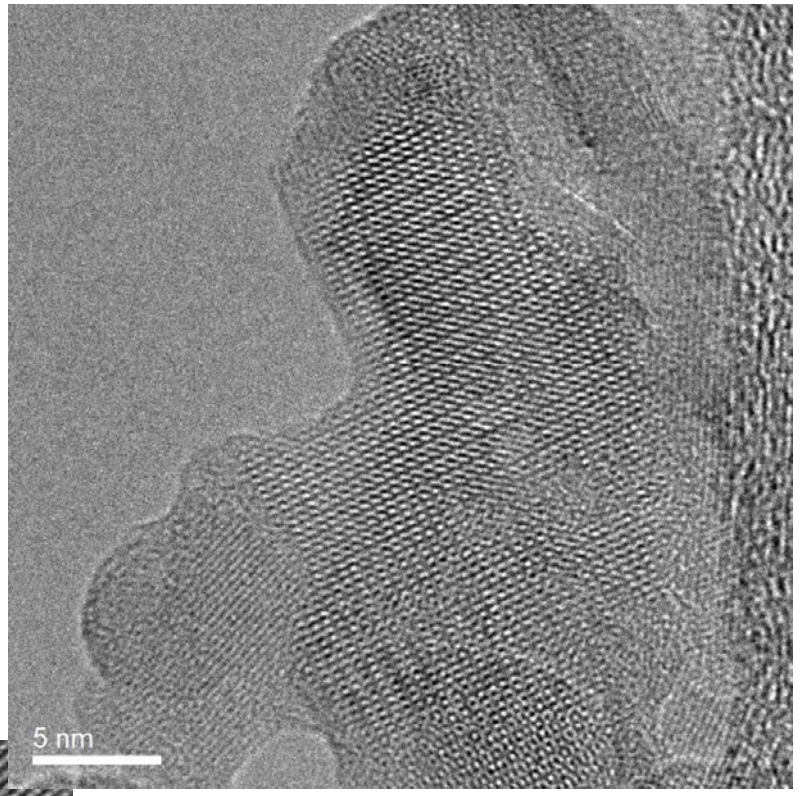

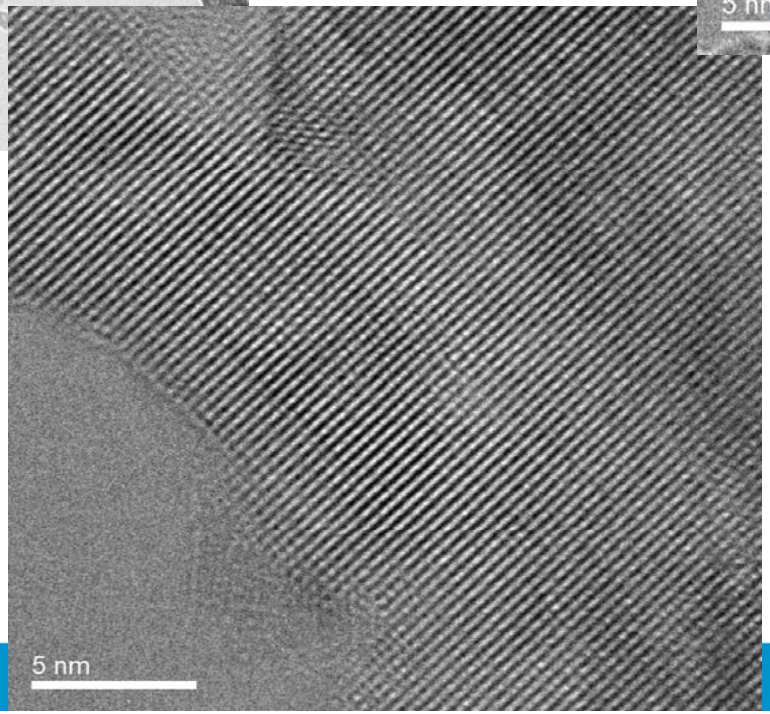

HRTEM (Un. TEXAS (Austin)
NanoXIM GEL Fluidinova S.A.

nanophased HA agglomerates after spray drying

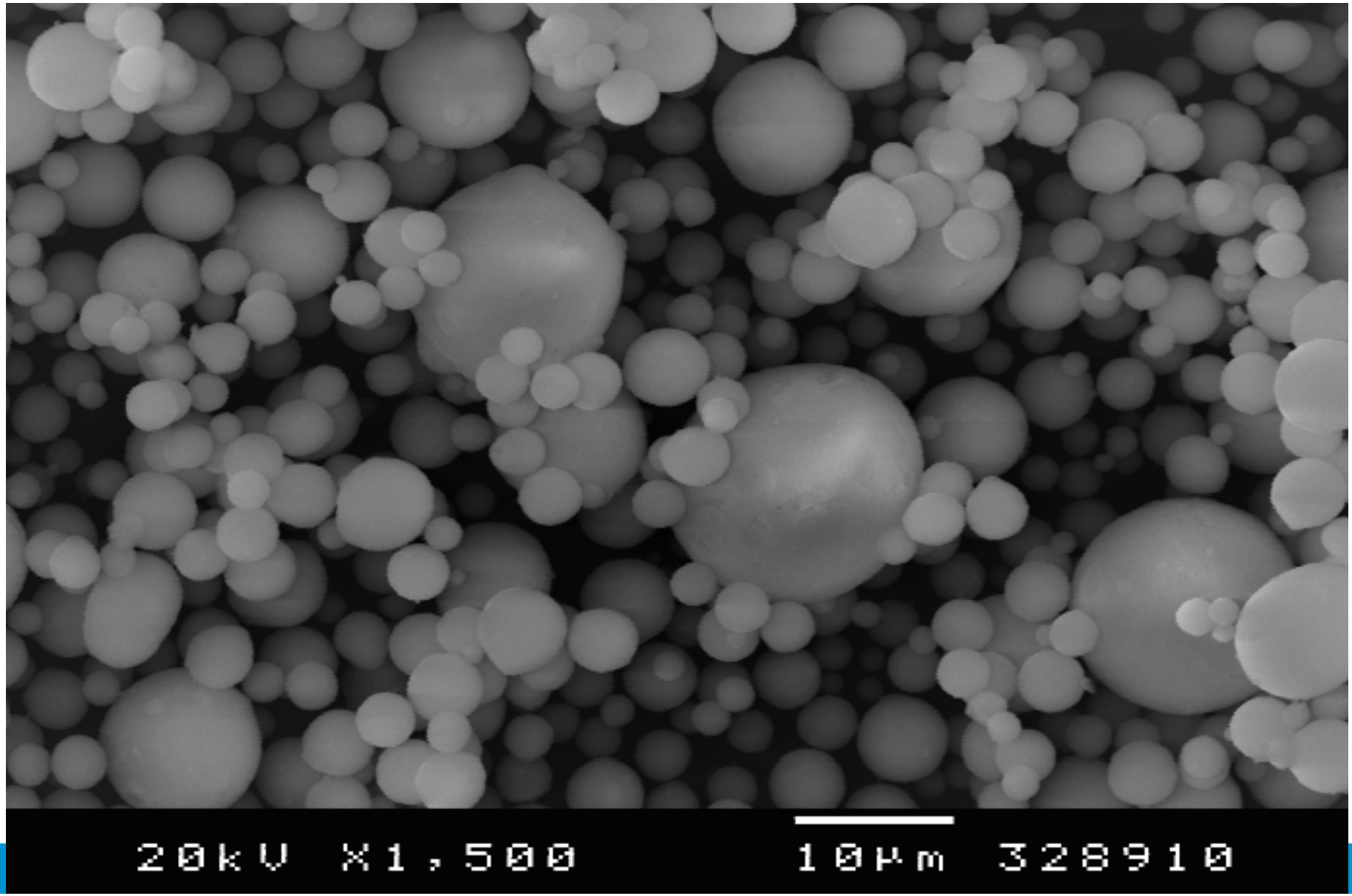

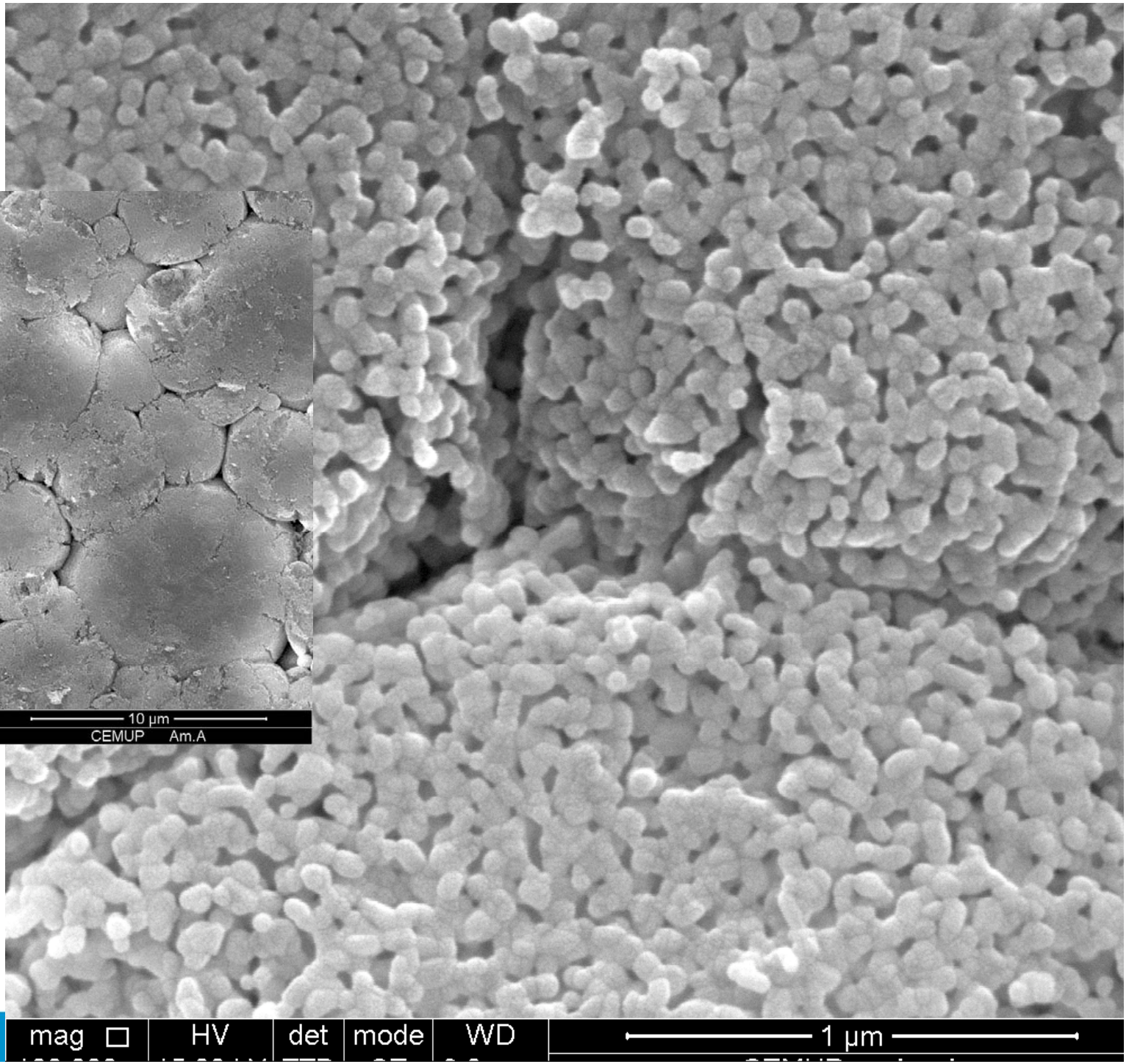

NanoHA

sintered at 830ºC
(2D disks)

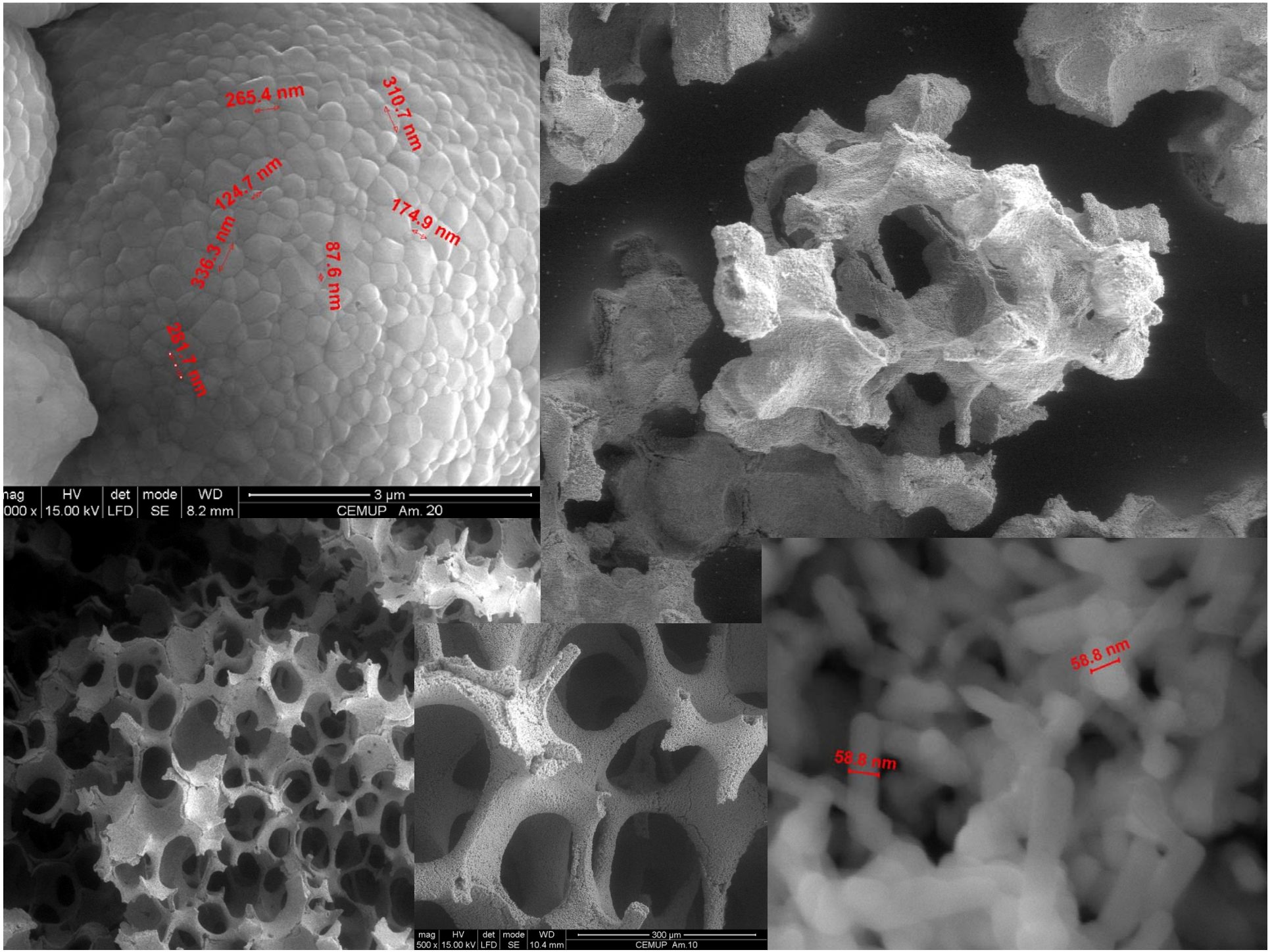
265.4 nm
310.7 nm
124.7 nm
174.9 nm
336.3 nm
87.9 nm
281.7 nm
mag HV det mode WD
000 x 15.00 kV LFD SE 8.2 mm
3 µm
CEMUP Am. 20
58.8 nm
58.8 nm
mag HV det mode WD
500 x 15.00 kV LFD SE 10.4 mm
300 µm
CEMUP Am.10

Biological *in vitro* studies on 2D and 3D nanoHA structures

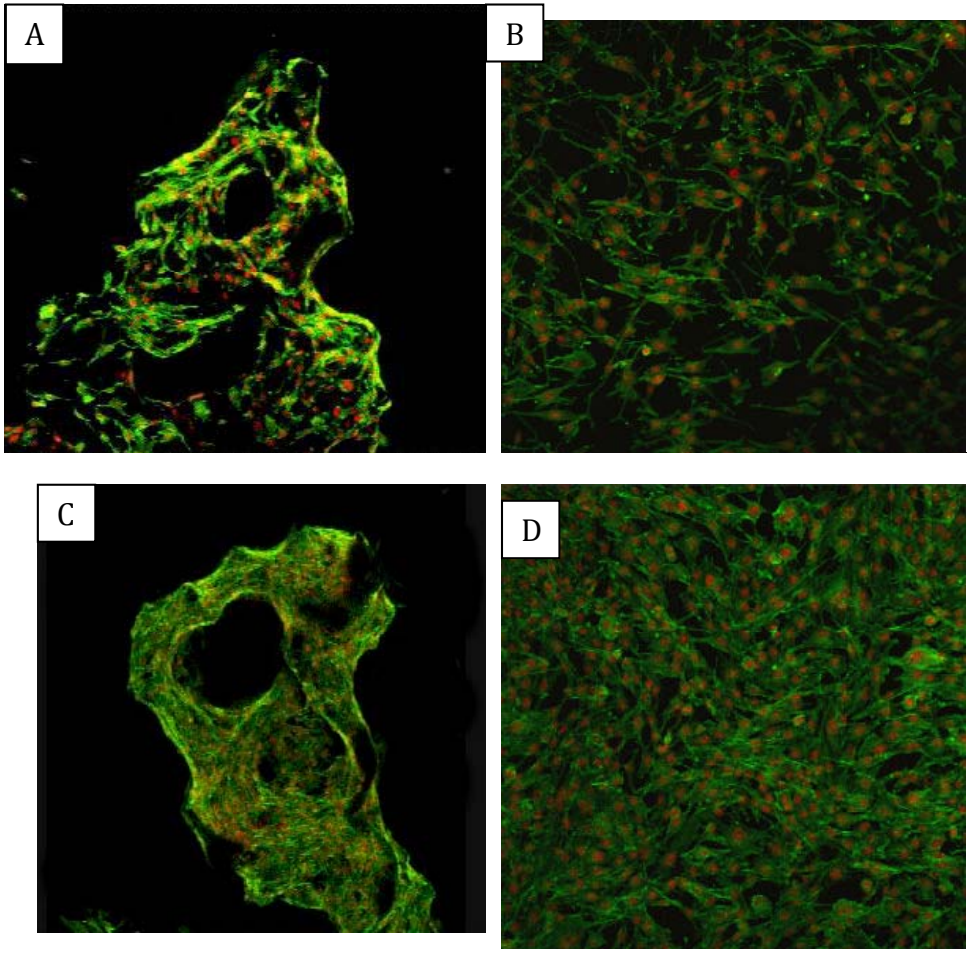

– Confocal Microscopy images of MG-63 Cultures on granules and disks after 3 days (A,B) e 6 ddays (C,D).

Biological *in vitro* studies on 2D and 3D nanoHA structures

A- Alkaline phosphatase activity on granules and disks after 6 days
B – Genetic expression of MG-63 on granules and disks after 6 days

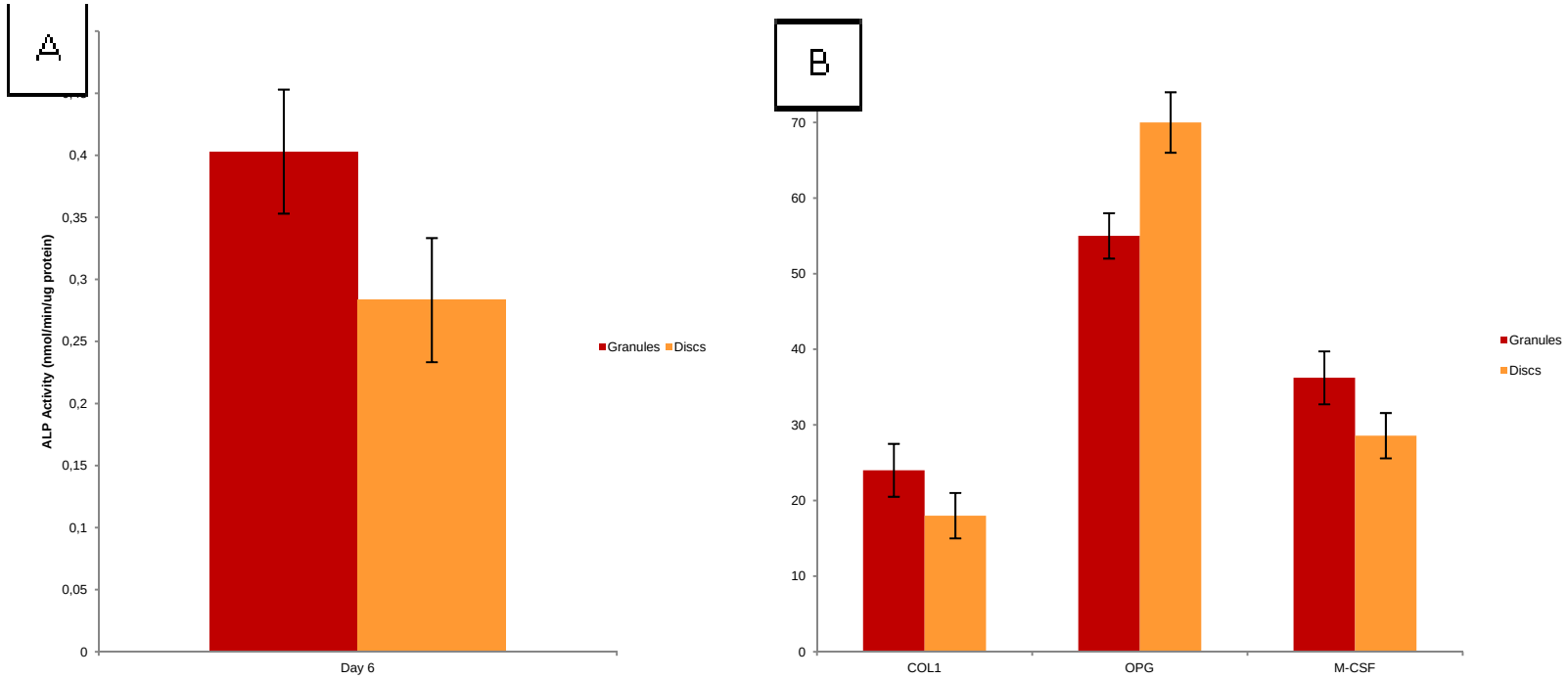

nanoHA granules in contact with Endothelial cells and osteoblasts

Marta Laranjeira

Mª Helena Fernandes

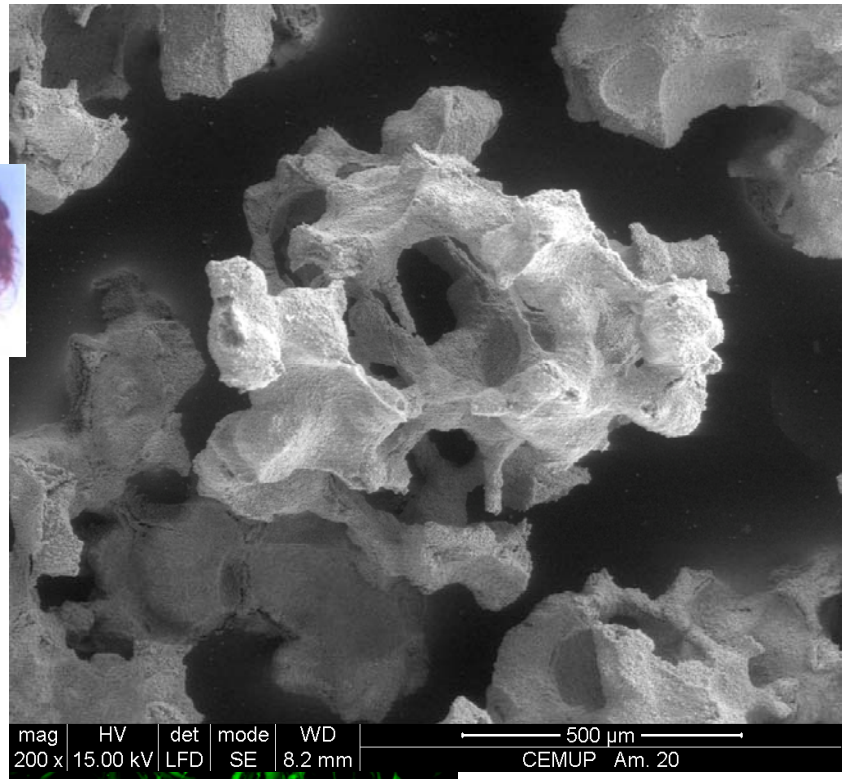

Confocal microscope images of 7d days co-culture of endothelial cell, and osteoblasts

Co-culture 7d

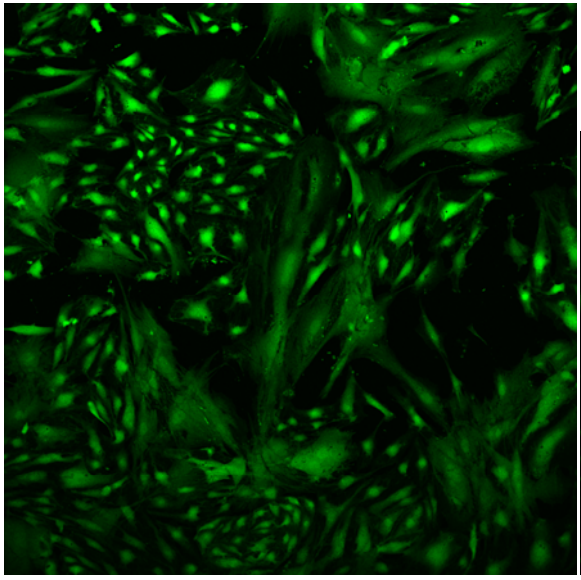

Osteoblasts

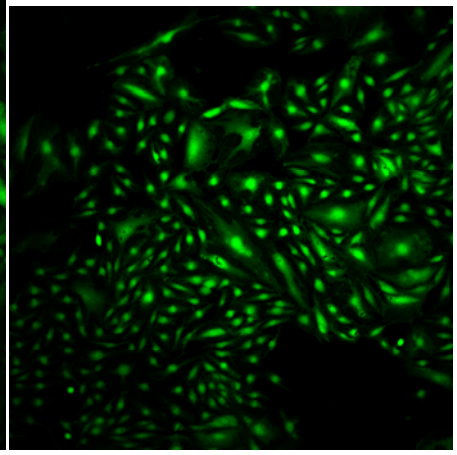

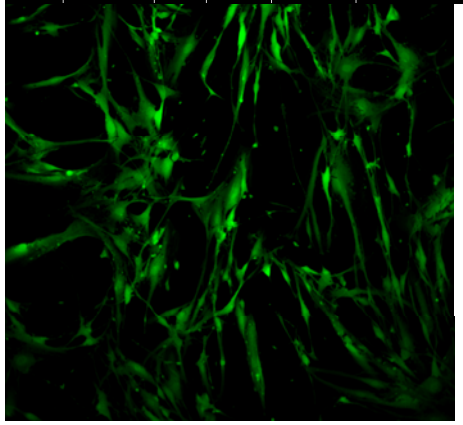

Endothelial 7d

Endothelial 7d

in vitro Biological studies on Nano HA porous granules of HbmMSC's and endothelial cells.

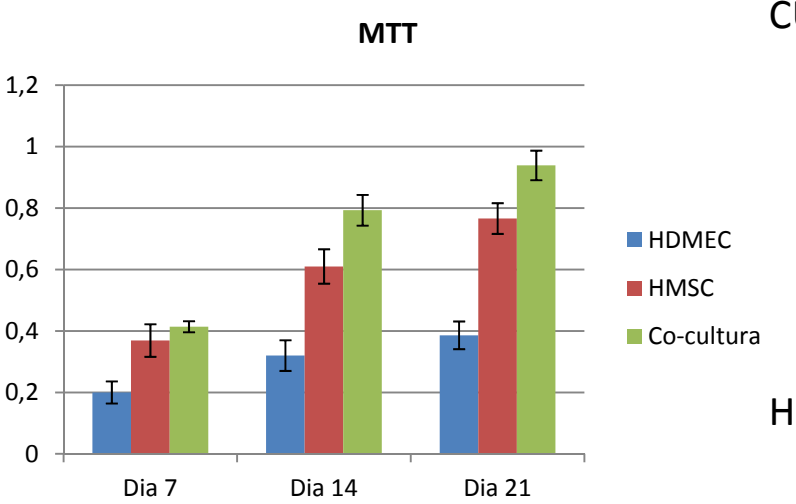

Day 21

CO-CULTURE

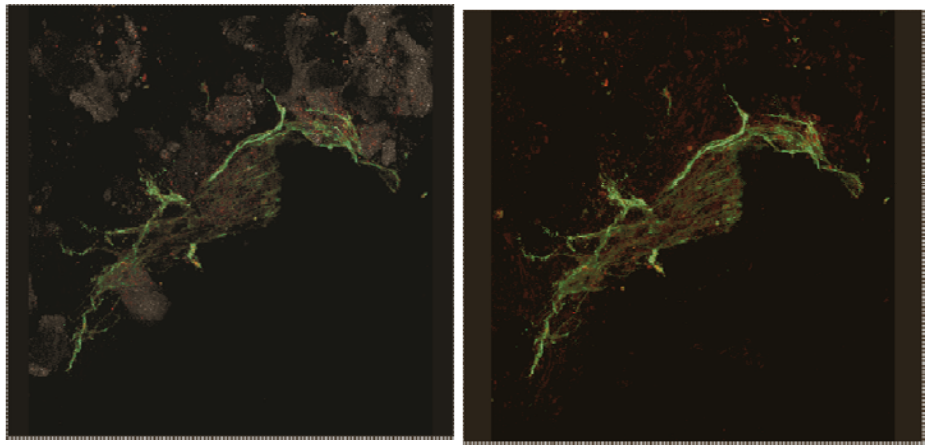

Day 21

HDMEC

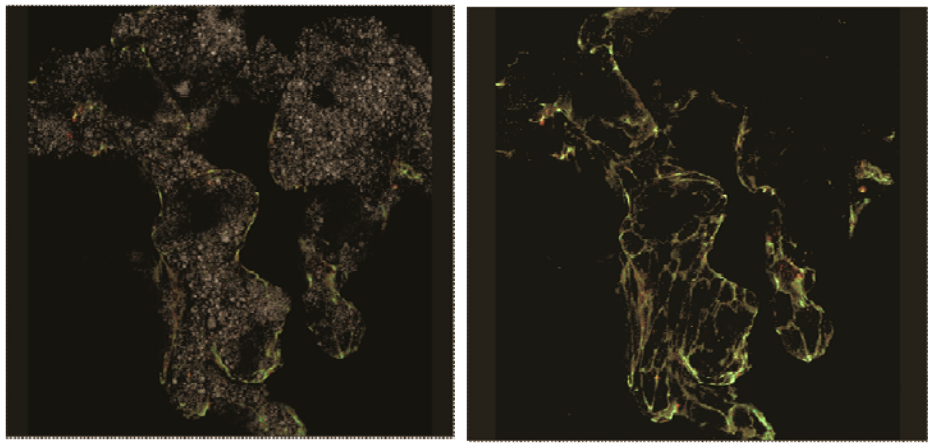

Day 21

HMSC

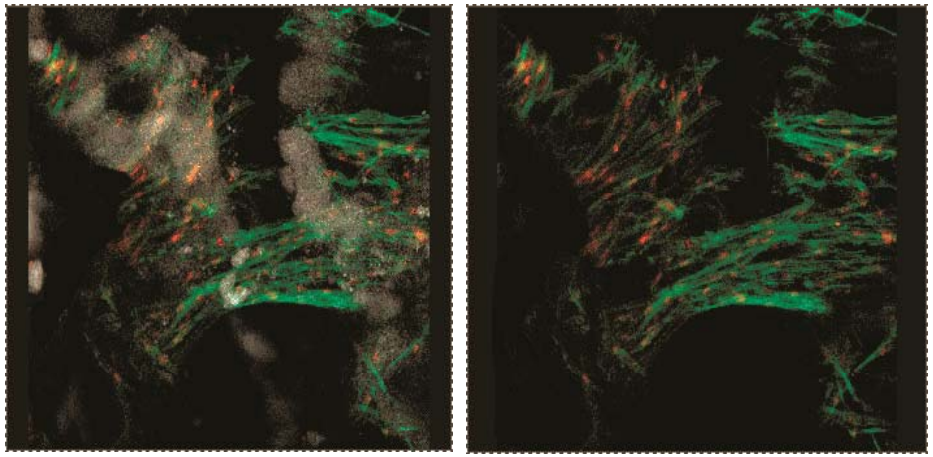

HDMEC e HMSC in monoculture e co-culture on granules after 21

INEB

Co-culture
Day 21

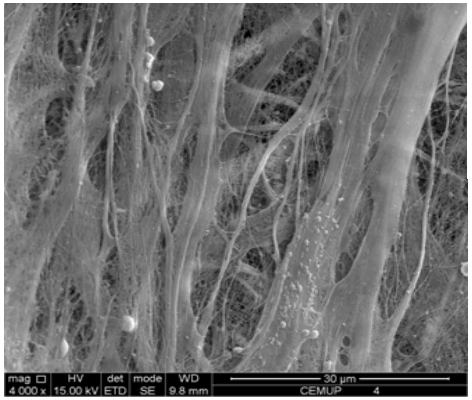

HDMEC
Day 21

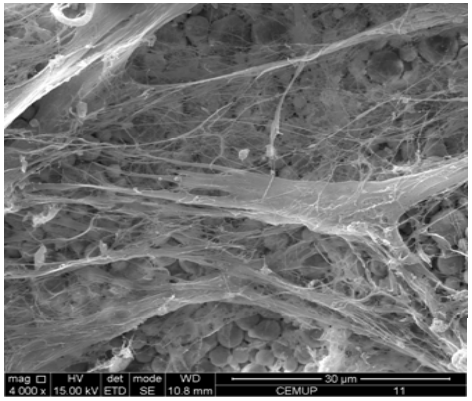

HMSC
Day 21

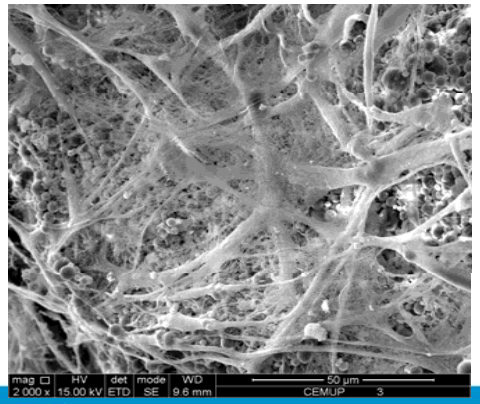

NanoHA granules provide adequate environment for adhesion. migration and differentiation of endothelial and HbmMSC, showing to be a promising material for bone regeneration

HDMEC e HMSC in monoculture e co-culture on granules after7,14 and 21 days

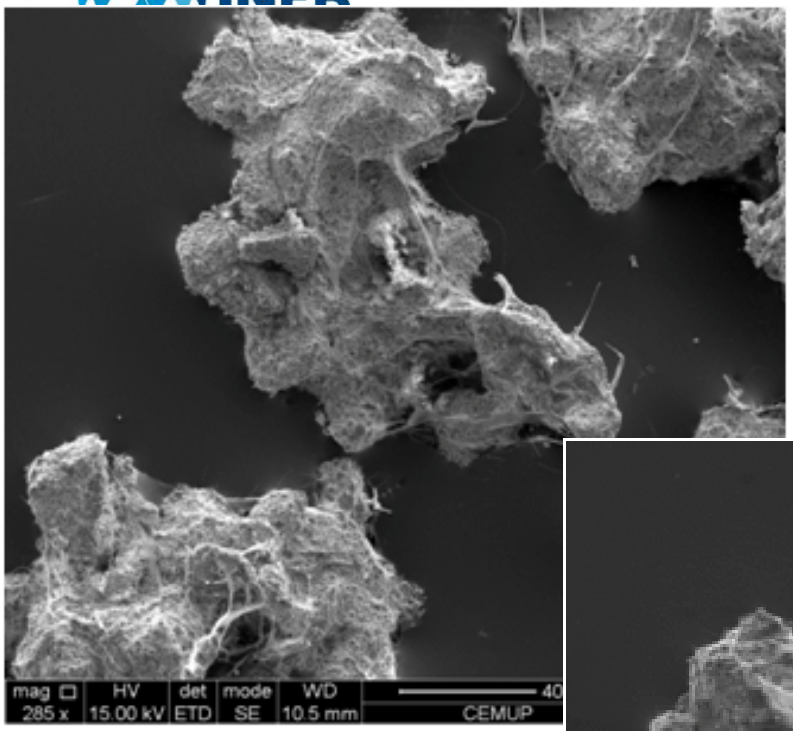

7 days

14 days

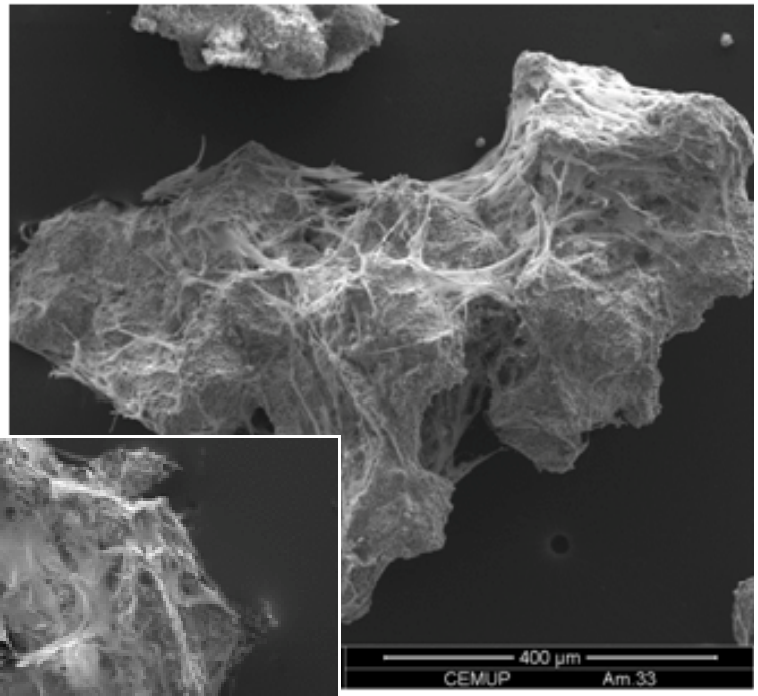

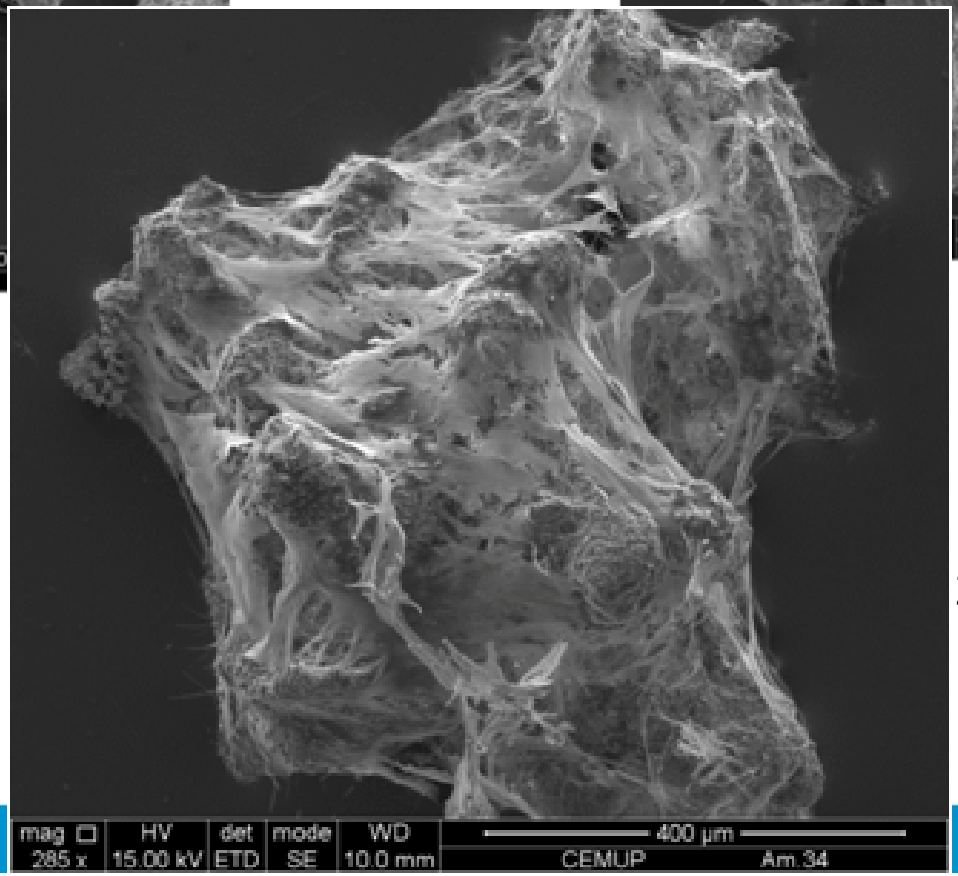

21 days

Osteomyelitis

S. aureus **infection**

↓

Osteomyelitis

↓

Bone necrosis

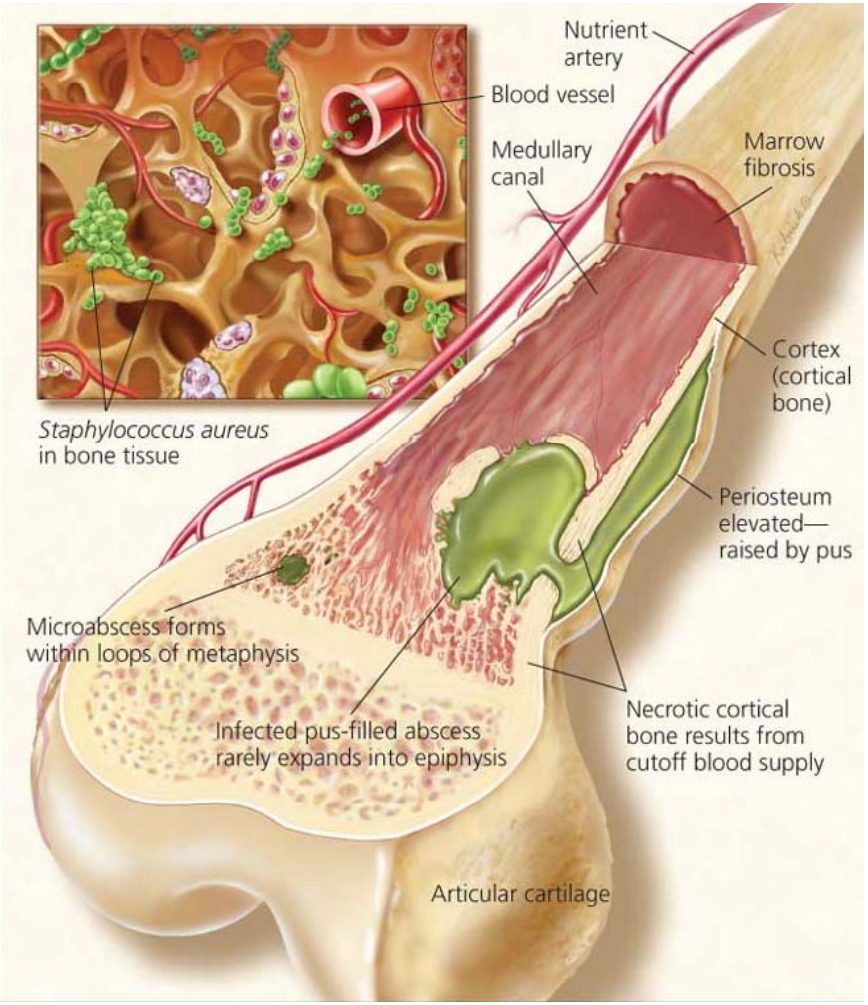

Illustration of hematogenous osteomyelitis in a tubular bone (Kibiuk, 2010).

Hydroxyapatite/ Collagen Scaffolds

Viviane Gomide/Susana Sousa/ Nuno Alegrete

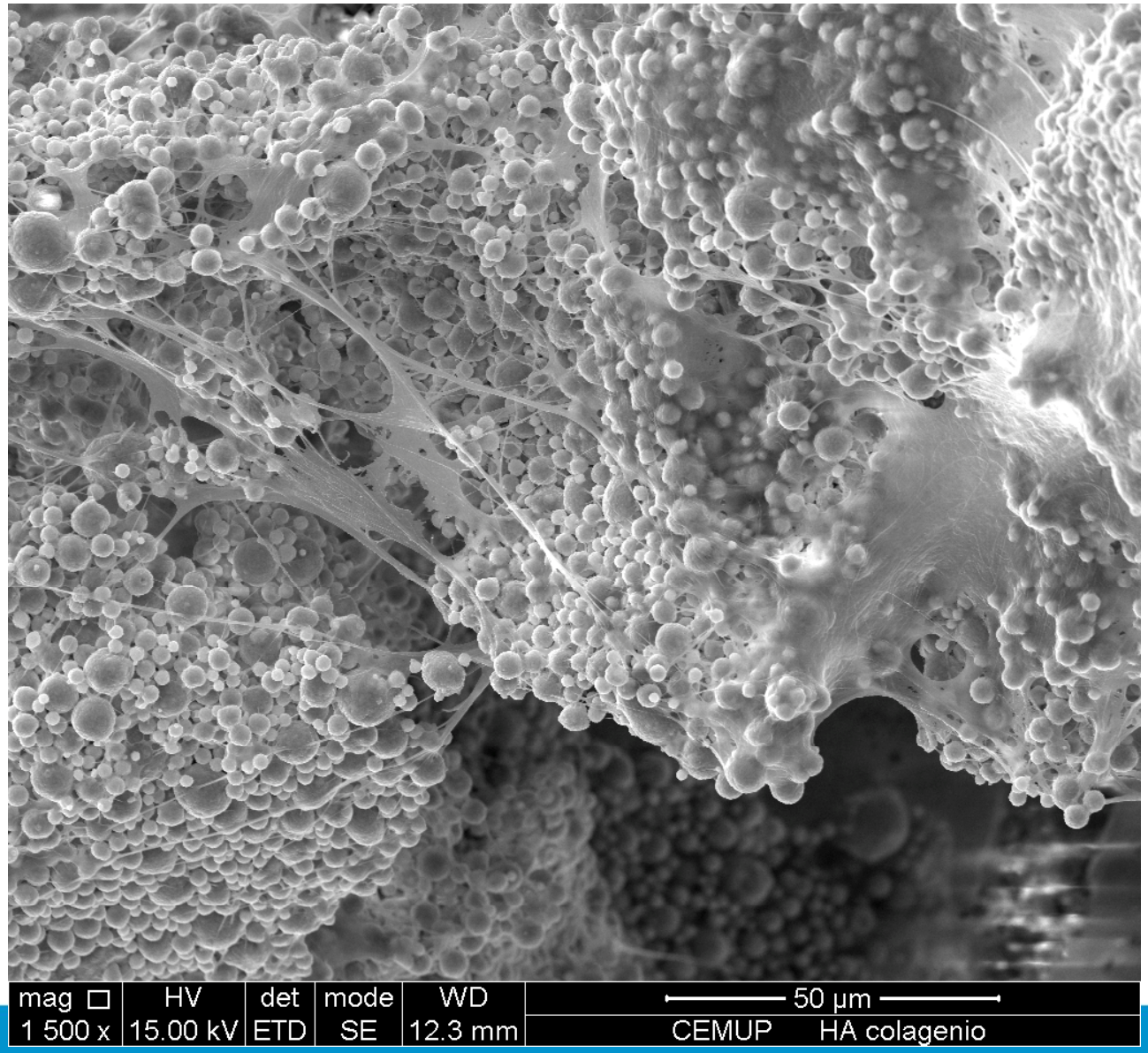

Hydroxyapatite/ Collagen scaffold

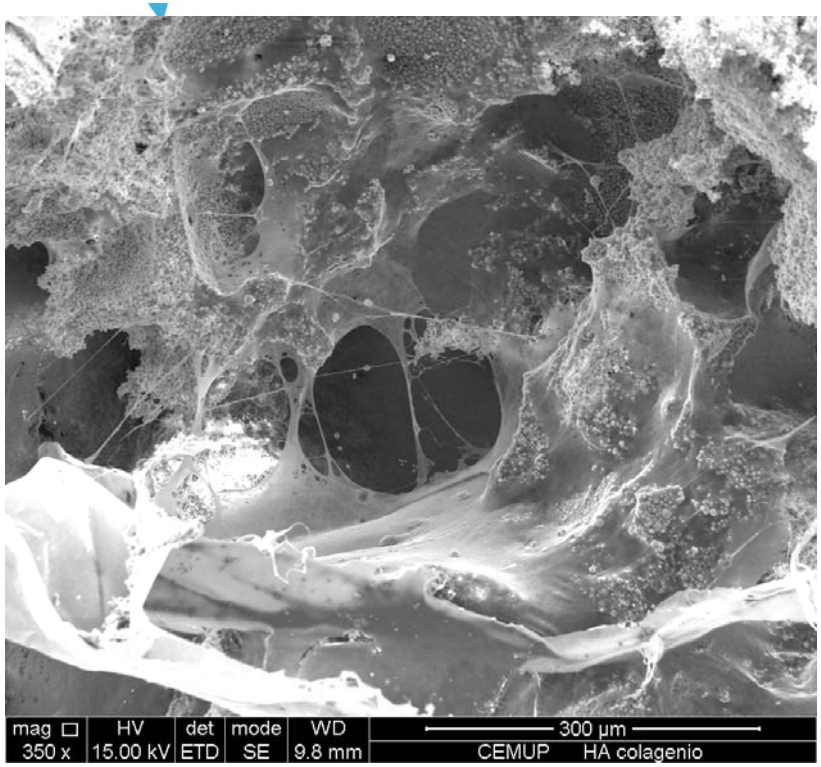

Polyurethane Sponges were impregnated with slurries
containing ceramics (mixtures of water, HA and surfactant) and heat-treated

Type I collagen solution was prepared from bovine Aquiles tendon , empregnating the HA sponges

Collagen was crosslinked with a mixture of N-(3-dimetilaminopropil)-N'-etilcarbodiimide hydrocloride (EDC)
and N-hydroxisuccinimide (NHS)

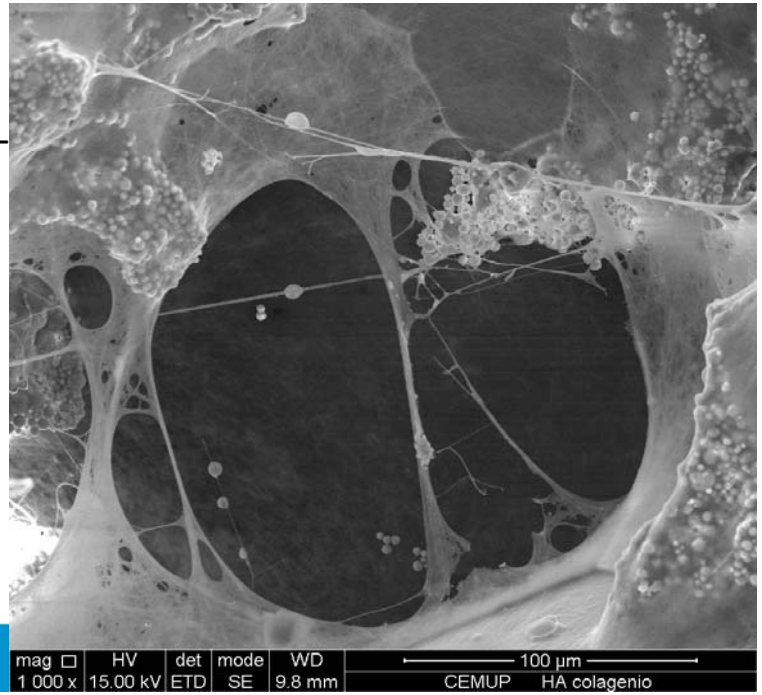

Our strategy

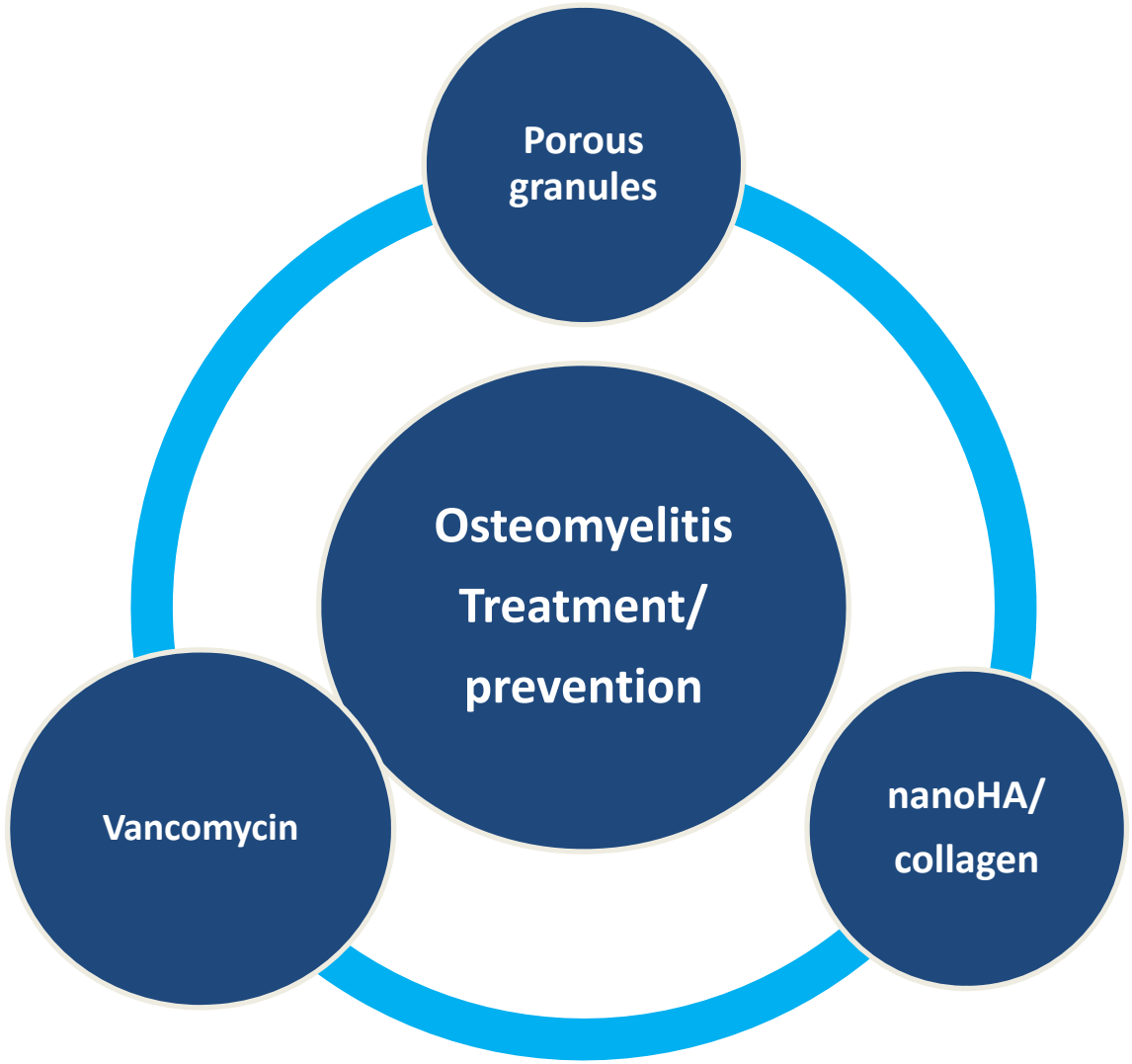

Osteomyelitis

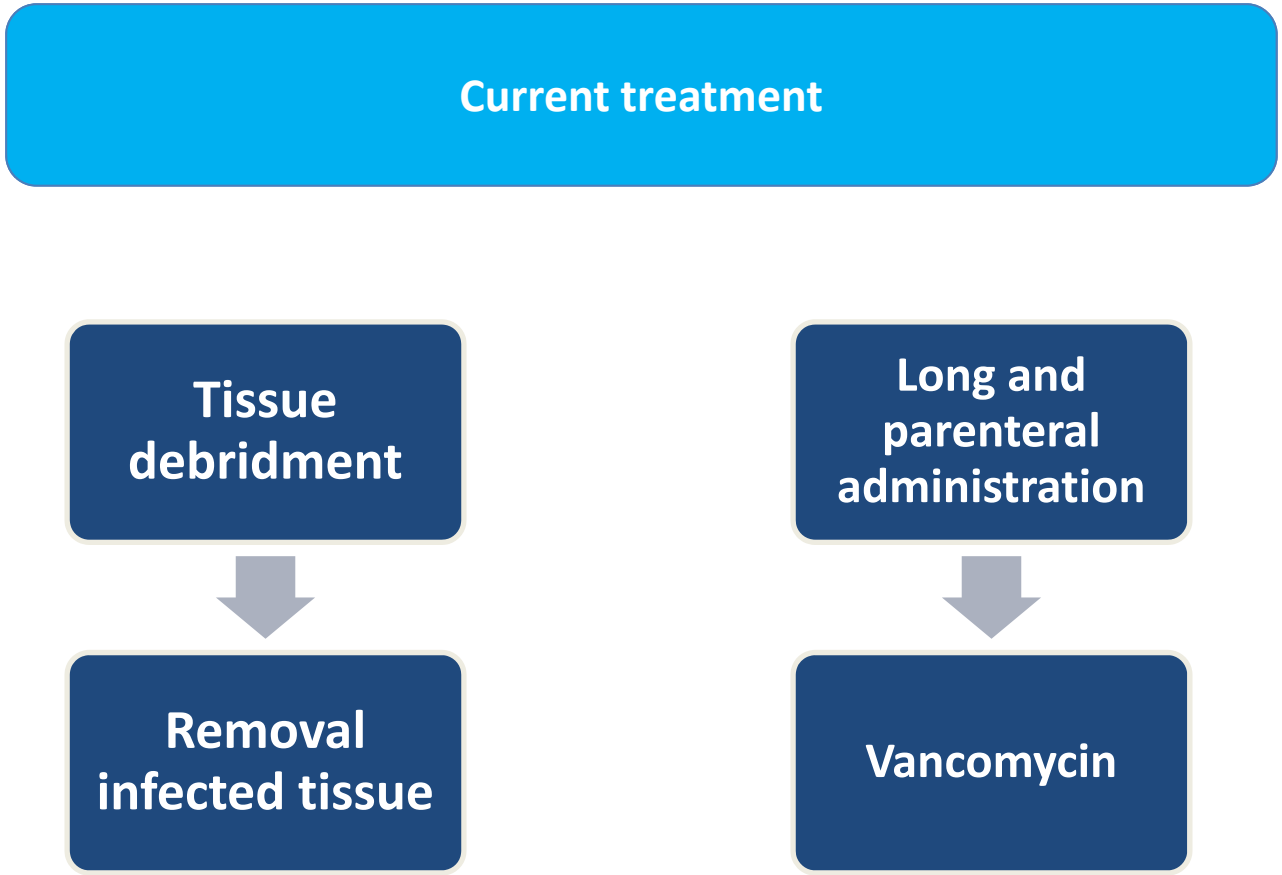

Organisms frequently isolated from osteomyelitis cases based on patient age. Adapted from (11).

Organisms Frequently Isolated in Osteomyelitis Based on Patient Age		
Infants (<1 year)	**Children (1 to 16 years)**	**Adults (>16 years)**
Group B streptococci	*Staphylococcus aureus*	*Staphylococcus epidermidis*
Staphylococcus aureus	*Streptococcus pyogenes*	*Staphylococcus aureus*
Escherichia coli	*Haemophilus influenzae*	*Pseudomonas aeruginosa*
		Serratia marcescens
		Escherichia coli

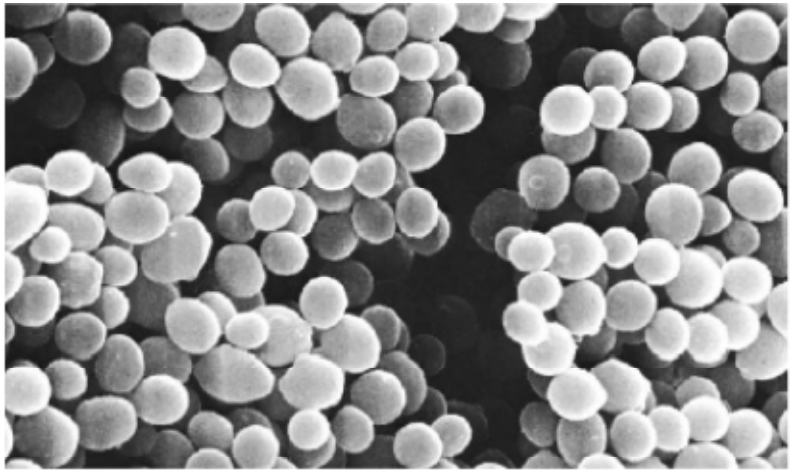

Scanning Electron Microscopy (SEM) depicted numerous clumps of *S. aureus*. 32000x magnification

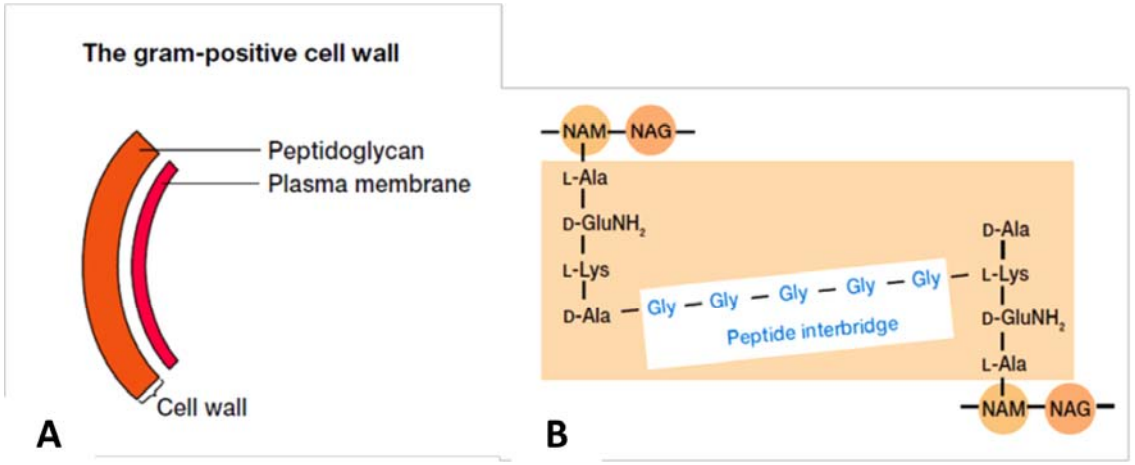

Figure 1: Characteristic gram-positive cell wall and *S. aureus* peptidoglycan. (A) The gram-positive cell wall. (B) *S. aureus* peptidoglycan. NAM: *N*-acetylmuramic acid. NAG: *N*-acetylglucosamine. Gly: Glycine.

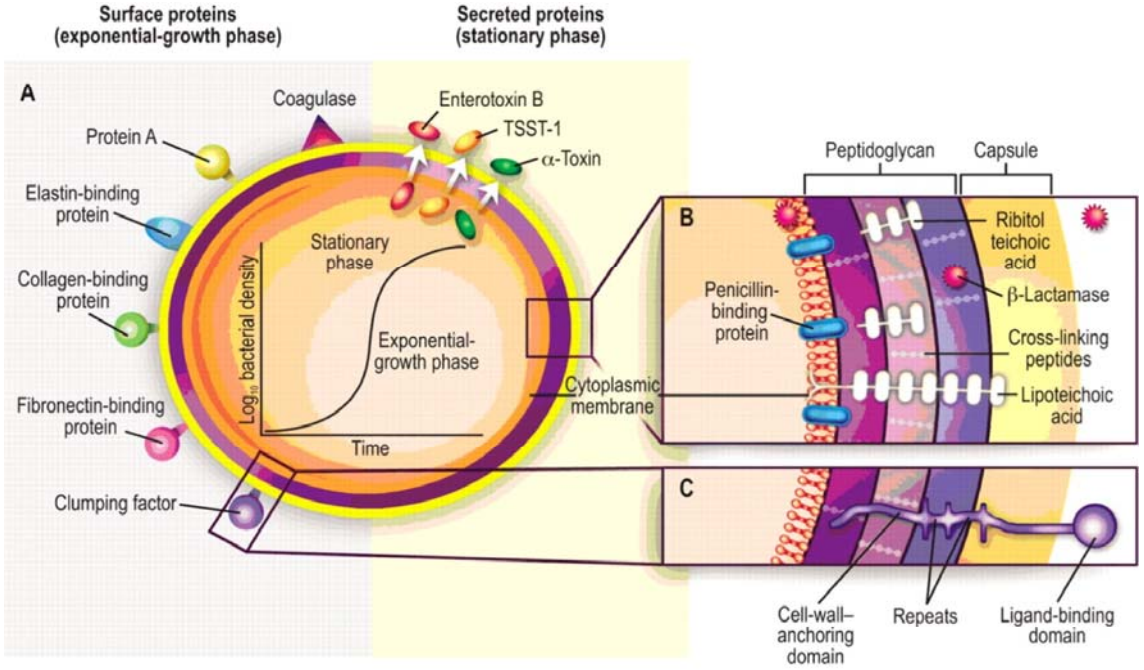

Figure 1: Pathogenic factors of *S. aureus*, with structural and secreted products both playing roles as virulence factors.
(A) Surface and secreted proteins. (B, C) Cross-sections of the cell envelope. TSST-1: toxic shock syndrome toxin 1

Vancomycin

Glycopeptide effective against *S. aureus;*

Low minimal inhibitory concentration (MIC, 1 µg/mL);

Low cytotoxicity for osteoblasts.

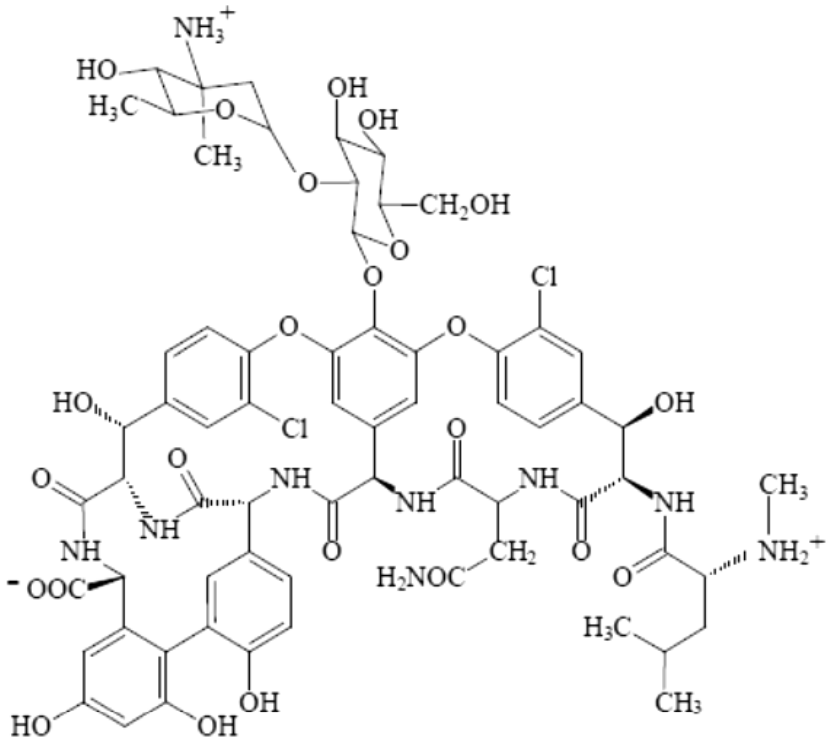

Chemical structure of vancomycin (Williams *et al*, 1999).

Novel approach for the treatment of Osteomyelitis

nanoHA and (nanoHA + Type I collagen composite) scaffolds for bone regeneration and for controlled release of Vancomycin

Patent application pending.

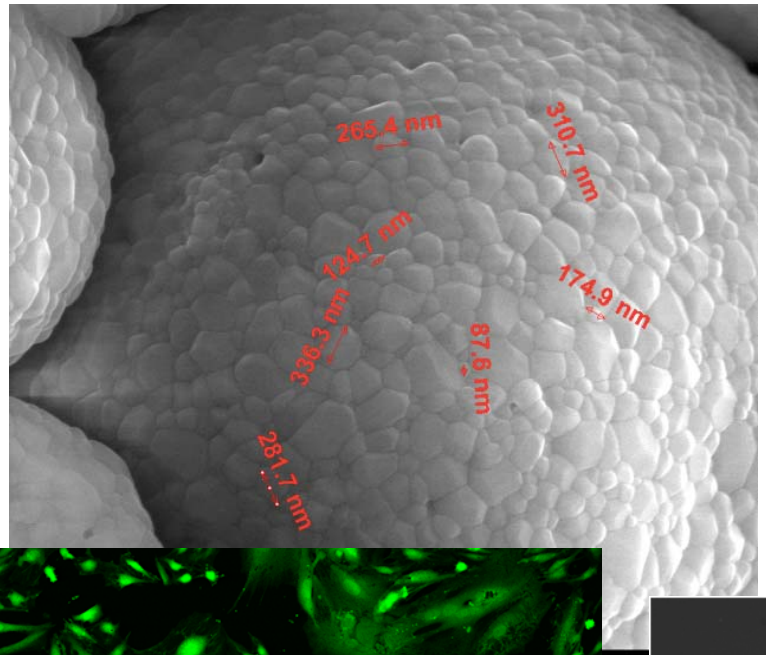

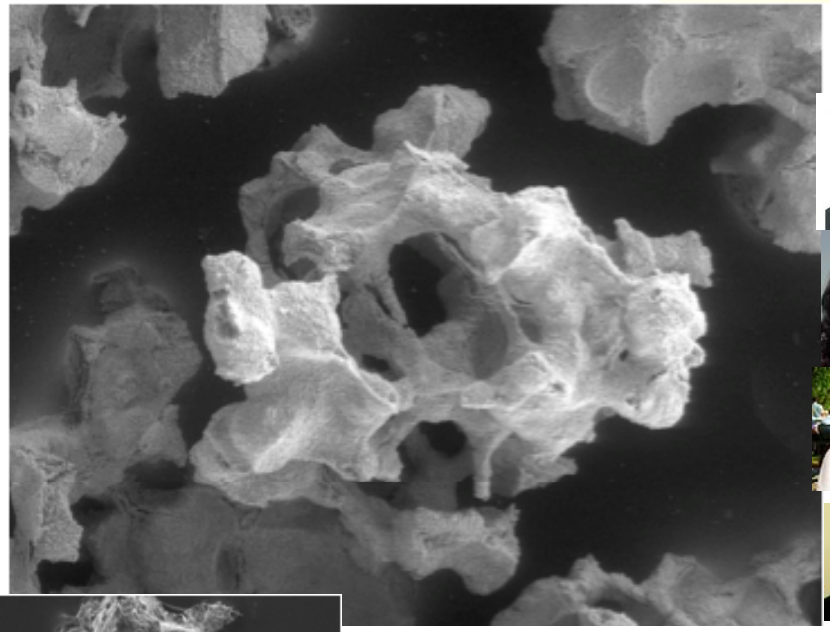

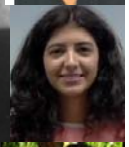

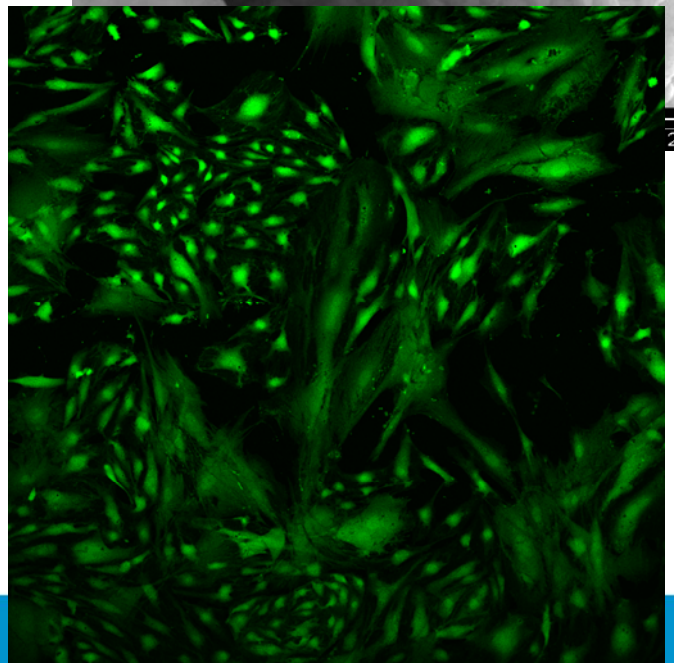

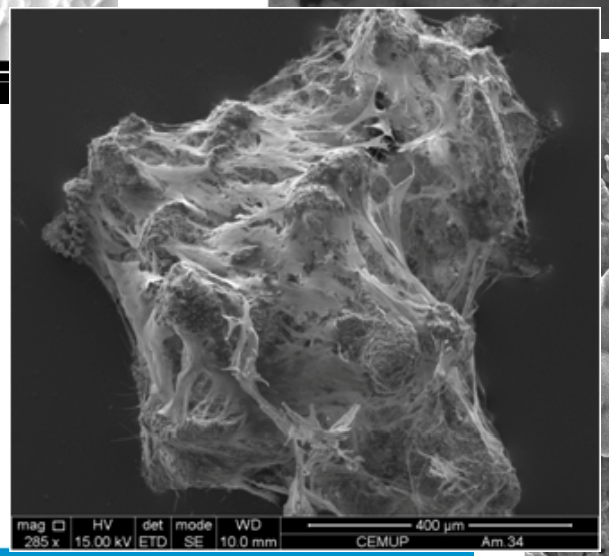

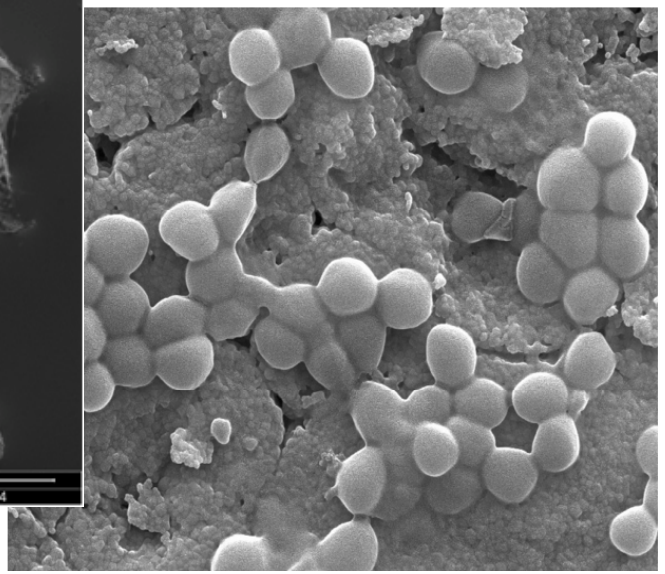

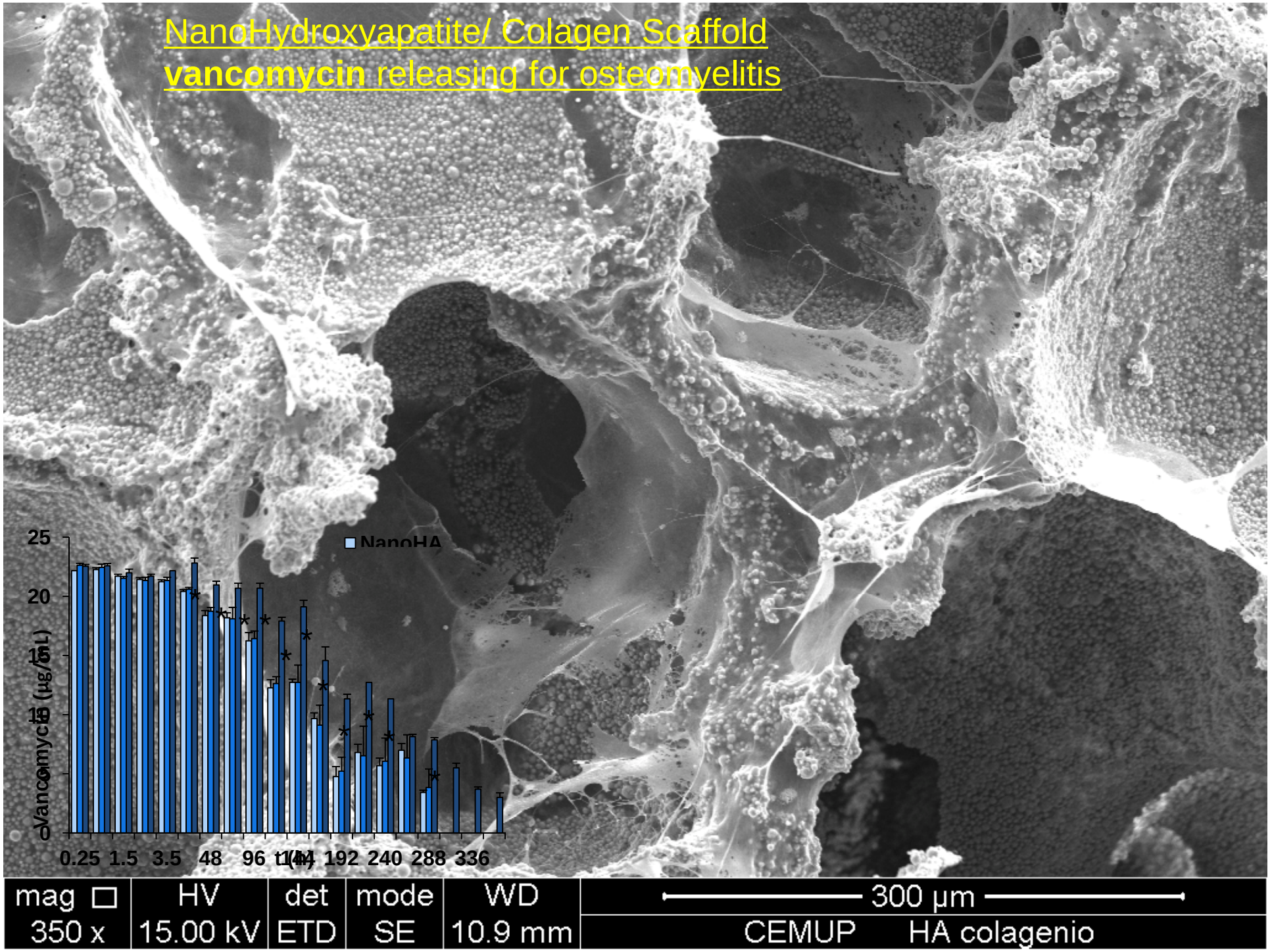
NanoHydroxyapatite/ Colagen Scaffold
vancomycin releasing for osteomyelitis
NanoHA
25
20
15
0
0.25 1.5 3.5 48 96 144 192 240 288 336
mag
350 x
HV
15.00 kV
det
ETD
mode
SE
WD
10.9 mm
300 µm
CEMUP HA colagenio

Bacterial adherence to nanoHA

Maria Pia Ferraz, Liliana Grenho, Marta Ribeiro

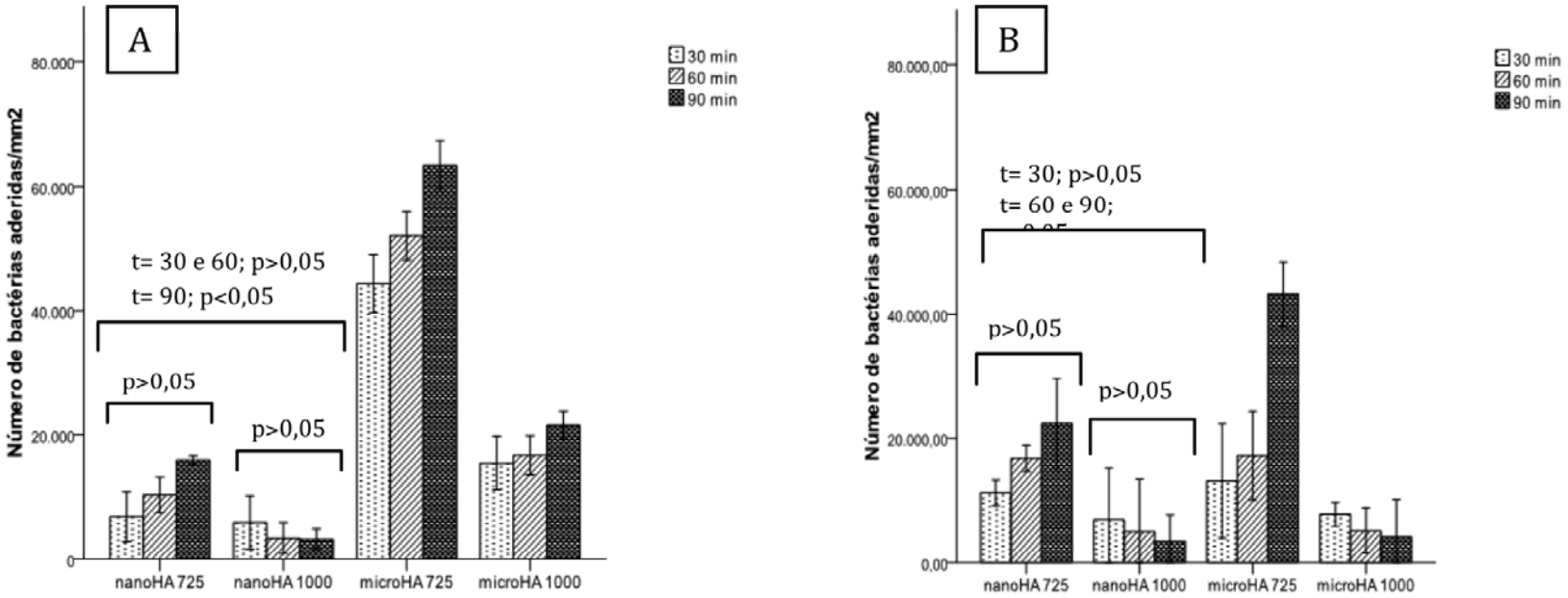

Two examples of the number of adherent bacteria per mm^2 for each material at different adhesion times (p-value according to Turkey HSD test).

S. aureus ATCC 25923

S. aureus MRSA isolated from an orthopaedic infection

Bacterial adherence to nanoHA

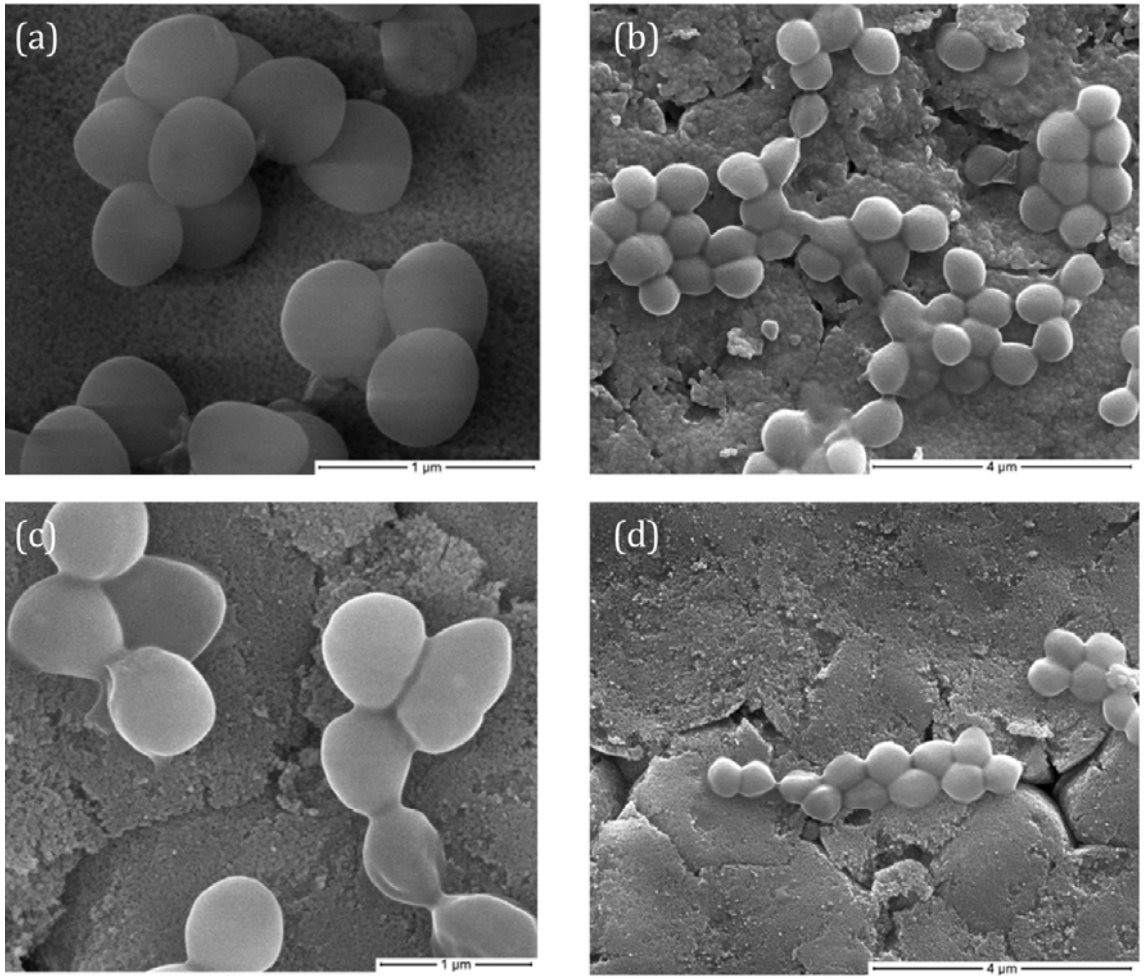

SEM images with bacteria showing lack of
slime production (a) and slime production (b, c and d).
S. aureus ATCC 25923 on nanoHA 725 at 90 min
S. aureus MSSA isolated from an orthopaedic infection
on nanoHA 1000 at 60 min
S. epidermidis RP62A on nanoHA 725 at 60 min
S. aureus MRSA isolated from an orthopaedic infection
on nanoHA 725 at 60 min

Influence of the presence of proteins on bacterial adherence to nanoHA

Graphs showing the influence of adsorbed FBS on the adhesion of *S. aureus* MSSA (A)and *S. aureus* MRSA (B) to nanoHA sintered at 725°C and at 1000°C.

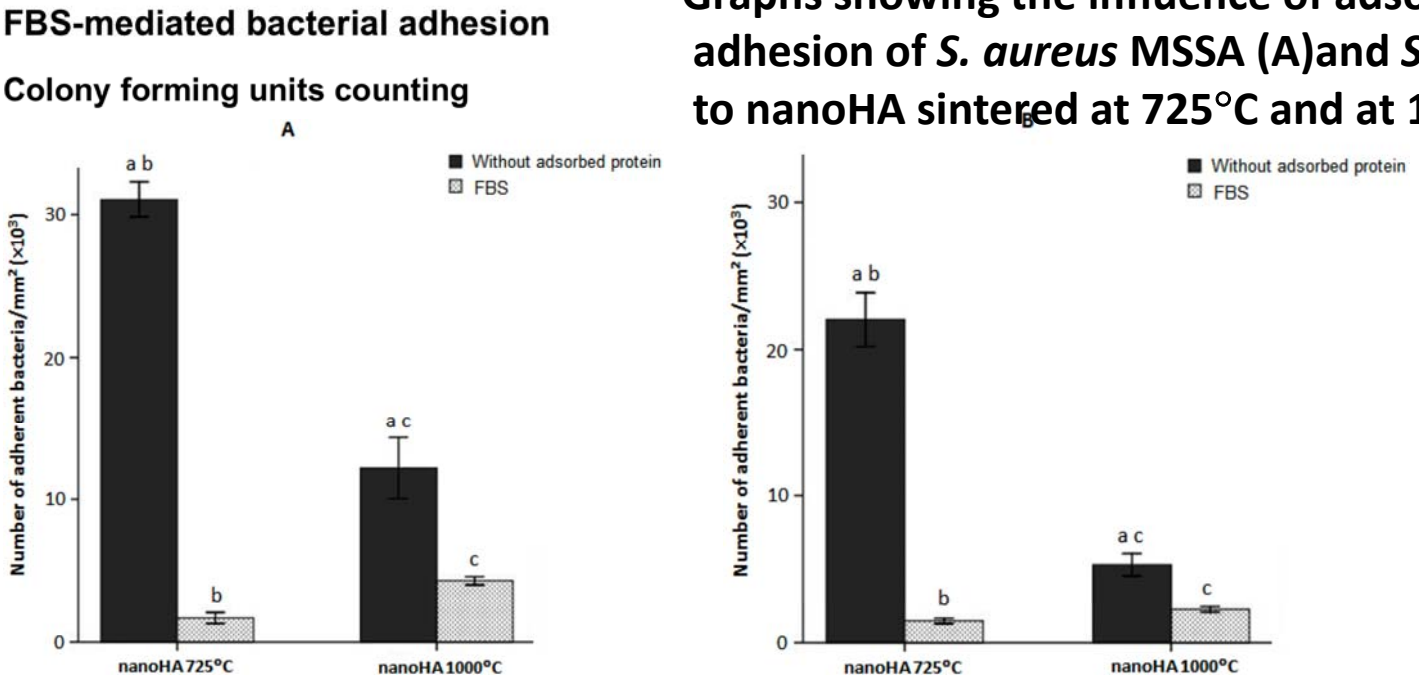

Influence of the presence of proteins on bacterial adherence to nanoHA

influence of adsorbed FBS on the adhesion of *S. epidermidis* RP62A (C) and S. epidermidis ORT (D) to nanoHA sintered at 725°C and at 1000°C.

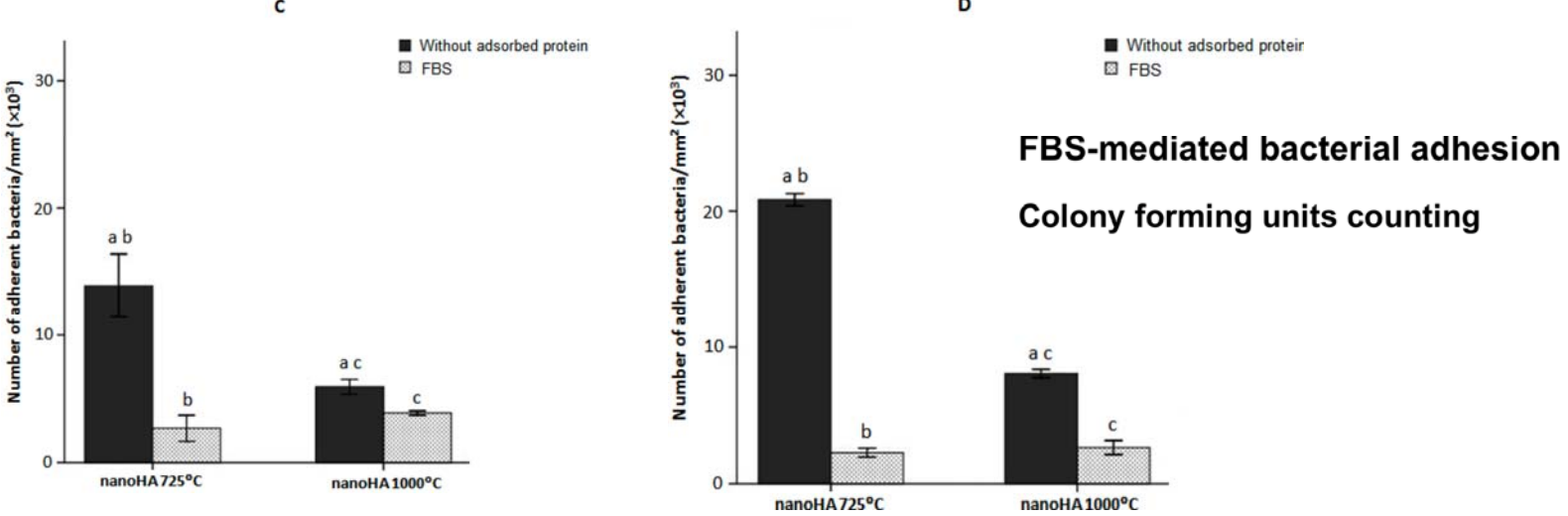

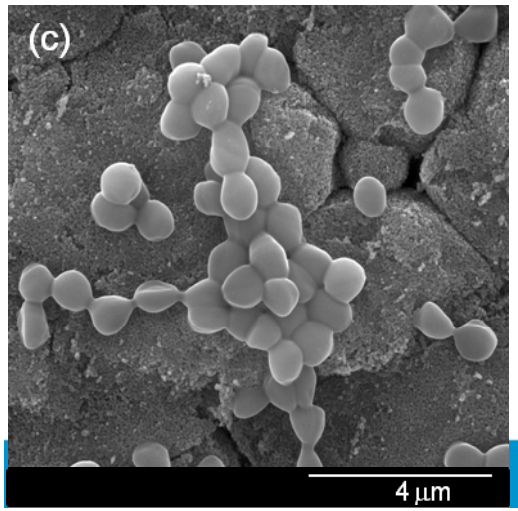

control

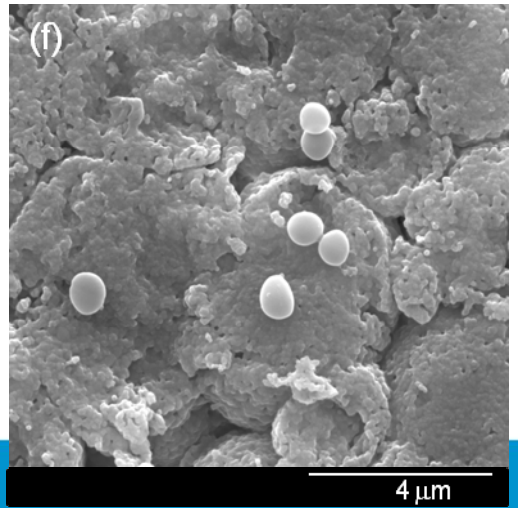

FBS

Vancomycin effect on MC3T

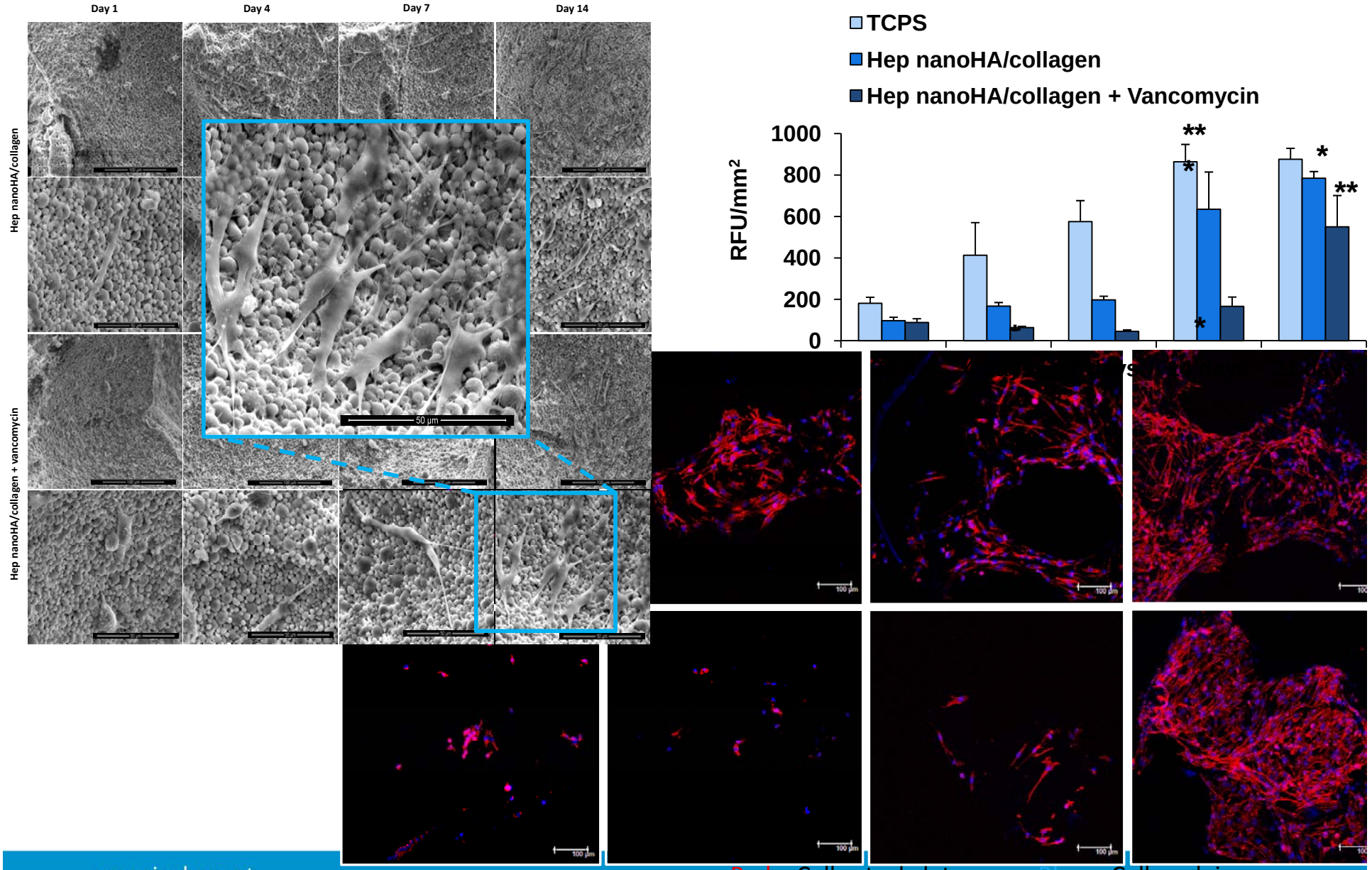

Red – Cell cytoskeleton Blue – Cell nuclei

Granules characterization

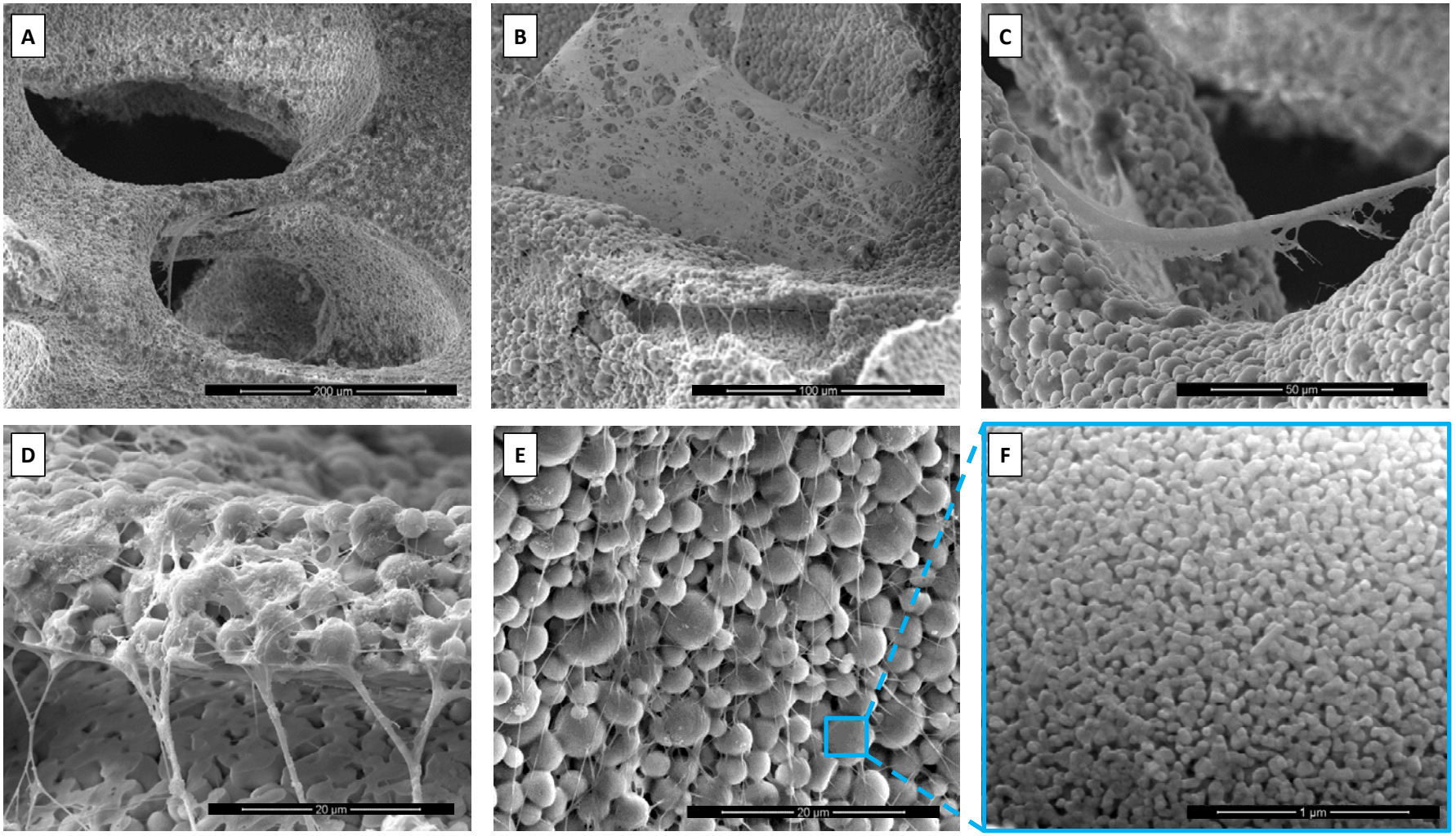

SEM

Vancomycin release

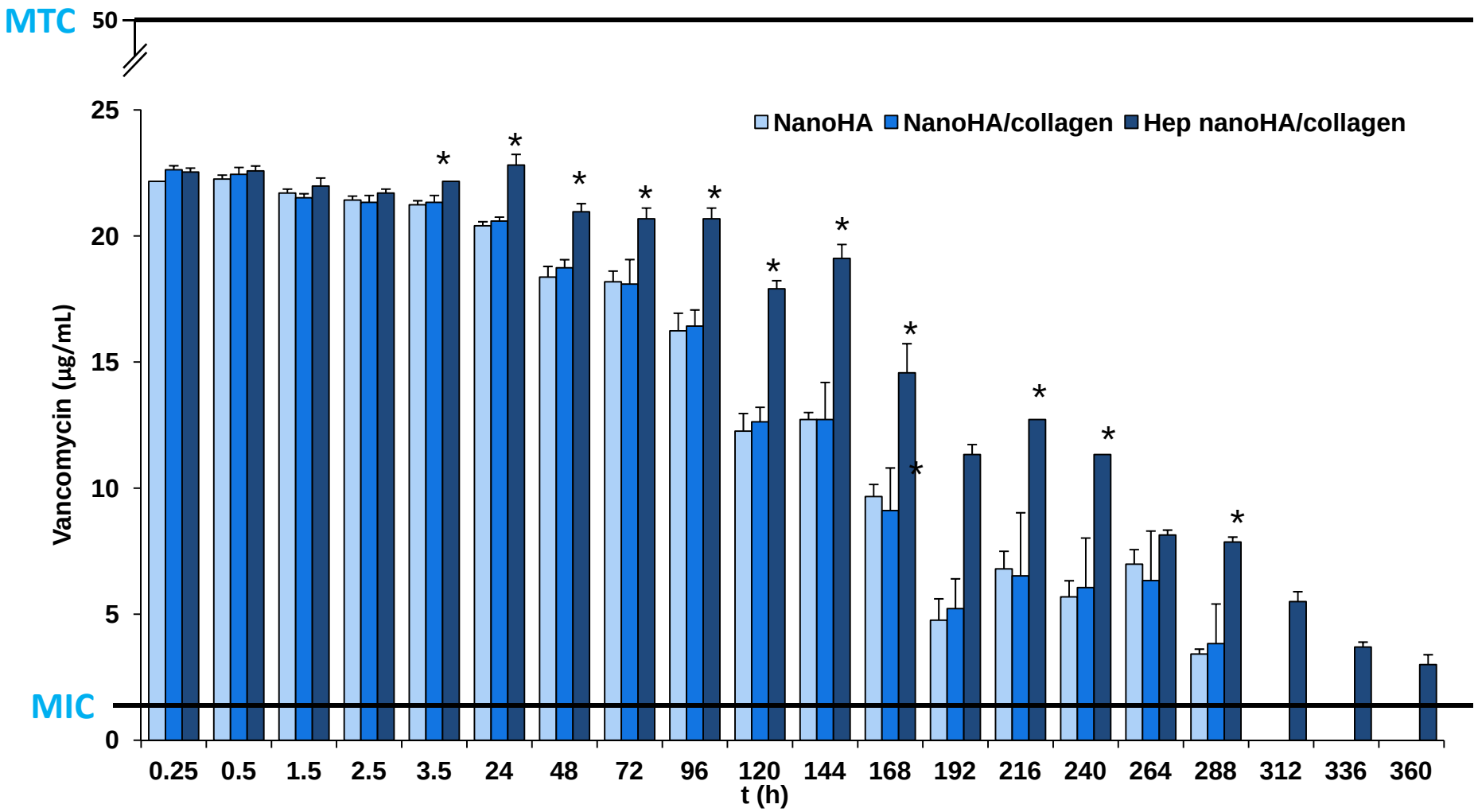

* Represents a statistical significant difference when compared to nanoHA and nanoHA/collagen granules for each time point ($p < 0.05$).

Vancomycin bioactivity

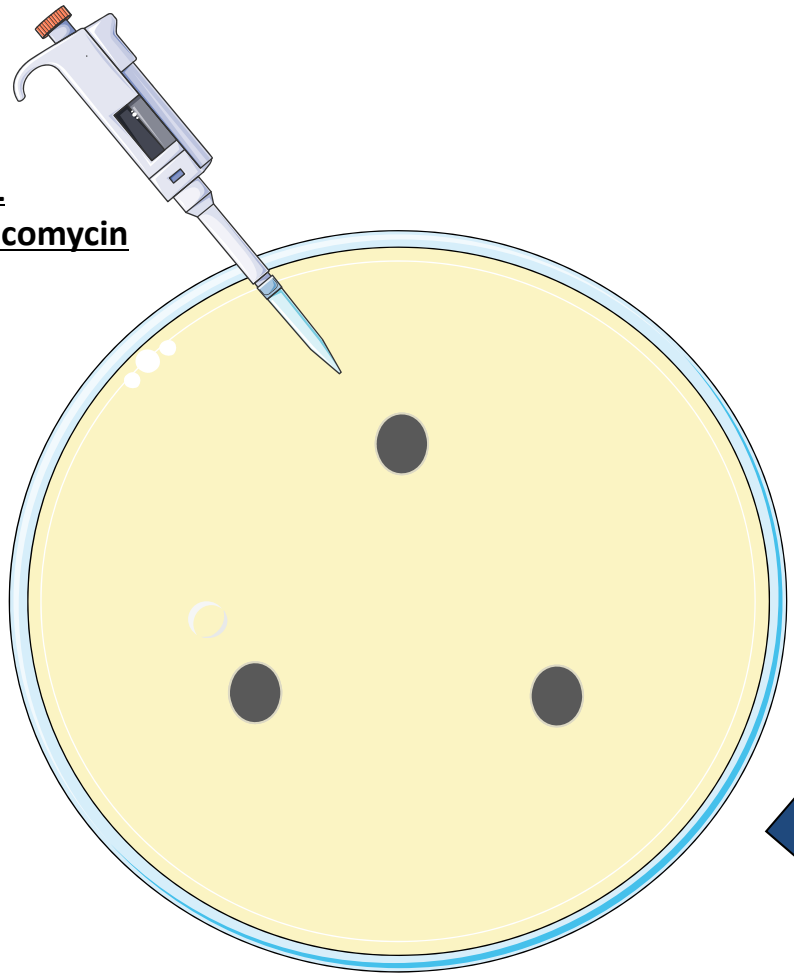

70 µL
released vancomycin

10 mm
stainless steel
cylinders

S. aureus ATCC 25923 suspension

Incorporation on nutrient agar

Incubation
18 h, 37 ºC

Agar diffusion method

Vancomycin bioactivity

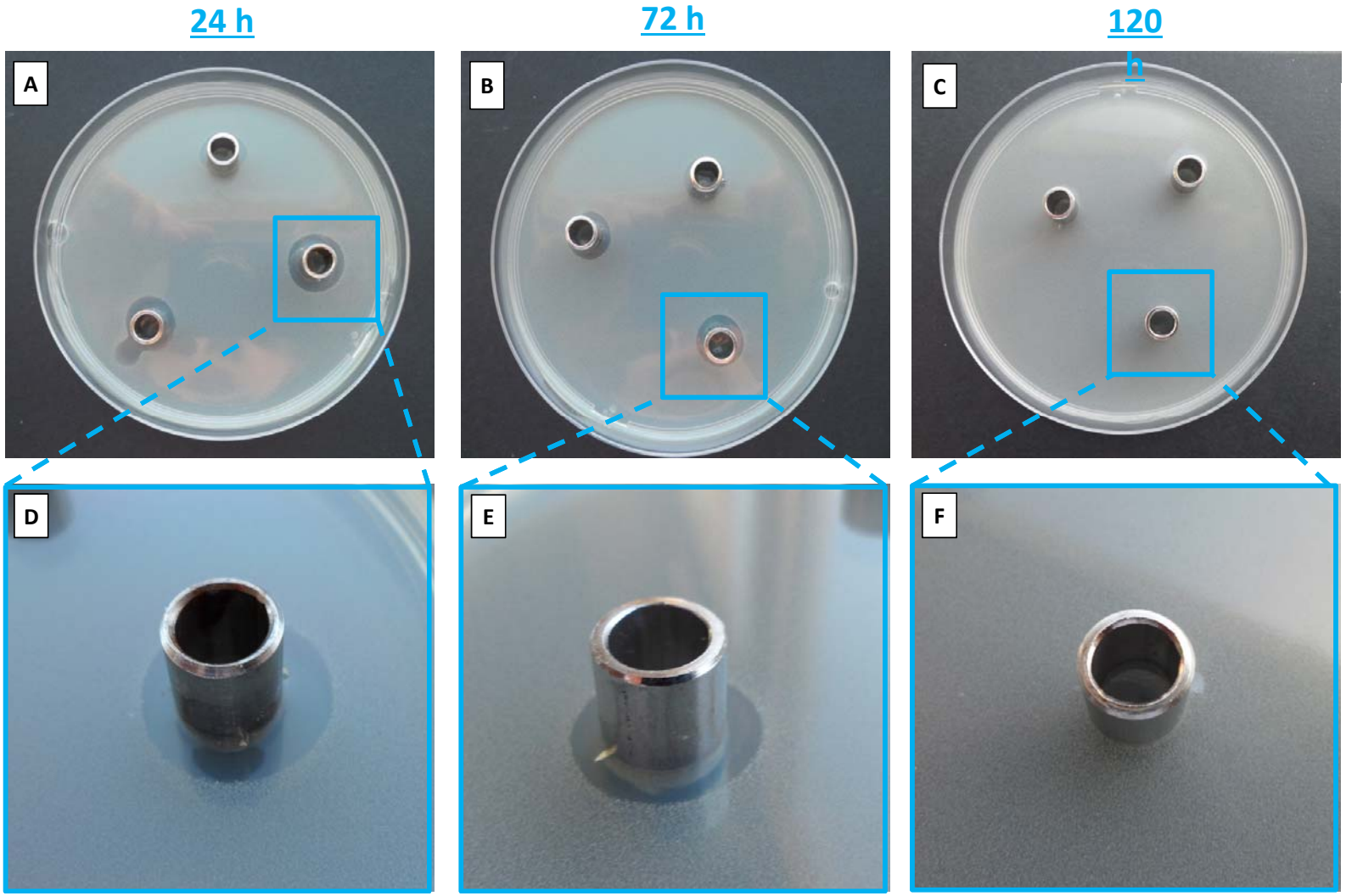

Lost bioactivity? Limit of detection?

Vancomycin bioactivity

	time (h)																
	0.25	0.50	1.5	2.5	3.5	24	48	72	96	120	144	168	192	216	240	264	288
Vancomycin (µg/mL)	2.254	2.258	2.198	2.170	2.217	2.281	2.096	2.069	2.069	1.791	1.911	1.457	1.133	1.272	1.133	0.814	0.786
S. aureus growth	-	-	-	-	-	-	-	-	-	-	-	-	-	-	+	++	+++

(-) No growth; (+) Growth in 1 replicate; (++) Growth in 2 replicates; (+++) Growth in 5 replicates.

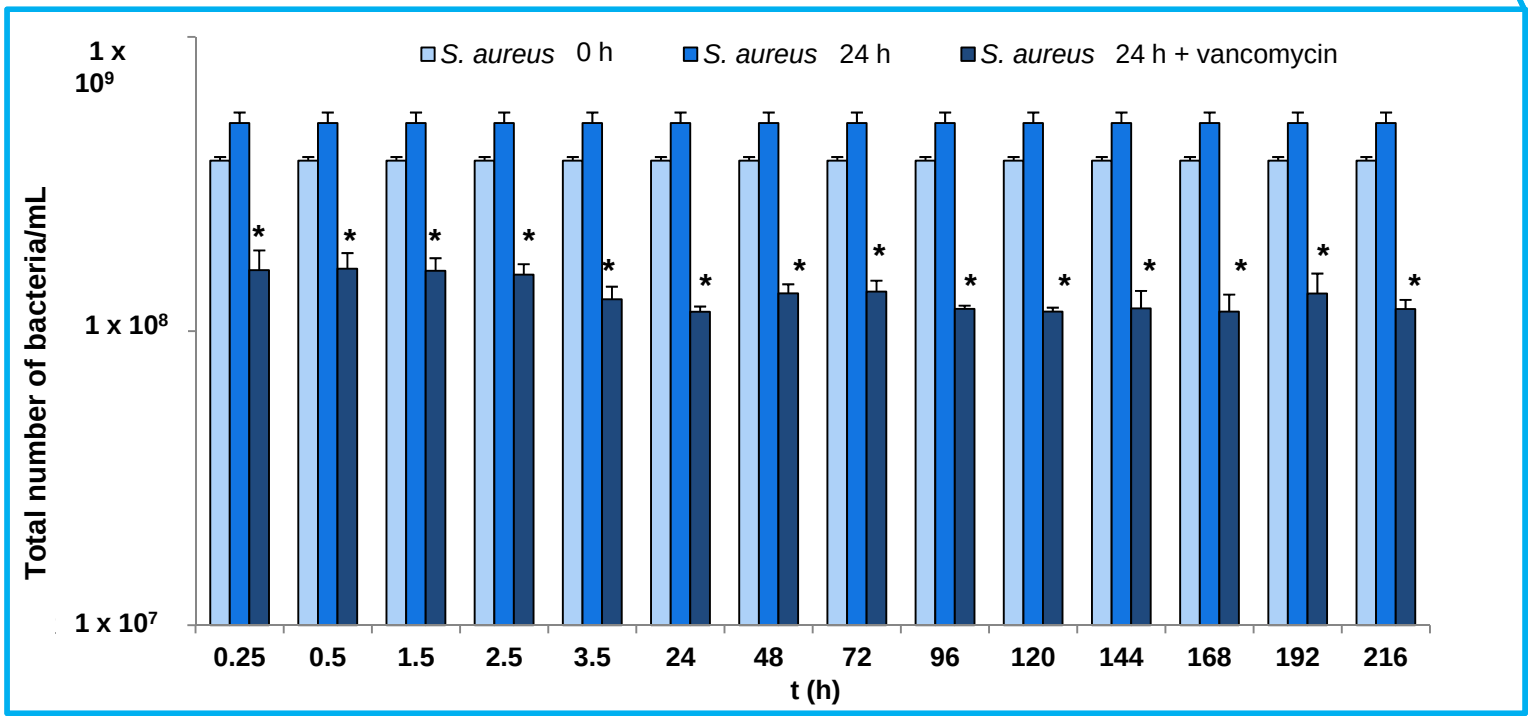

Total number of *S. aureus* in the absence of vancomycin, for 0 and 24 h of incubation, and in the presence of vancomycin after 24 h of incubation. * represents a statistical significant difference when compared with *S. aureus* 0 h and *S. aureus* 24 h ($p < 0.05$).

S. aureus adhesion on granules

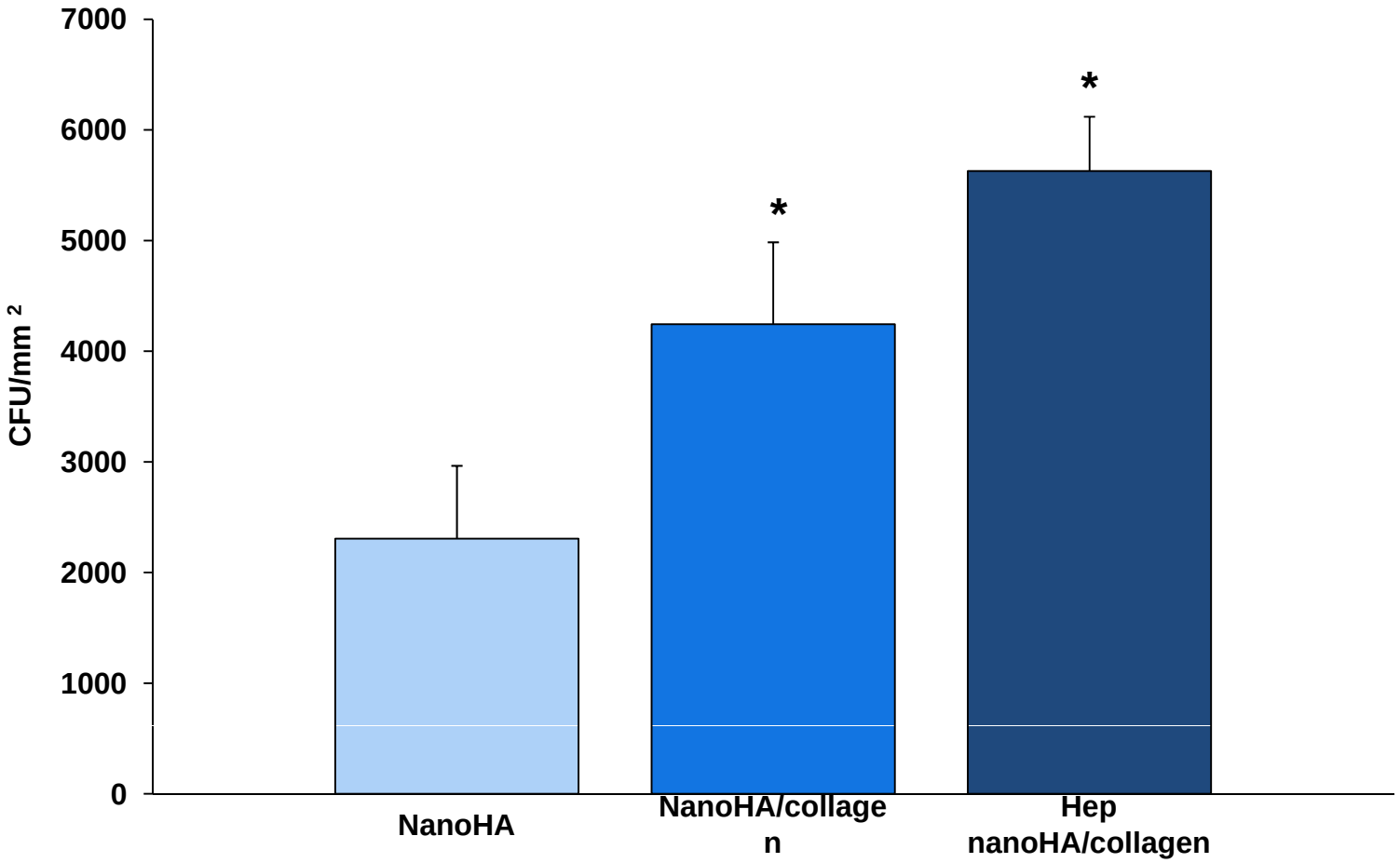

* Represents a statistical significant difference when compared to nanoHA granules ($p < 0.05$).

S. aureus adhesion on granules

NanoHA | NanoHA/collagen | Hep nanoHA/collagen

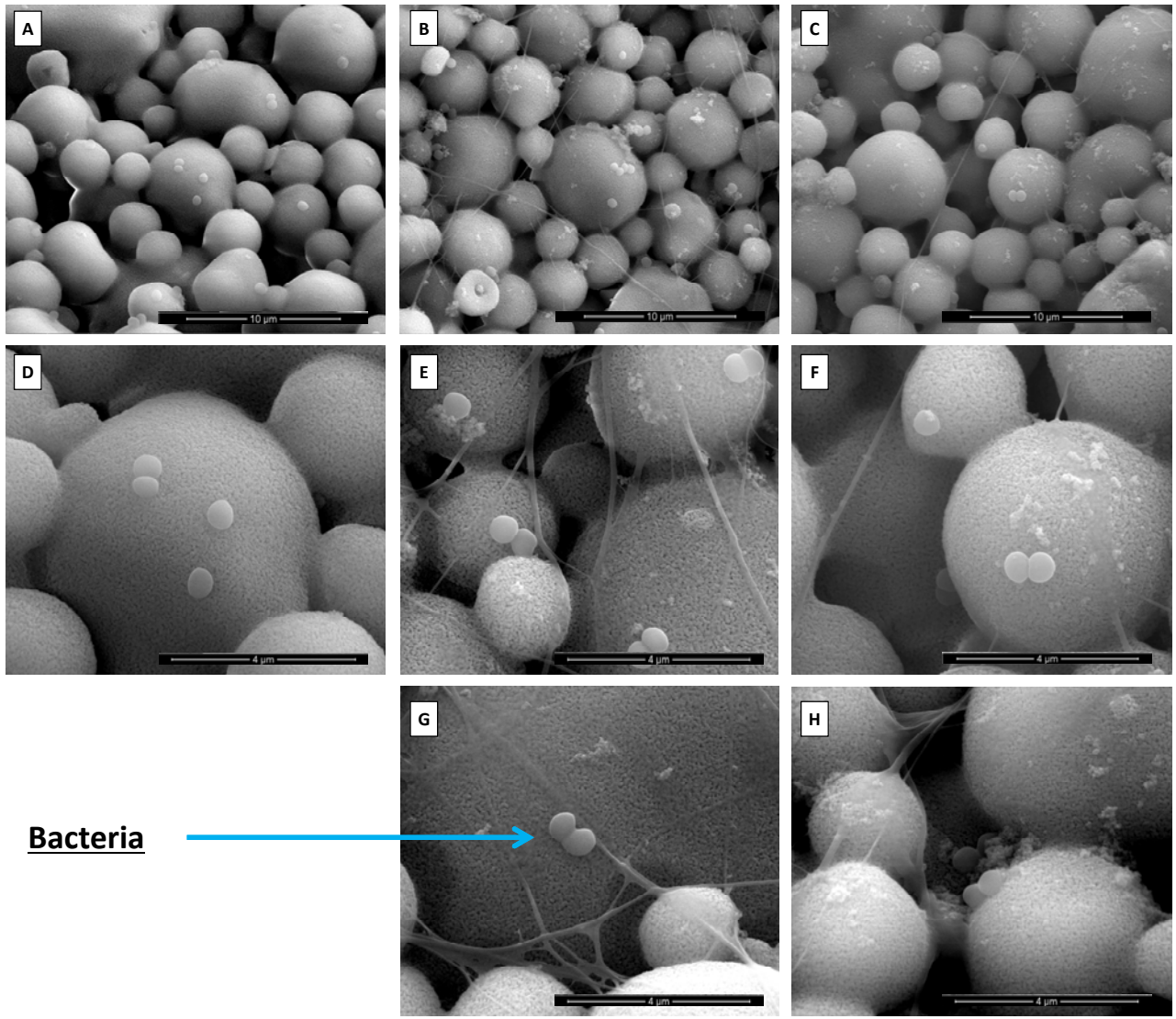

Bacteria

SEM

Case Study 2

Collagen based (functionalised) spongy-like scaffolds for bone tissue engineering

SIBLING proteins Functionalized Collagen scaffolds for critical bone defects

Abhishek Sahu , Christiane Salgado e Sandra Rodrigues

Collagen/ nanoHA Scaffolds obttained by “cryogelation” crosslinked by EDC/NHS

Collagen/ nanoHA biocomposites with immobilized SIBLING proteins for Bone tissue engineering

(OPN(osteopontin e BSP bone sialoprotein are memebers of SIBLING (Small Integrin-Binding LIgand, N-linked Glycoprotein) family

In vitro and In vivo studies of activity on functionalized scaffolds for bone formation, angiogenesis and bone remodelling

3D porous Collagen-Nanohydroxyapatite Biocomposite Scaffolds

Abhishek Sahu Christiane Salgado and Sandra Rodrigues

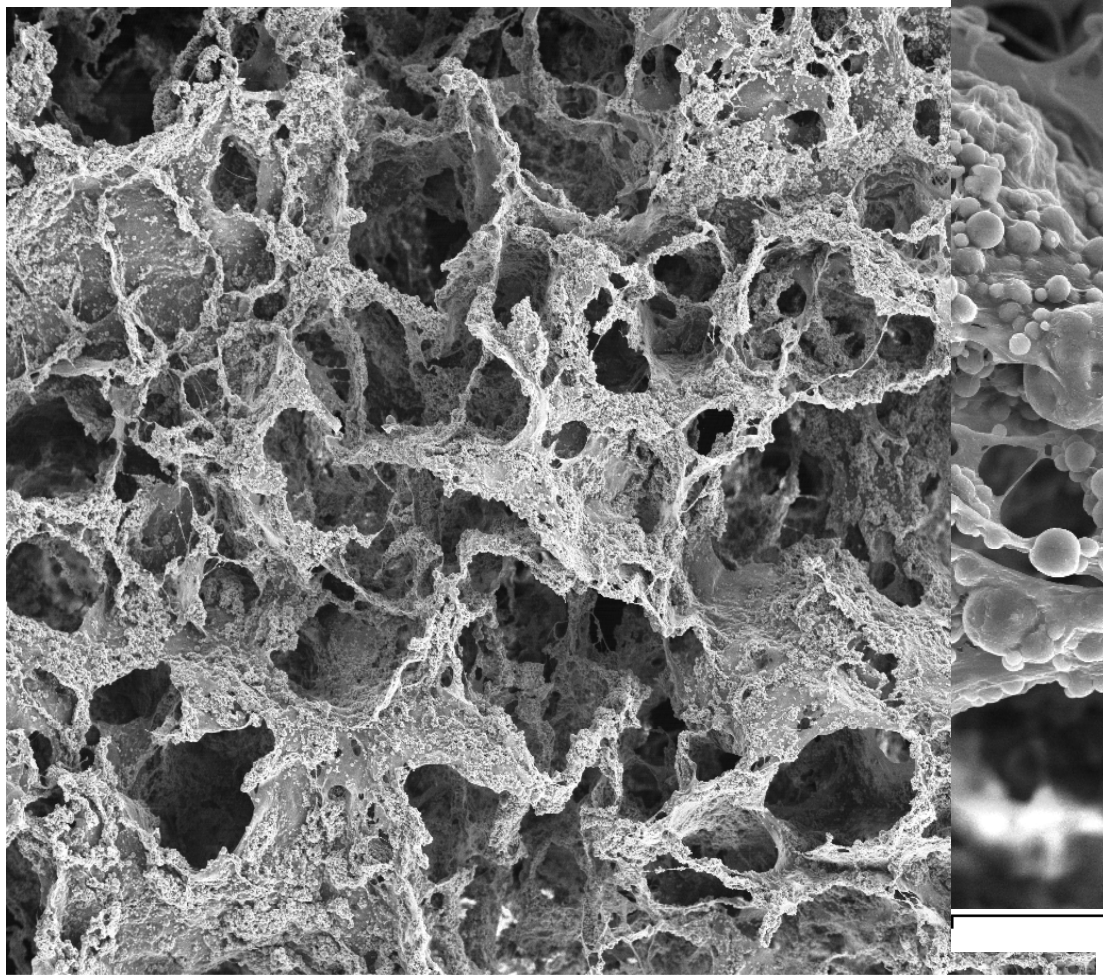

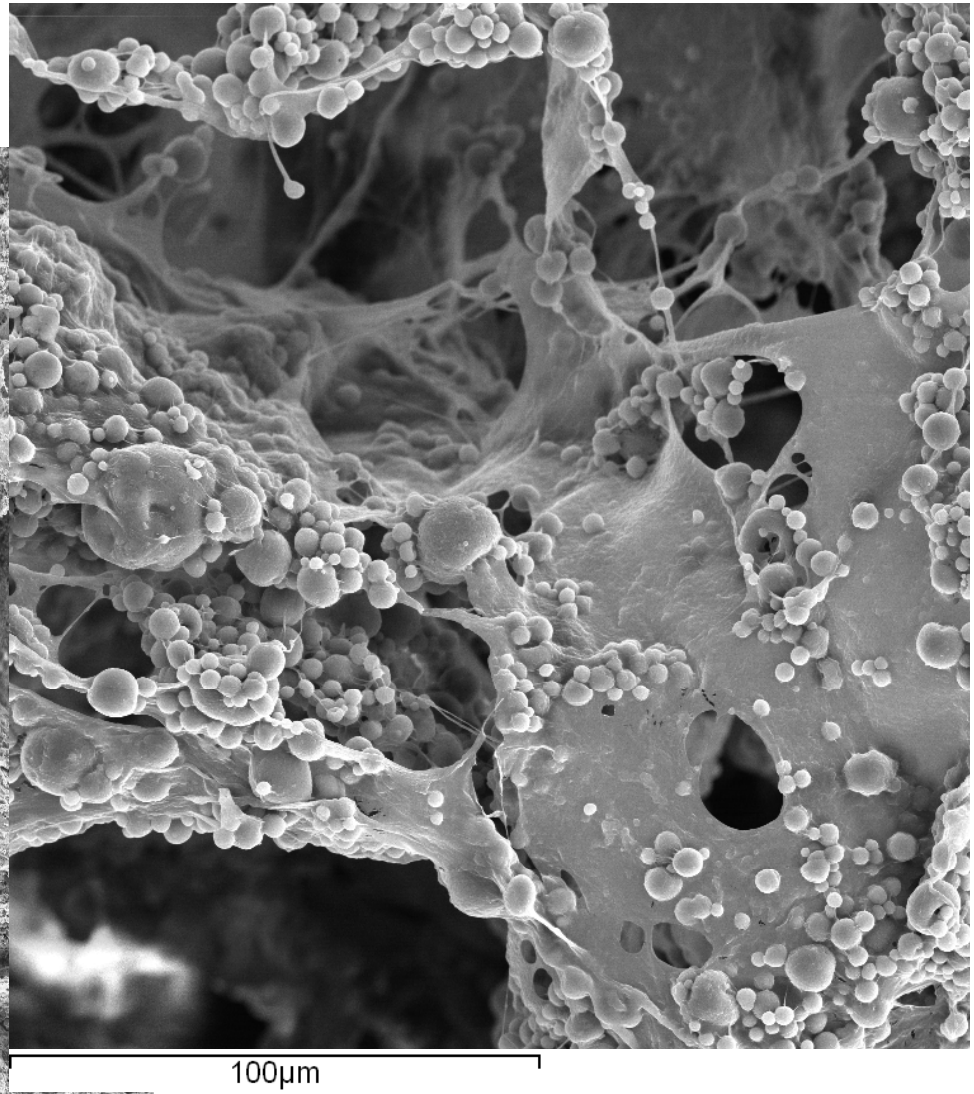

3D porous Collagen-Nanohydroxyapatite Biocomposite Scaffolds

Abhishek Sahu, Christiane Salgado and Sandra Rodrigues

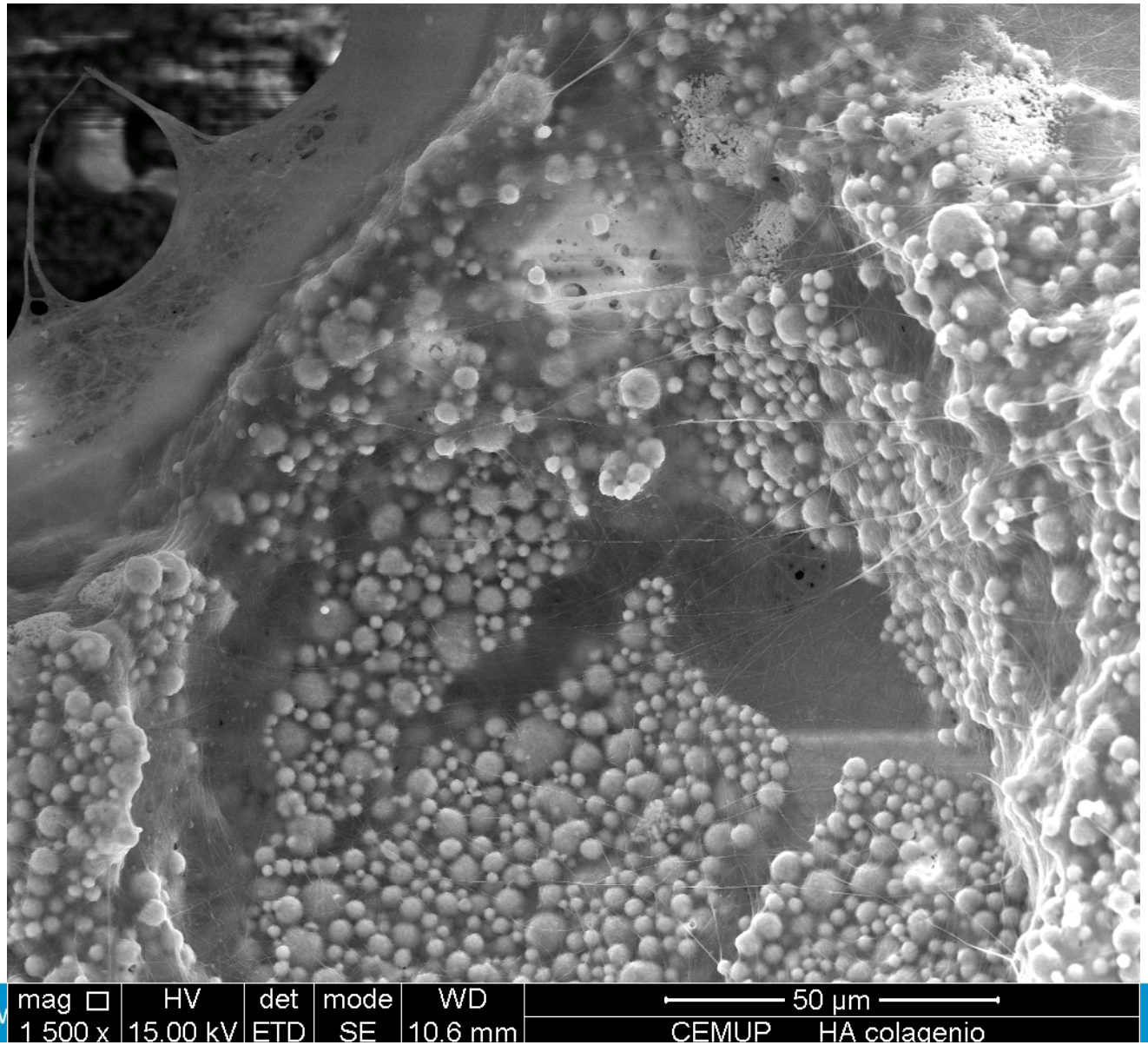

3D porous Collagen-Nanohydroxyapatite Biocomposite Scaffolds

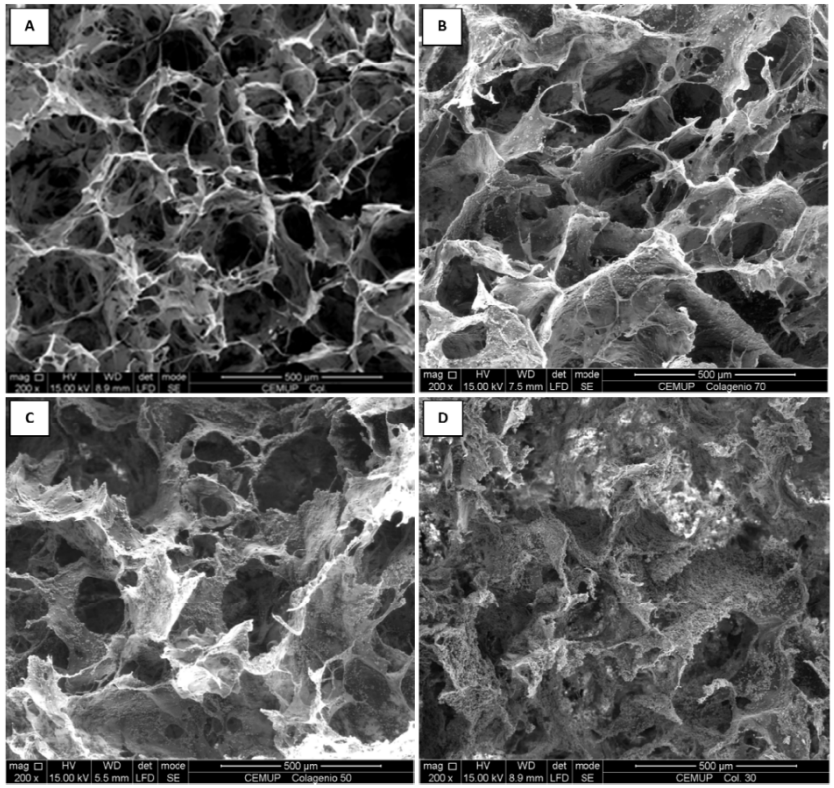

Figure . Scanning electron micrographs (SEM) of the cross-sections of (A) collagen scaffold (B) collagen-nanoHA (70:30) scaffold, (C) collagen-nanoHA (50:50) scaffold and (D) collagen-nanoHA (30:70) scaffold. Magnification: x 200.

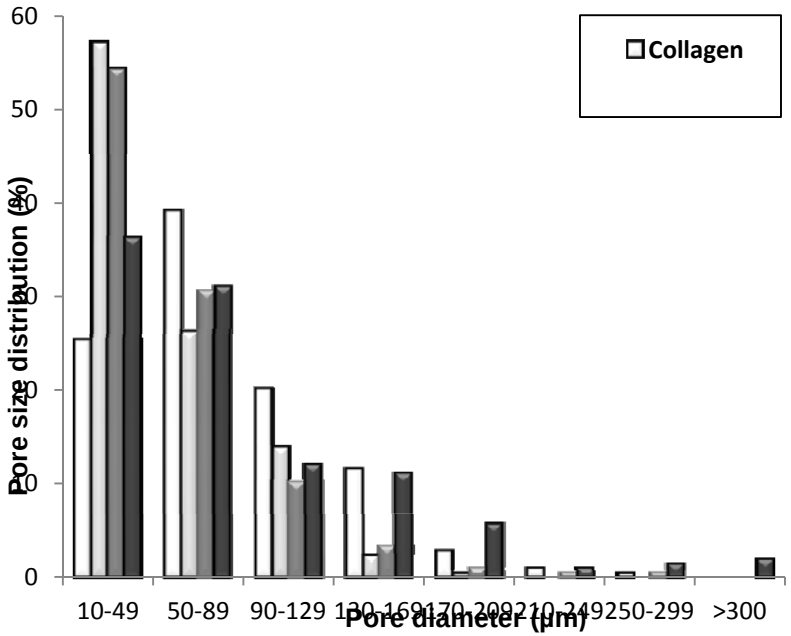

3D porous Collagen-Nanohydroxyapatite Biocomposite Scaffolds

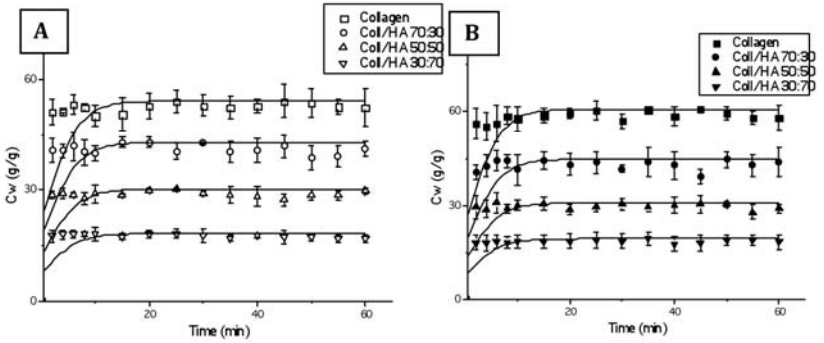

Figure 3: Swelling Kinetics of collagen and collagen-hydroxyapatite biocomposi cryogel scaffolds in PBS buffer (A) and (B) in distilled water.

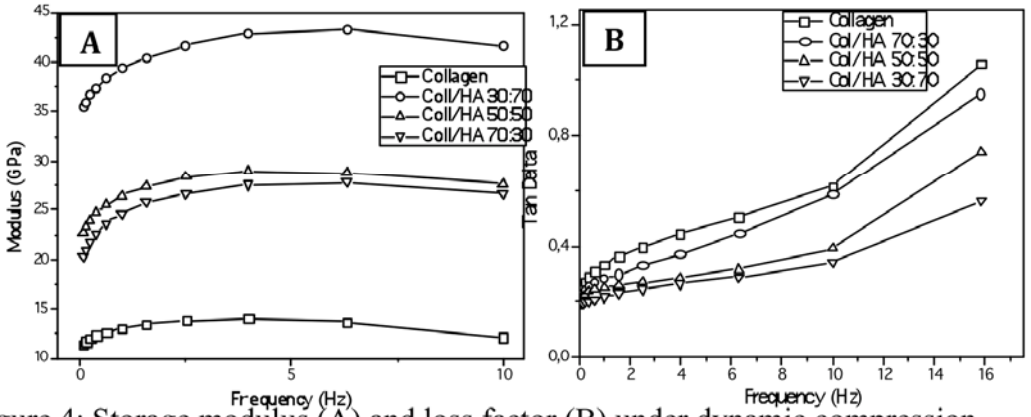

Figure 4: Storage modulus (A) and loss factor (B) under dynamic compression solicitation of increasing frequencies ranging from 0,1 to 10 Hz.

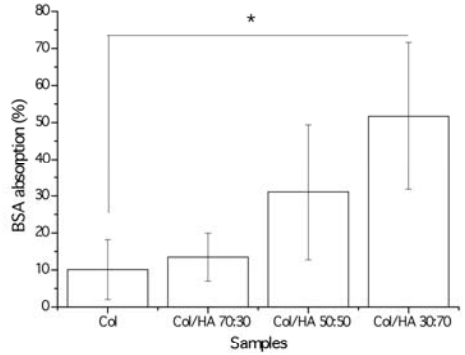

Figure 6: Albumin adsorption on the different composition of Col/nanoHA composites compared to collagen scaffols.

DNA extraction and ALP activity analyses

osteoblast culture (MG63).

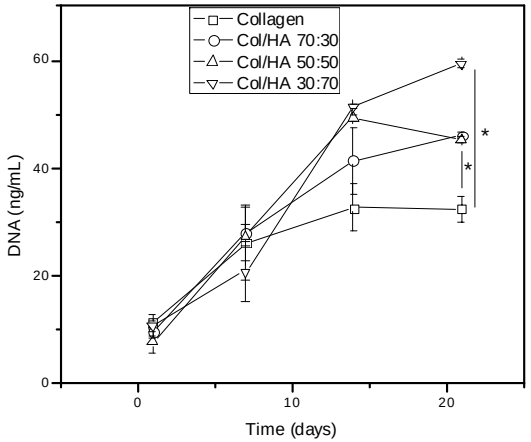

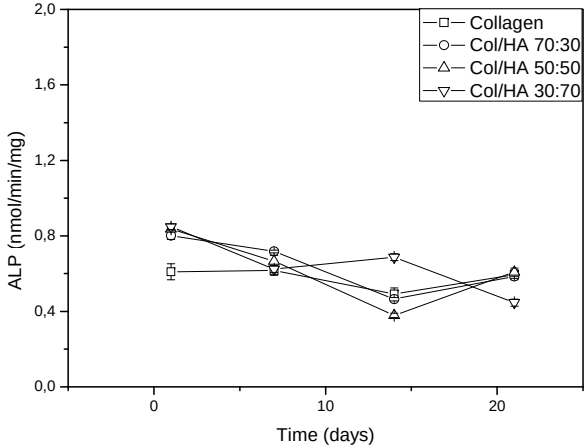

human mesenchymal stem cells (hMSC).

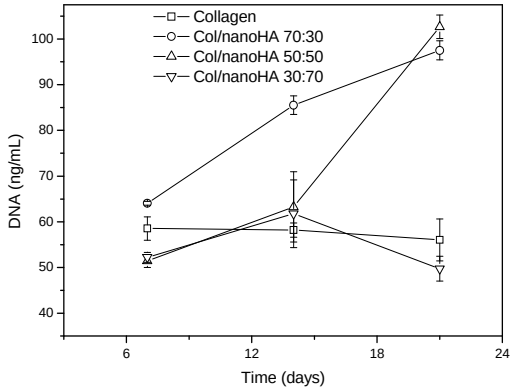

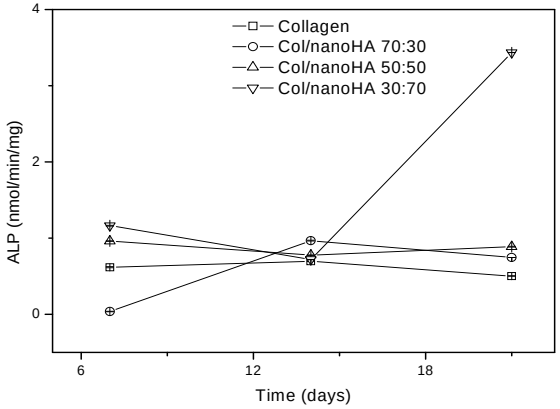

3D porous Collagen-Nanohydroxyapatite Biocomposite Scaffolds

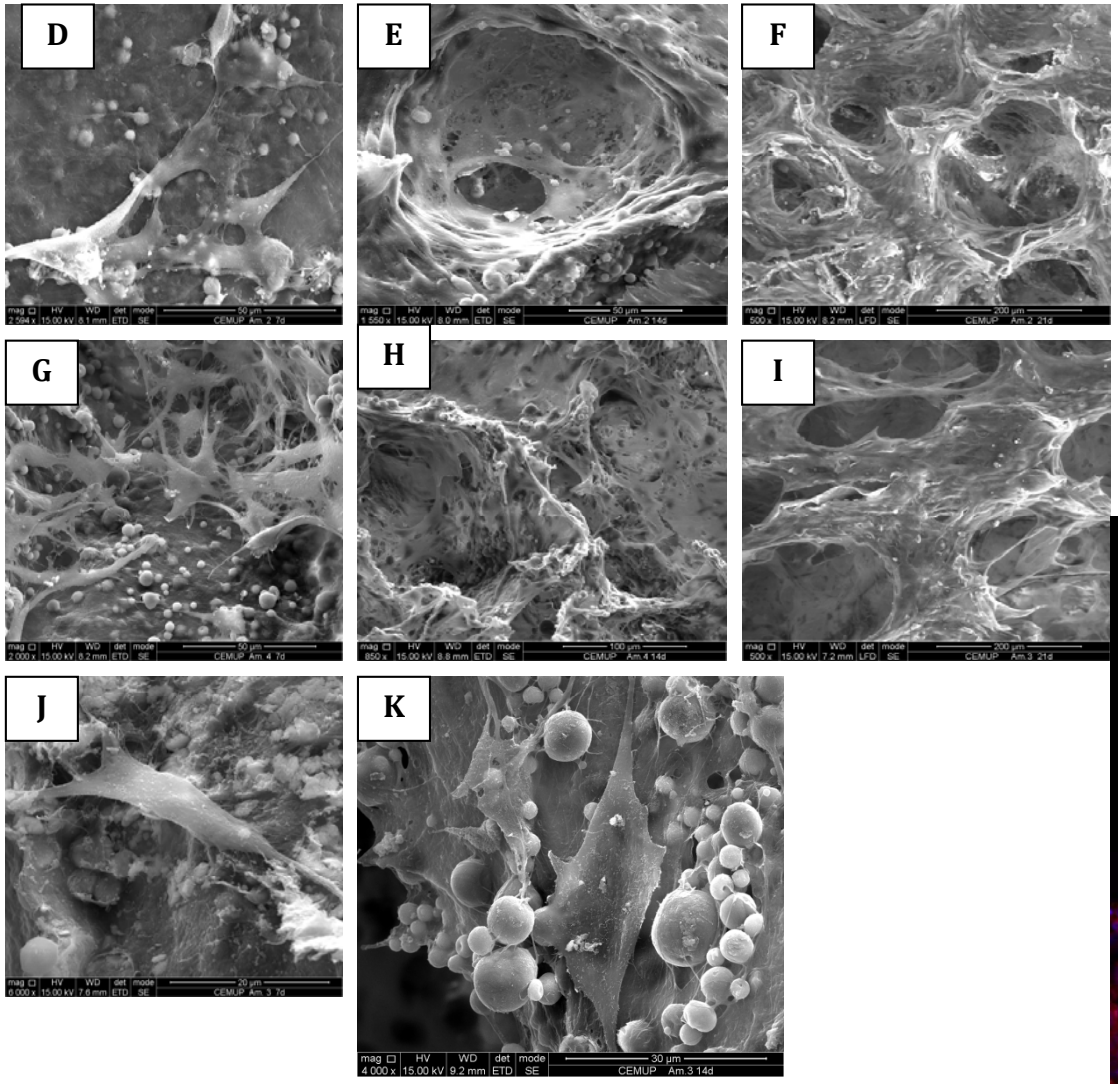

SEM images of cryogels' materials D, E and F - col/nanoHA 70:30; G, H and I - col/nanoHA 50:50; J and K - col/nanoHA 30:70) with osteoblast culture after 7days (A, D, G and J), 14 days (B, E, H and K) and 21 days (C, F and I).

Confocal Laser Microscopy images of cryogels' materials (A - collagen; B - col/nanoHA 70:30 ; C - col/nanoHA 50:50; D - col/nanoHA 30:70) with osteoblast culture after 21 days.

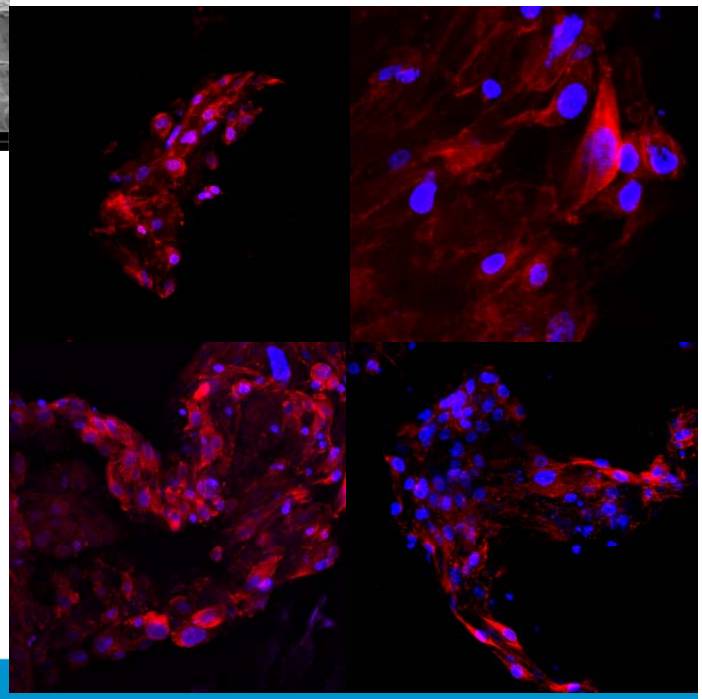

3D porous Collagen-Nanohydroxyapatite Biocomposite Scaffolds

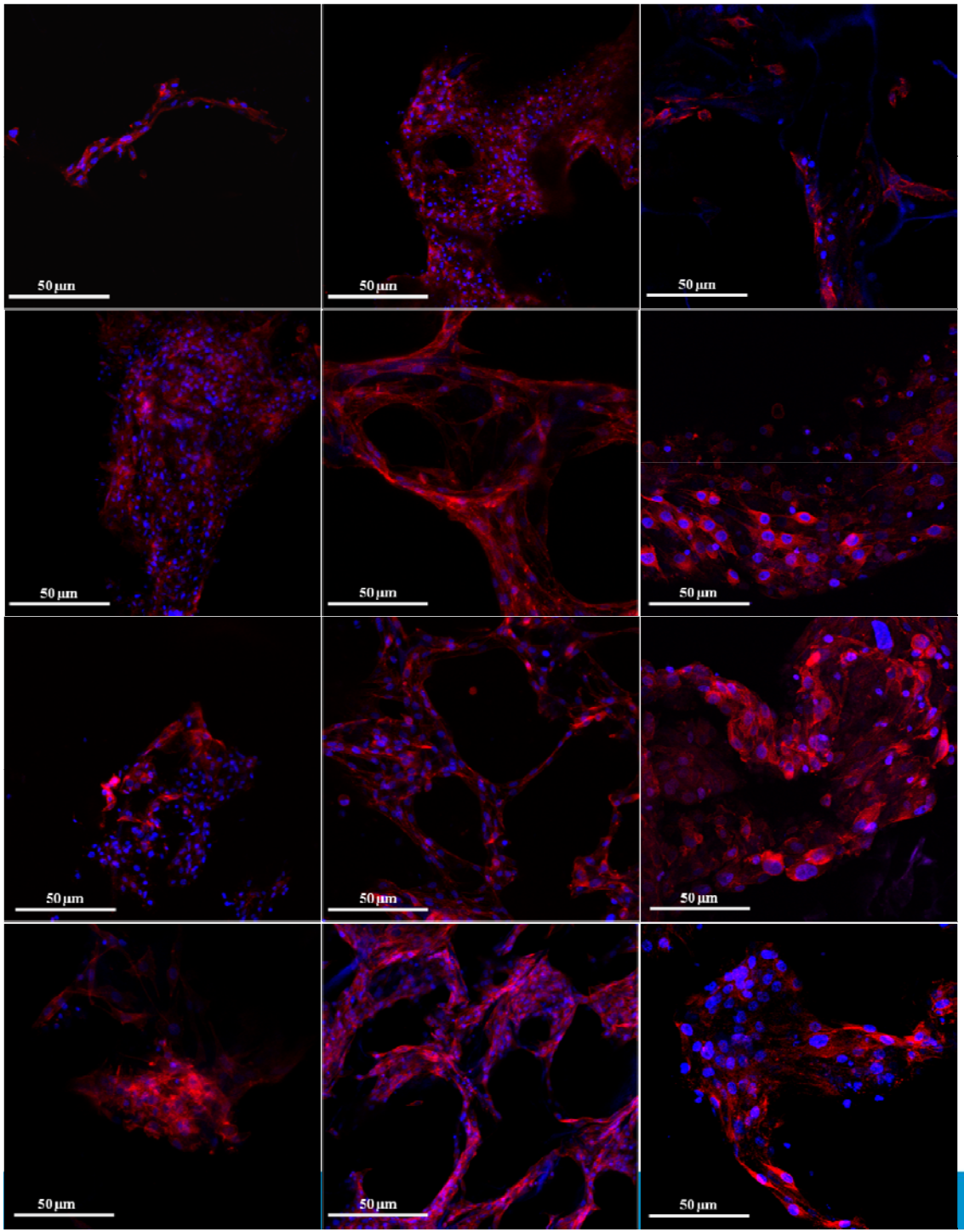

CLSM images of cells cultured for 7, 14 and 21 days on collagen and collagen-nanoHA biocomposite scaffolds.

Examples: **Fibronectin**

- **Fibronectin plays an important role in cell adhesion, migration and differentiation of different sources of mesenchymal cells;**
- **In bone, it is involved in the early stages of osteogenesis.**

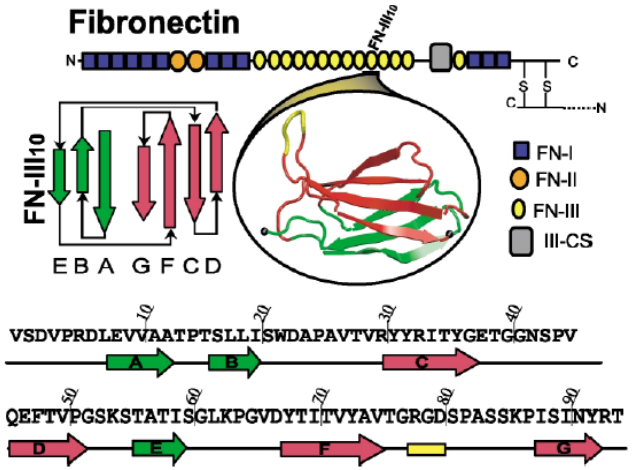

Osteopontin

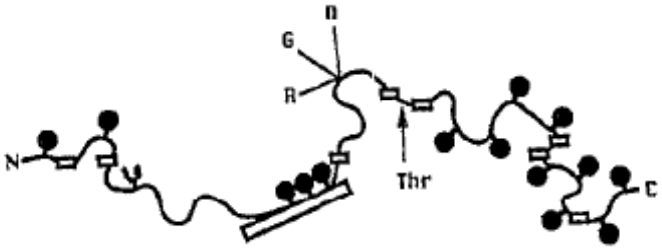

is a member of SIBLING (Small Integrin-Binding LIgand, N-Linked Glycoprotein) present in bone, teeth, kidney, epithelial lining tissue, being expressed by osteoblasts, osteocytes, osteoclasts, chondrocytes and odontoblasts.

- A family of non-collagenous proteins;
- Can be found in mineralized tissues;
- They are secreted into the extracellular matrix during the formation and mineralization of those tissues.

Characterization of collagen films

- The chemical composition of collagen films with and without adsorbed proteins were proved by FT-IR.

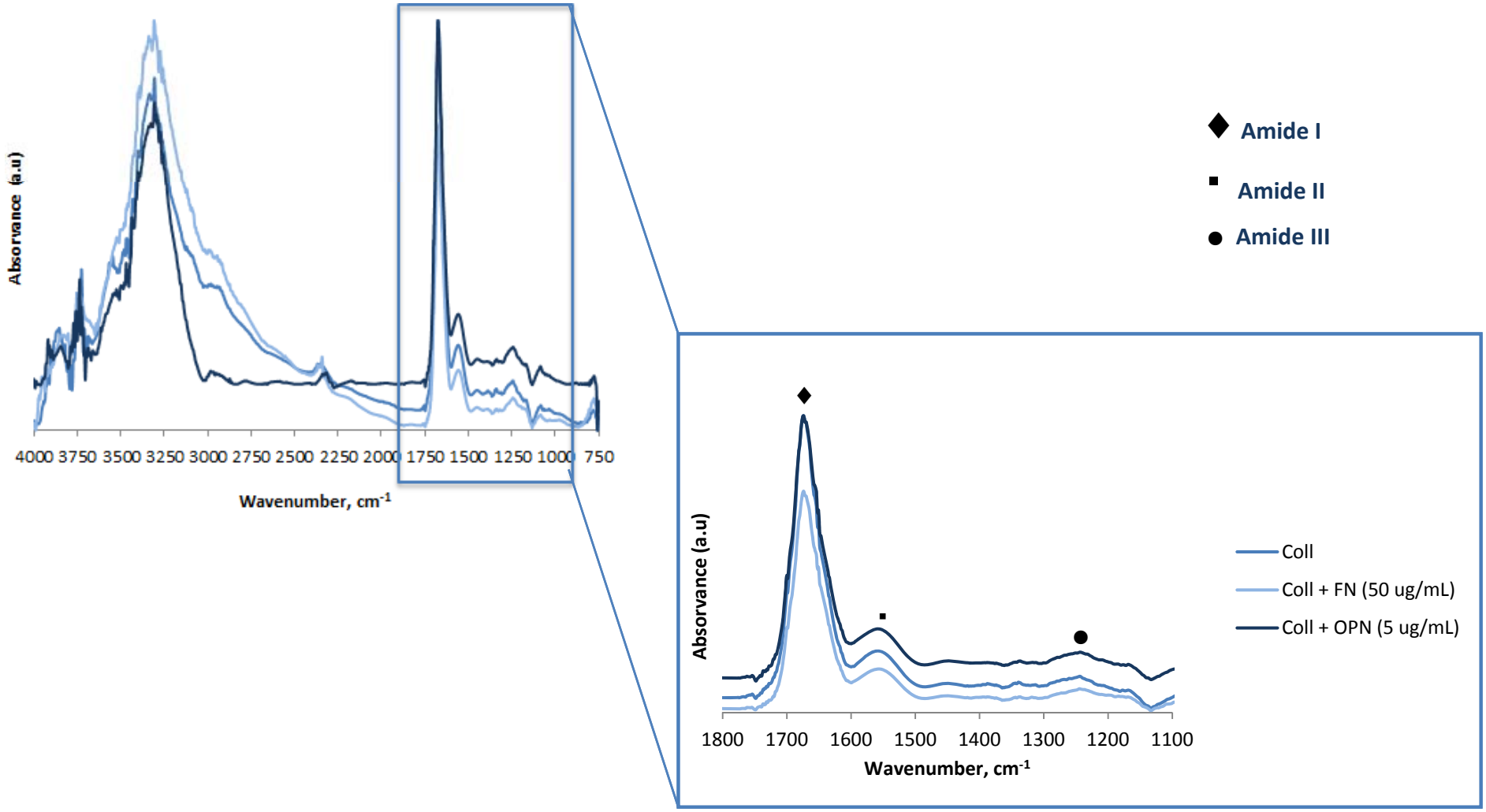

Characterization of collagen films

- **The topography of collagen films with and without adsorbed proteins were evaluated by AFM.**

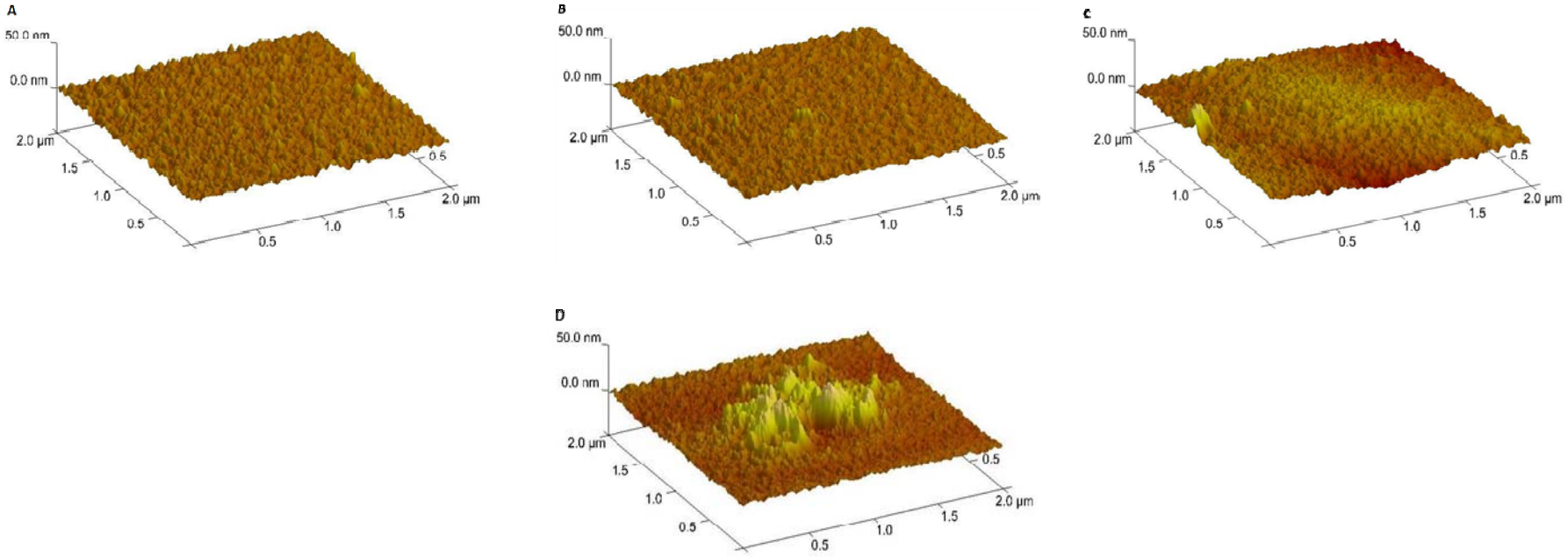

AFM images of gold substrates (A) modified with collagen (B), collagen with adsorbed fibronectin (C) and collagen with adsorbed osteopontin (D). Images were obtained using Tapping Mode and the scan size were 2 µm x 2 µm.

Characterization of collagen films

- **The fibronectin and osteopontin adsorption was confirmed by immunohistochemistry with CLSM.**

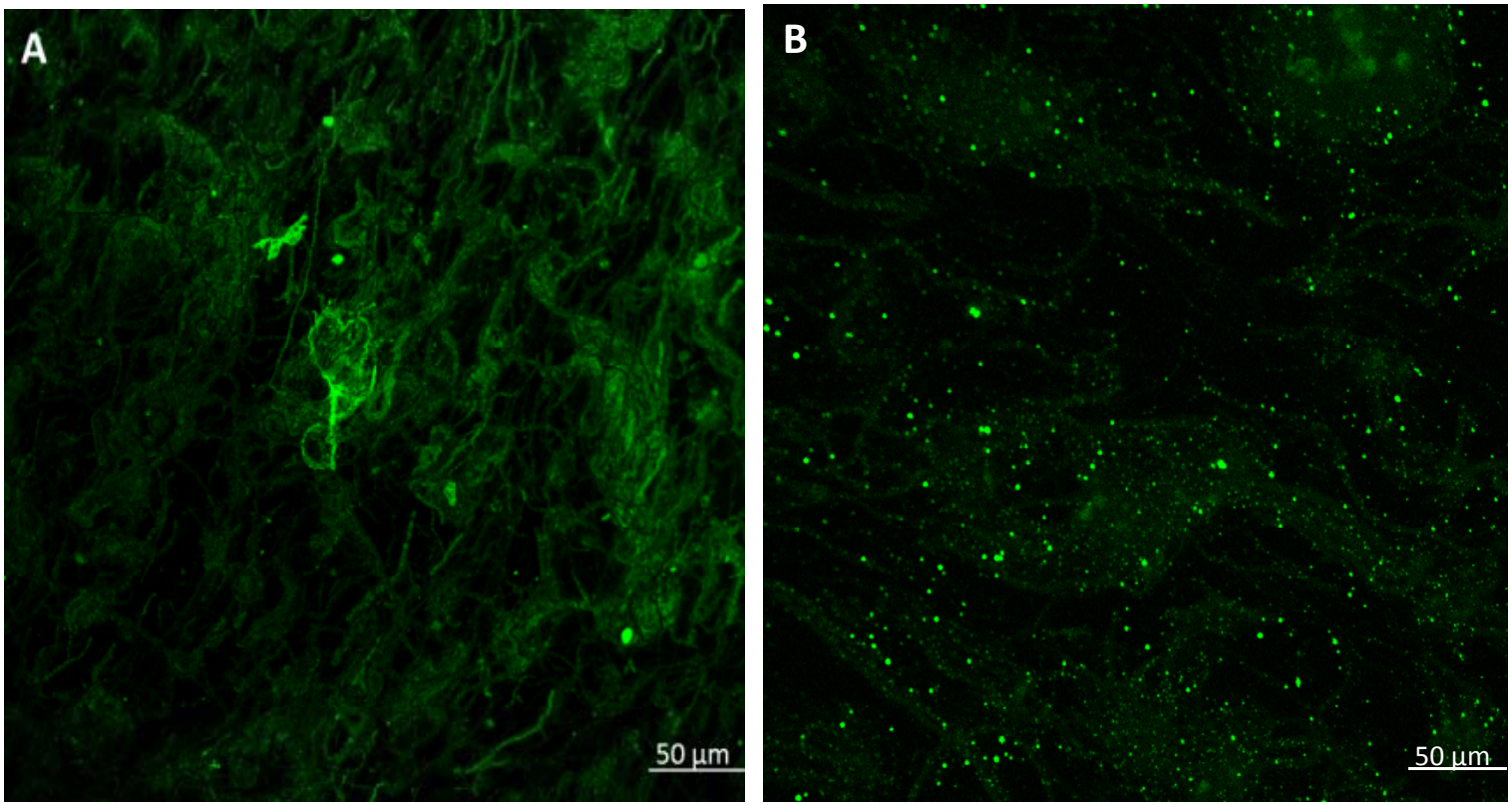

Confocal images of collagen films with adsorbed fibronectin (A) and osteopontin (B). (Control with secondary antibody was negative (data not shown)). Magnification: 40x.

MC3T3-E1 culture on collagen surfaces

In vitro biological studies

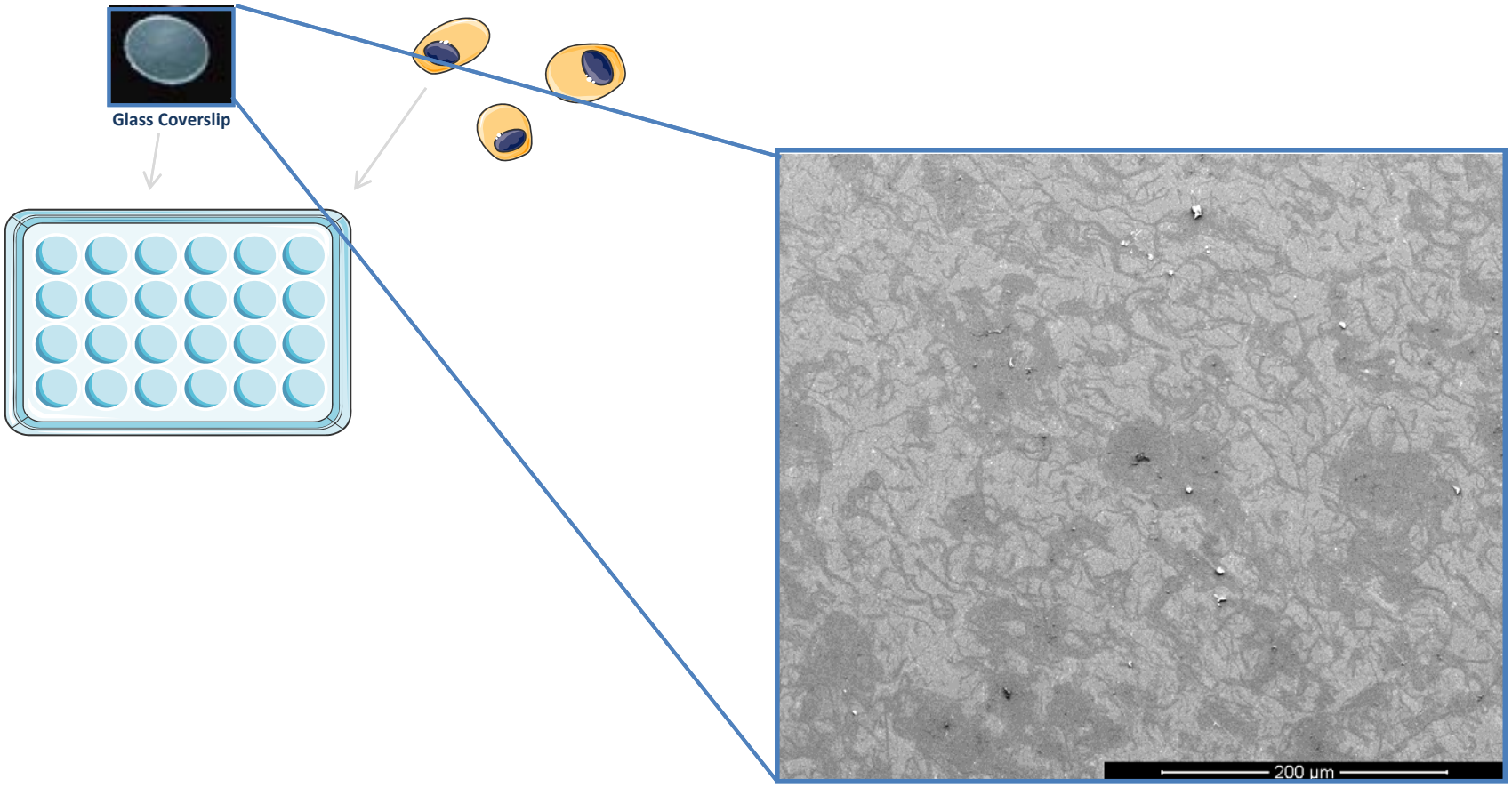

Collagen films on glass coverslips.

MC3T3-E1 culture on collagen surfaces

In vitro biological studies

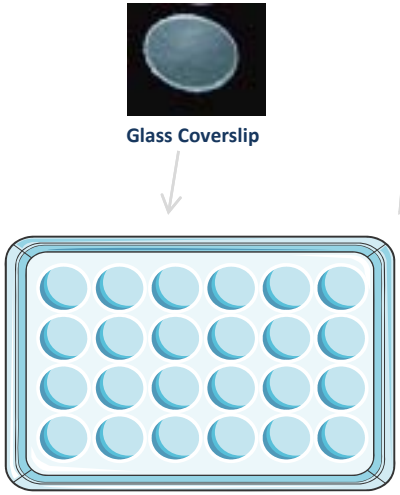

MC3T3-E1 pre-osteoblasts → 4 x 10^4 cells/mL

- Metabolic Activity (Resazurin)
  4 h, 24 h, 3 days and 7 days
- Cell Morphoplogy (SEM and CLSM)
  4 h, 24 h, 3 days and 7 days
- Alkaline Phosphatase Activity (ALP)
  24 h, 3 days and 7 days

MC3T3-E1 culture on collagen surfaces

In vitro biological studies

- MC3T3-E1 metabolic activity was evaluated by Alamar Blue (resazurin).

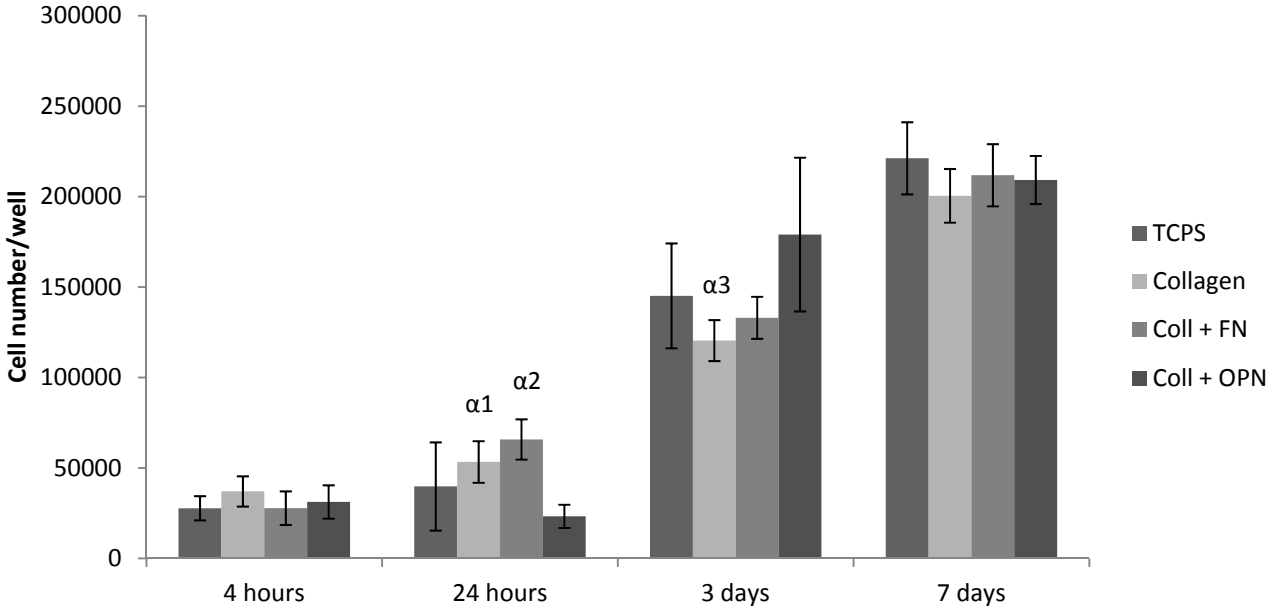

Metabolic activity of MC3T3-E1 cultured on TCPS, Collagen, Coll + FN and Coll + OPN during 7 days, estimated by Alamar Blue assay.
Metabolic activity of MC3T3-E1 was expressed in number of cell per well. α1 (Collagen) and α2 (Coll + FN) represent a significant difference comparing with Coll +OPN after 24 hours of culture, while α3 (Collagen) represents a significant difference comparing with Coll + OPN after 3 days of culture ($p<0.05$).

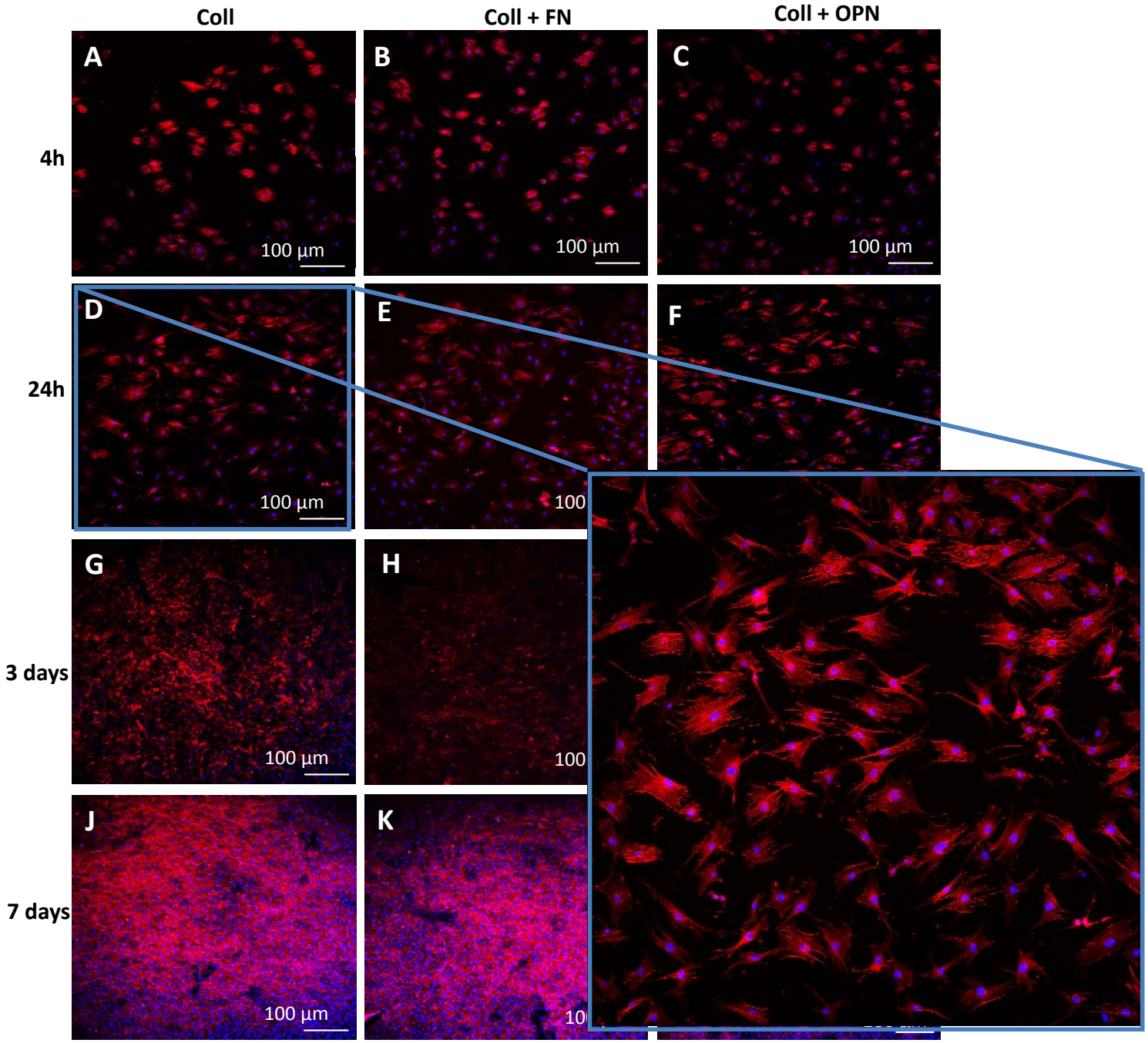
Coll
Coll + FN
Coll + OPN
4h
24h
3 days
7 days
A
B
C
D
E
F
G
H
J
K
100 µm

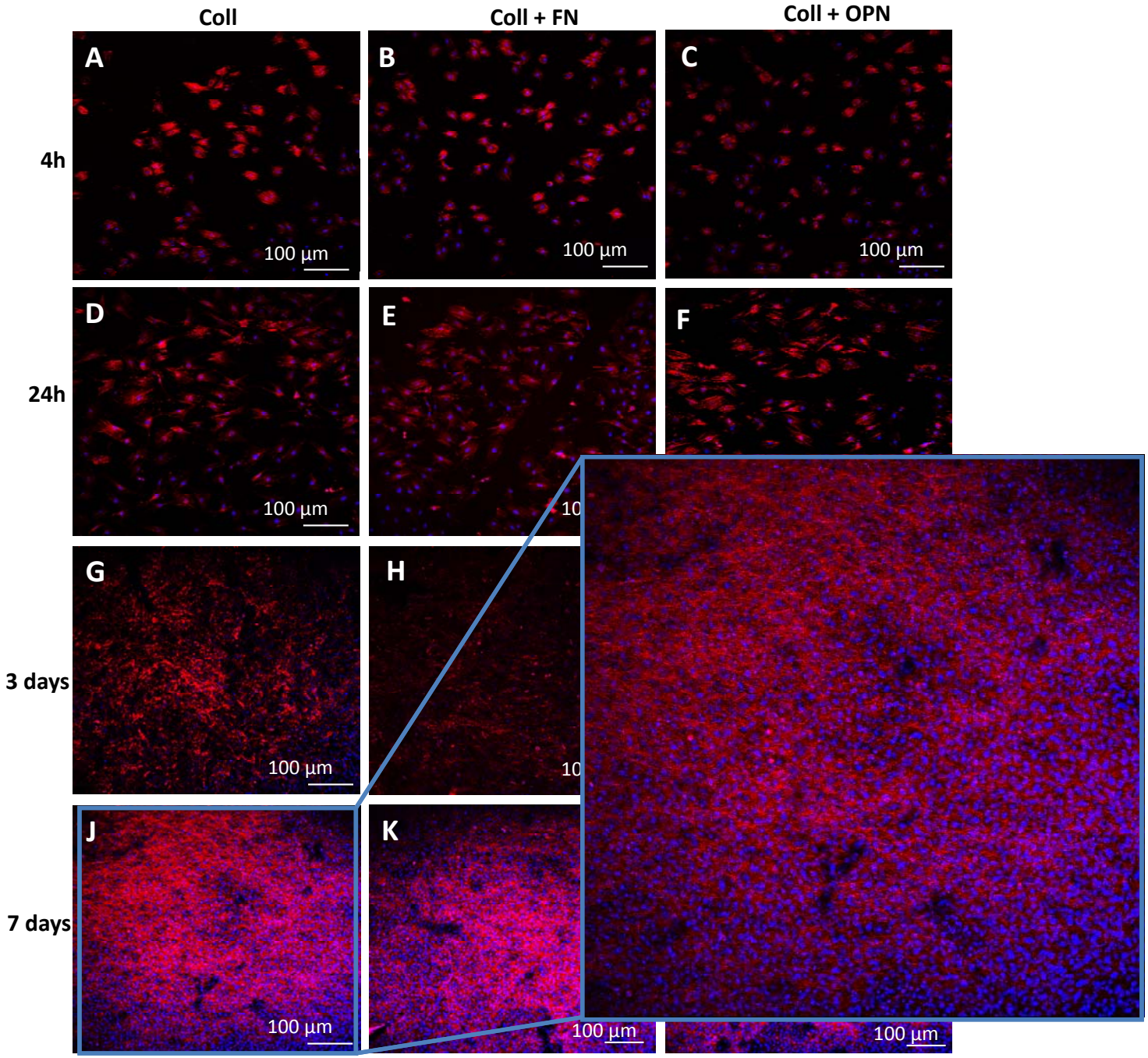
Coll
Coll + FN
Coll + OPN
4h
24h
3 days
7 days
A
B
C
D
E
F
G
H
J
K
100 µm

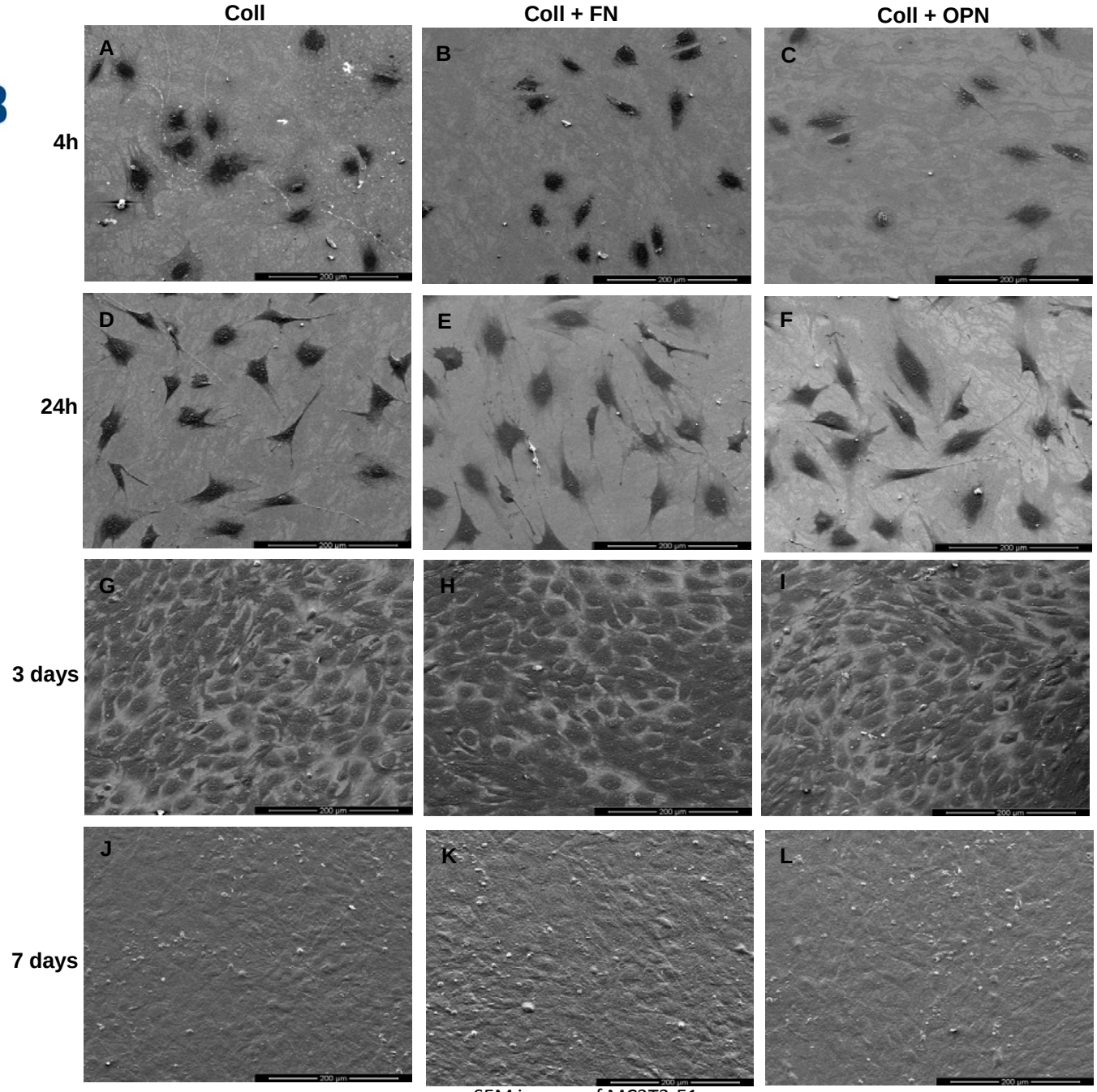

SEM images of MC3T3-E1.

MC3T3-E1 culture on collagen surfaces

in vitro biological studies

- The functional activity of MC3T3-E1 cells on collagen surfaces was evaluated by measuring the Alkaline Phosphatase Activity (ALP) normalized with Total Protein Content.

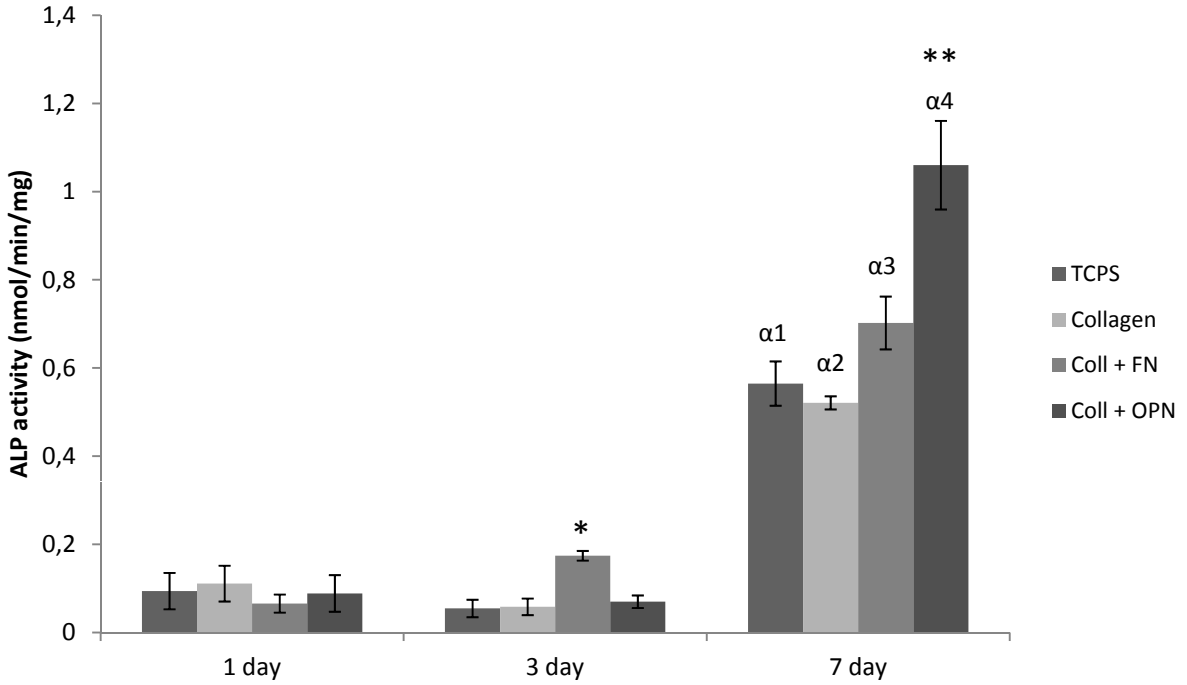

Alkaline phosphatase activity for MC3T3-E1 on TCPS, Collagen films, Coll + FN and Coll + OPN for different time-points.
* represents a significant difference from Coll + FN within the respective time-point while ** represents a significant difference from Coll + OPN within the respective time-point ($p<0.05$); α1 (TCPS), α2 (Collagen), α3 (Coll + FN), and α4 (Coll + OPN) represents a significant difference comparing the respective material in distinct time-points ($p<0.05$).

Collagen/ nanoHA cryogel scaffolds functionalized with SIBLING protein for critical bone defects

Salgado C., Sahu A., Rodrigues S., Monteiro F.J.

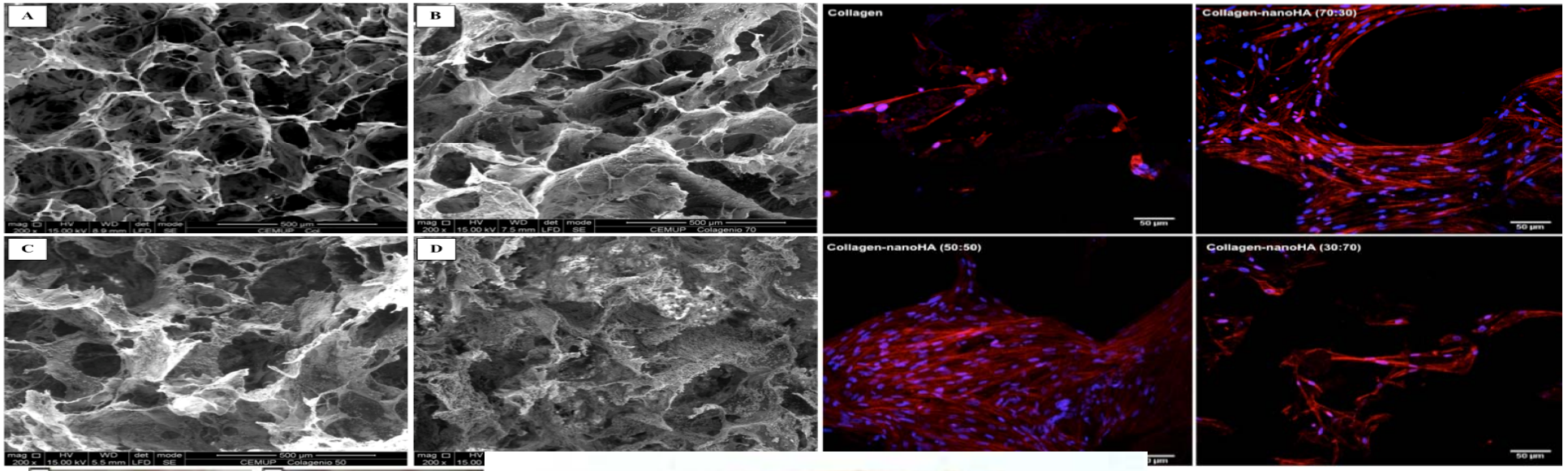

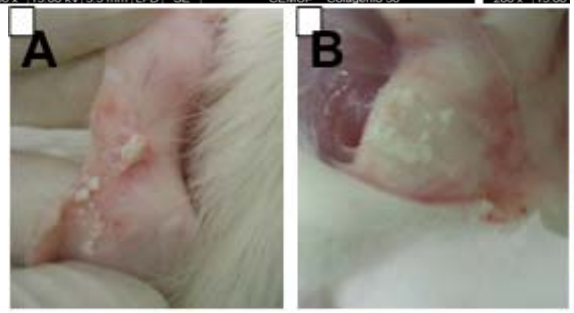

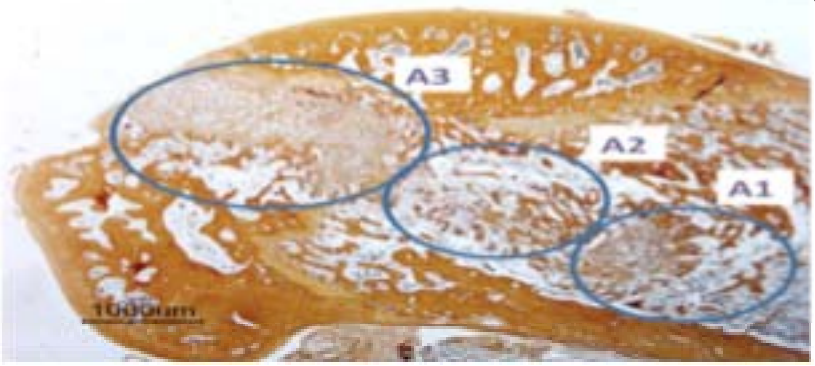

Preparation and characterization o
f collagen-nanohydroxyapatite biocomposite
scaffolds by cryogelation method for bone
tissue engineering applications. J Biomed Mater
Res A, [Volume: 101A Issue: 4
Pages: 1080-1094
DOI: 10.1002/jbm.a.34394, 2013

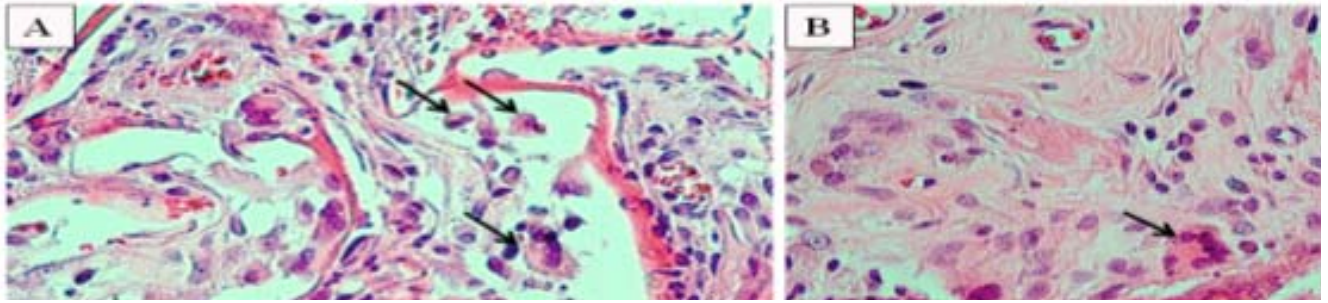

Composite cryogels for bone tissue regeneration

Type I collagen/nanoHA sponges for bone tissue enginnering

25 YEARS ADVANCING

Transmission electron microscopy (TEM)

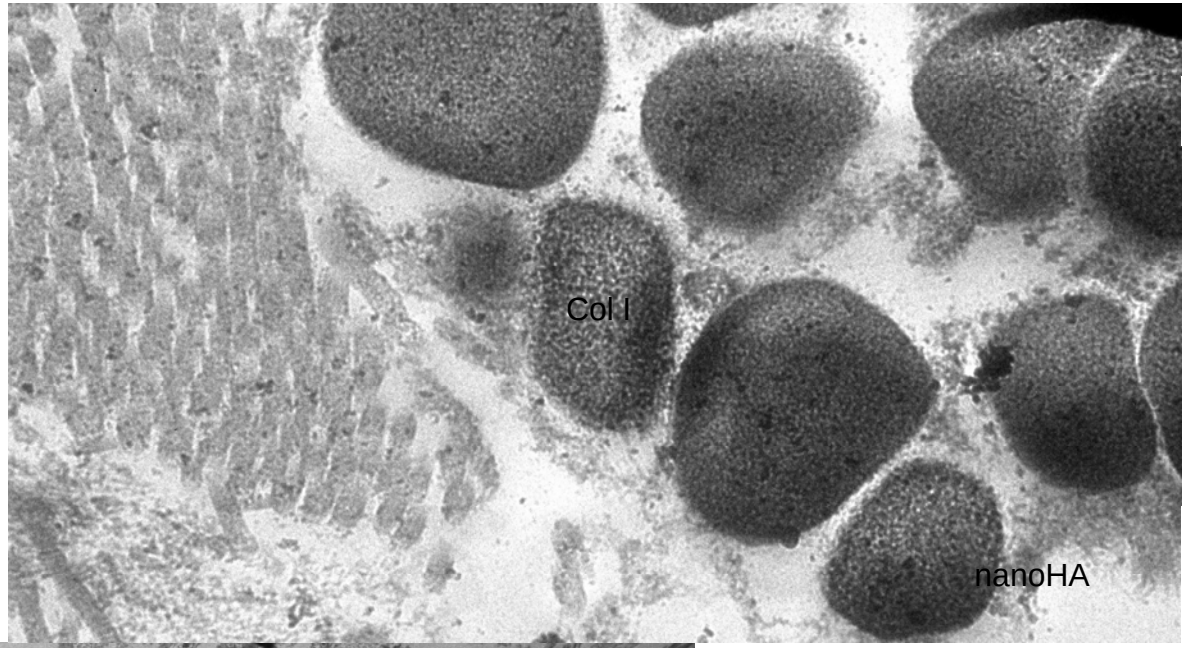

In vivo characterization

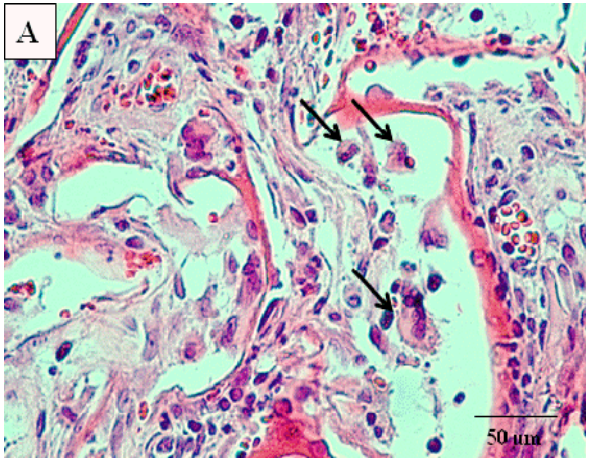

Coll/nanoHA 70:30

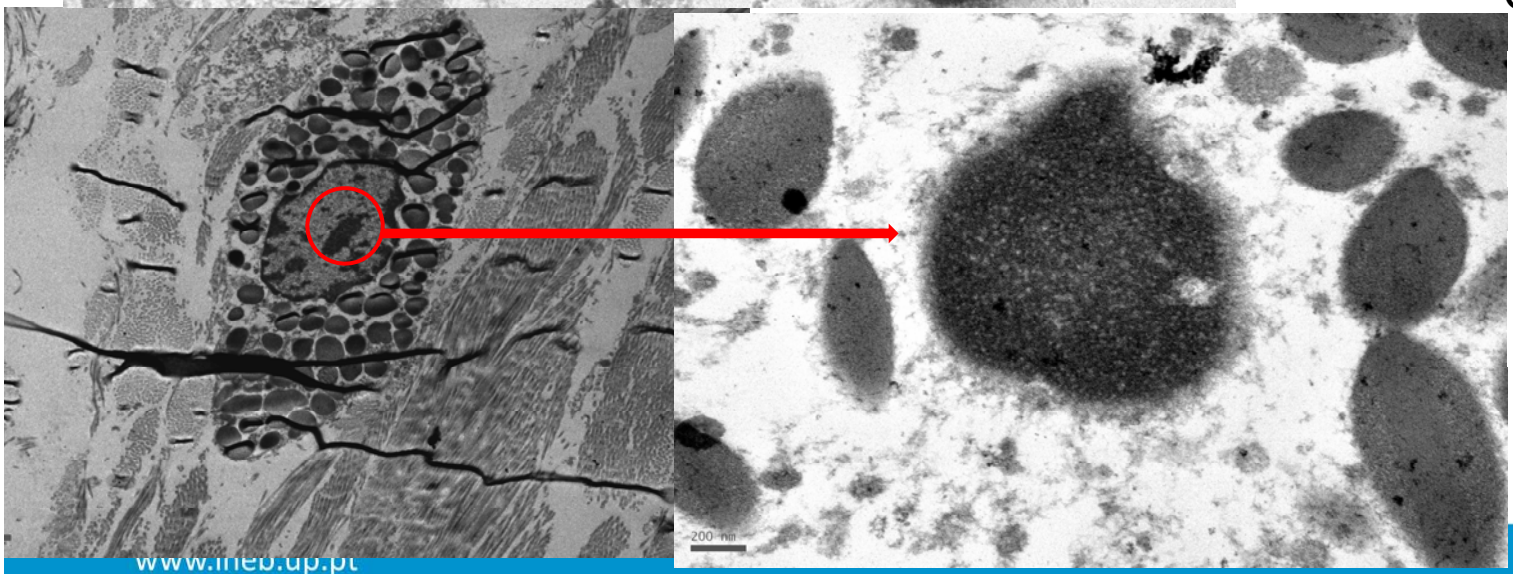

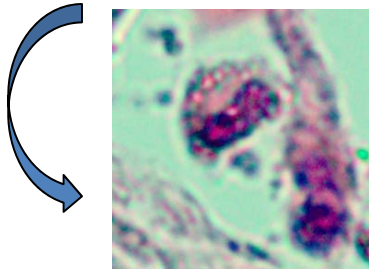

Histology

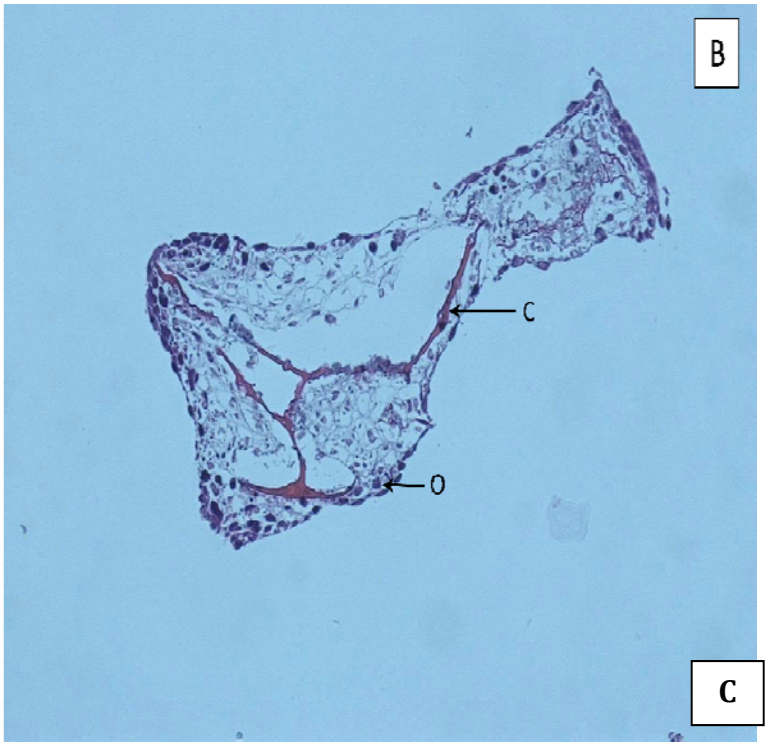

H&E staining of, b) collagen-nanoHA (70:30) scaffold,
and d) collagen-nanoHA (30:70) scaffold
cultured with osteoblast-like cells for 21 days.

Osteoblast-like cells (O) and collagen (C) were observed in all the scaffolds.

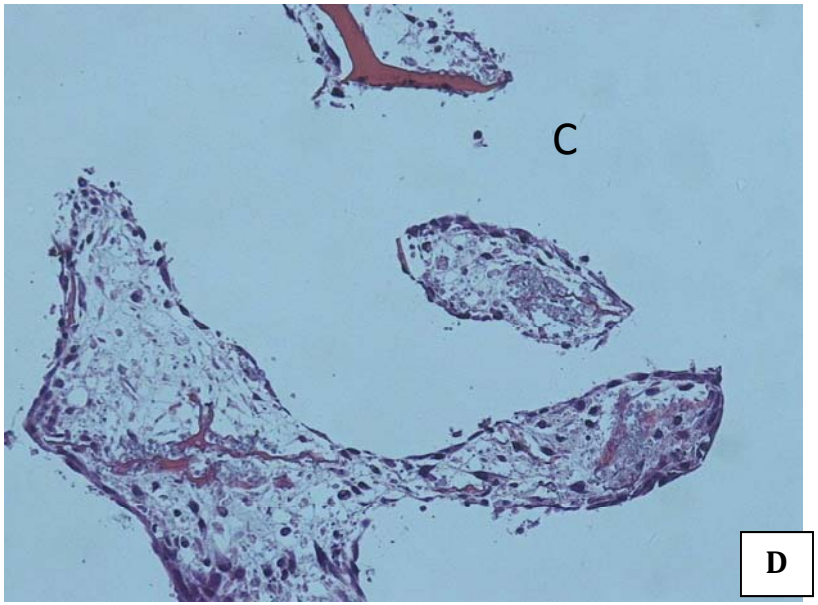

In vivo Materials Characterization

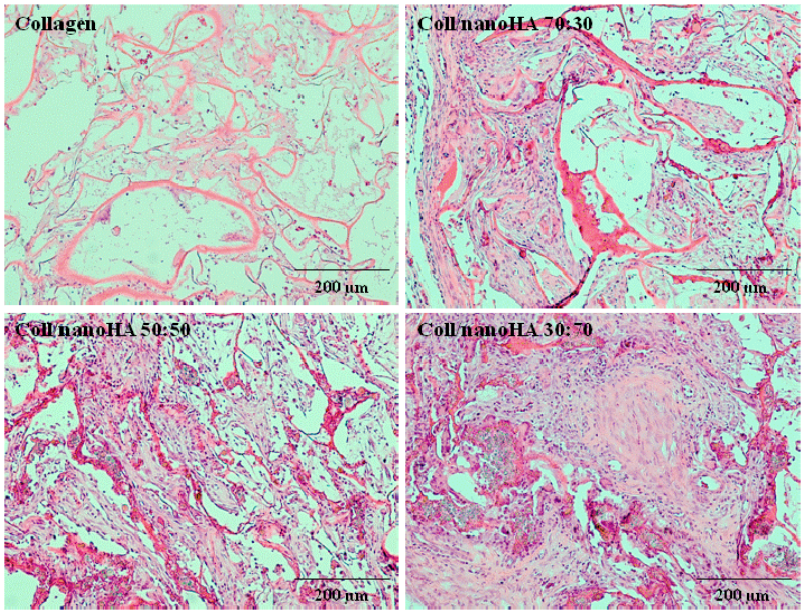

H&E stained scaffold sections after 7 days of *in vivo* implantation.

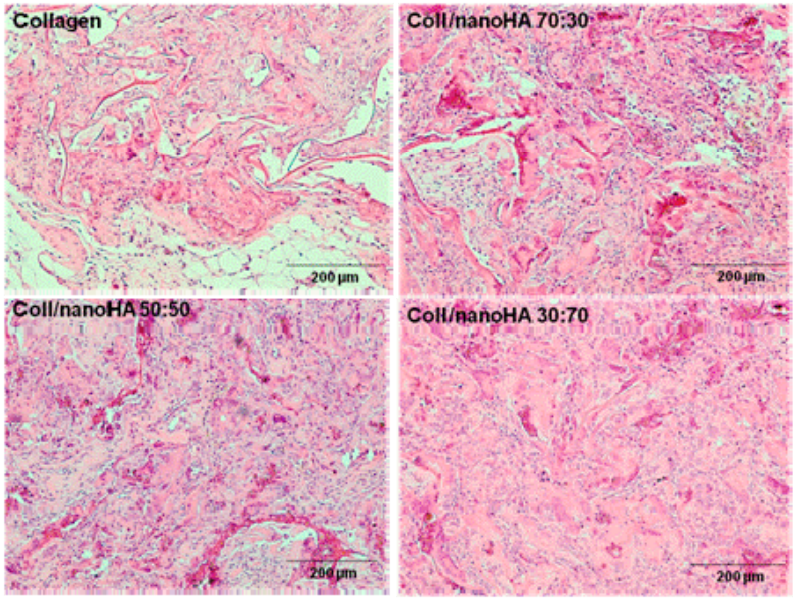

H&E stained scaffold sections after 30 days of *in vivo* implantation.

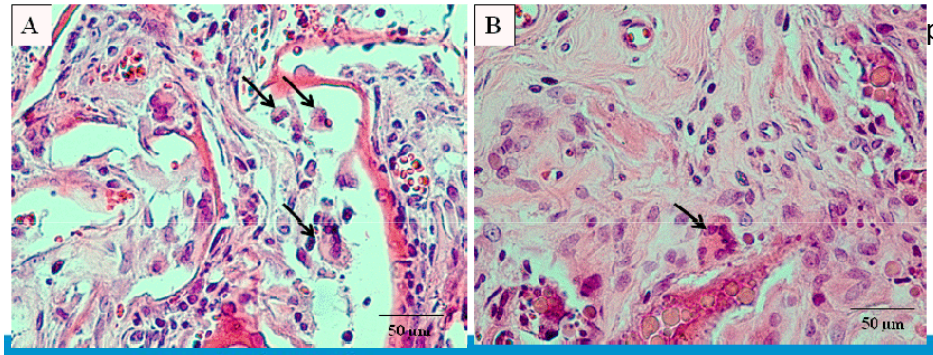

Optical micrographs of H&E stained scaffold sections after 30 days of ***in vivo*** implantation (Coll/nanoHA 50:50). (A) Arrows show presence of nanoparticles inside macrophage cells. (B) Arrow shows presence of giant cells.

Collagen nanofibers/nanohydroxyapatite Biocomposite for skin and bone repair

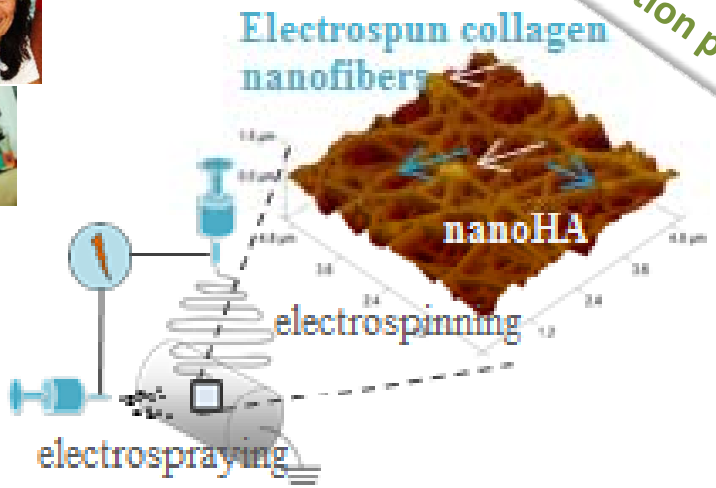

Patent application pending.

- Bone regeneration
- Skin regeneration

The development of a 3D immunocompetent model of human skin

David Y S Chau[1,3], Claire Johnson[2,3], Sheila MacNeil[2,4], John W Haycock[2,3] and Amir M Ghaemmaghami[1,4]

control: no cells | upper (epidermis): keratinocytes | bottom (dermis): fibroblasts

Influence of electrospun collagen on wound contraction of engineered skin substitutes

Heather M. Powell[a,*], Dorothy M. Supp[a,b], Steven T. Boyce[a,b]

Acta Biomaterialia

journal homepage: www.elsevier.com/locate/actabiomat

Electrospun synthetic human elastin:collagen composite scaffolds for dermal tissue engineering

Jelena Rnjak-Kovacina[a,1], Steven G. Wise[a], Zhe Li[b], Peter K.M. Maitz[b], Cara J. Young[c], Yiwei Wang[b], Anthony S. Weiss[a,*]

Calcium ions:

- play an important role in the regeneration of skin and connective tissue (L. Gennero *et al.*, 2011)
- regulate the activation of the MMPs, which is also required for the migration of the keratinocytes (L.H. Cornelissen, 2004).
- play a vital role in the growth and differentiation of keratinocytes (B. Pomahac *et al.*, 1998)

Multi-functional and biospecific hydrogels for cell delivery

Molecularly designed natural polymers (alginate- and pectin-based) as artificial 3D extracellular matrices

Cell adhesion on
RGD-alginate

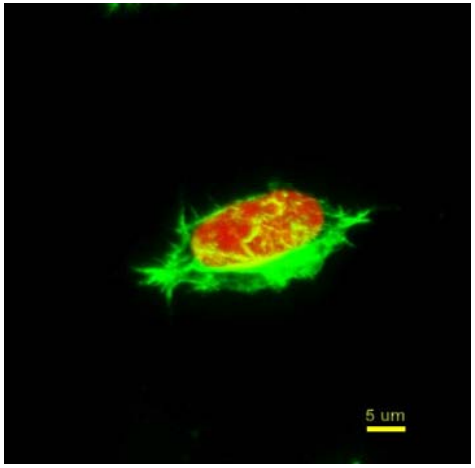

Evangelista, Biomaterials (2007)
Bidarra, Biomacromolecules (2010)

Cell adhesion and migration on
PVGLIG-RGD-alginate

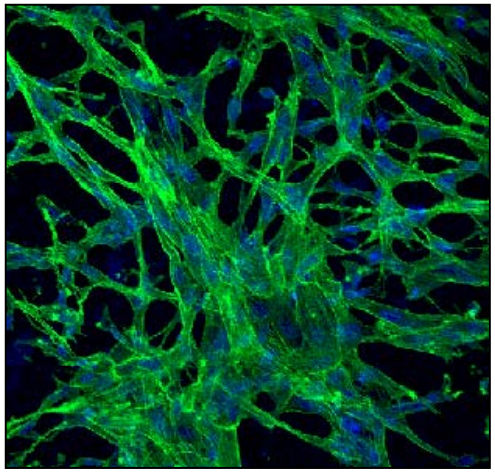

Fonseca, Acta Biomater (2011)
Fonseca, Soft Matter (2013)
Fonseca, Biomacromolecules (2014)

Cell differentiation on
OGP-PVGLIG-RGD-alginate

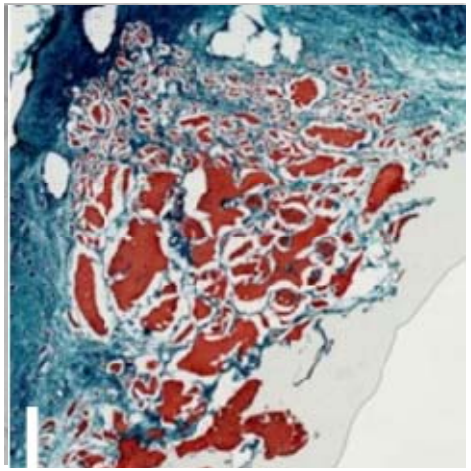

Maia, Acta Biomater (2013)
Maia, J Control Rel (2014)
Maia, Acta Biomater (2014)

3D Printing for skin Tissue Engineering

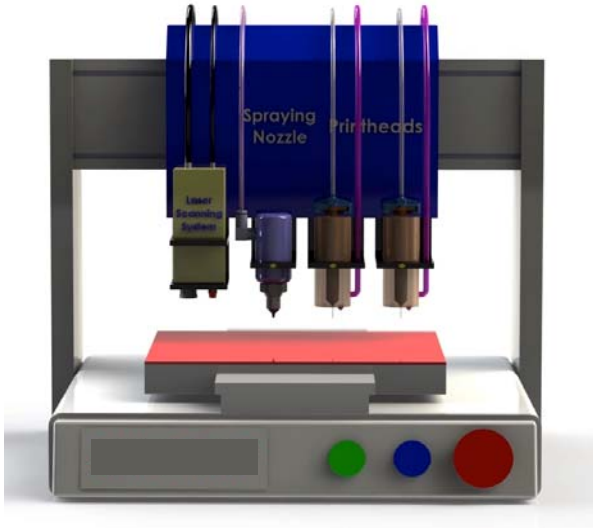

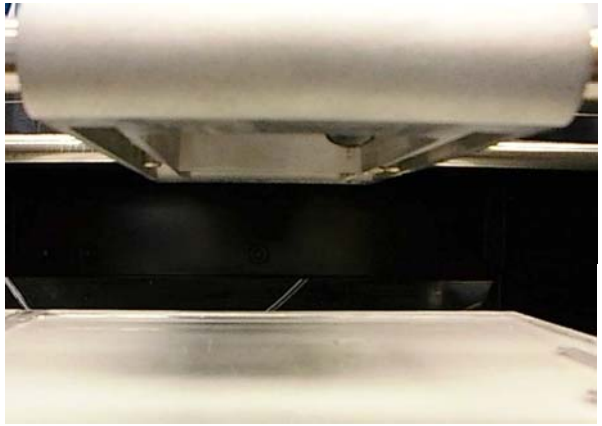

3D bioprinting system with syringes containing different hydrogel-based materials with entrapped skin cells

UV crosslinkable, biodegradable RGD-pectin hydrogels for skin regeneration

Subcutaneous implantation of RGD-Pectin (1 week)

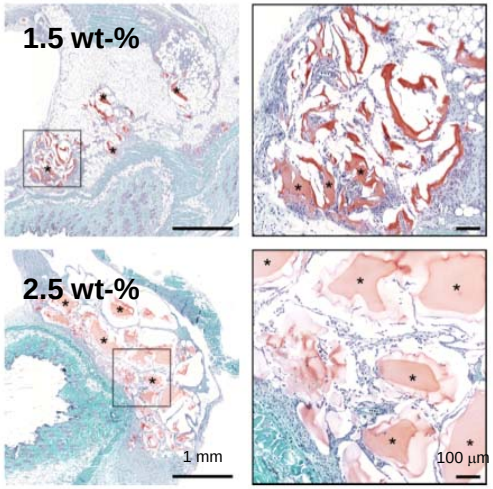

Light crosslinkable pectin functionalized with methacrylic anhydride

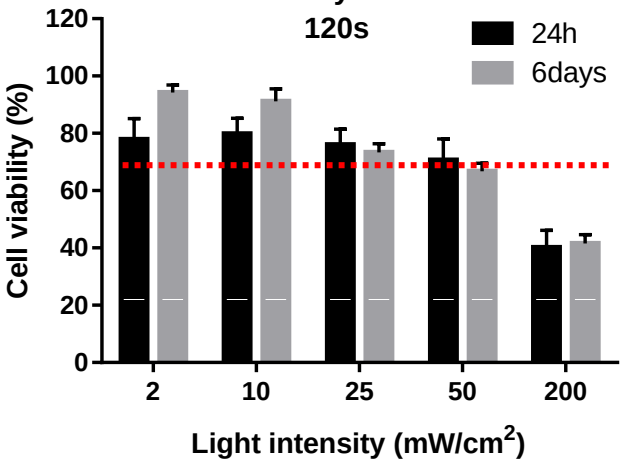

*Pereira, **Granja** +, Nanomedicine (2013)*

*Neves, **Granja** +, J Mater Chem B (2015)*

*Pereira, **Granja** +, In Preparation (2015)*

Our Partners

Thank You for your attention!